This electronic thesis or dissertation has been downloaded from the King's Research Portal at https://kclpure.kcl.ac.uk/portal/

ESCRT-III/Vps4 controls heterochromatin-nuclear envelope tethering and the establishment of nuclear compartmentalisation through the inner nuclear membrane protein complex Lem2-Nur1

Pieper, Gerard

Awarding institution:
King's College London

The copyright of this thesis rests with the author and no quotation from it or information derived from it may be published without proper acknowledgement.

END USER LICENCE AGREEMENT

Unless another licence is stated on the immediately following page this work is licensed

under a Creative Commons Attribution-NonCommercial-NoDerivatives 4.0 International

licence. https://creativecommons.org/licenses/by-nc-nd/4.0/

You are free to copy, distribute and transmit the work

Under the following conditions:

- Attribution: You must attribute the work in the manner specified by the author (but not in any way that suggests that they endorse you or your use of the work).
- Non Commercial: You may not use this work for commercial purposes.
- No Derivative Works - You may not alter, transform, or build upon this work.

Any of these conditions can be waived if you receive permission from the author. Your fair dealings and other rights are in no way affected by the above.

Take down policy

If you believe that this document breaches copyright please contact librarypure@kcl.ac.uk providing details, and we will remove access to the work immediately and investigate your claim.

Download date: 31. Oct. 2023

ESCRT-III/Vps4 controls heterochromatin-nuclear envelope tethering and the establishment of nuclear compartmentalisation through the inner nuclear membrane protein complex Lem2-Nur1

Gerardus Hendrikus Pieper

King's College London

PhD Supervisor: Prof. Snezhana Oliferenko

A thesis submitted for the degree of

Doctor of Philosophy

King's College London

December 2019

Declaration and contributions

All experiments in this thesis were performed and analysed by Gerard Pieper except for the following: All the *in vitro* binding experiments in Fig. 5-1 were performed by Simon Sprenger of the lab of Dr. David Teis at the Medical University Innsbruck. Simon Sprenger also created the Vps24, Vps4 and Vps4^{EQ} tagged constructs, validated their functionality (Fig. 4-1A, B) and initiated the experiments on ESCRT-III/Vps4 localisation.

Parts of this thesis are parts of a manuscript in preparation for publication as: Gerard H. Pieper, Simon Sprenger, David Teis and Snezhana Oliferenko. ESCRT-III/Vps4 controls heterochromatin-NE tethering.

Summary

The nucleus contains almost all of the genetic material of eukaryotes. The nuclear envelope (NE) is the boundary of this structure. It not just compartmentalises the chromosomes, it also organises the genome in the nucleus through interactions with inner nuclear membrane (INM) proteins. A wide spectrum of mitotic NE remodelling strategies exists. Different species have found different ways of dealing with the nuclear membrane to properly segregate its chromosomes. On one end of the continuum, an impressive number of events coordinated in space and time break-down and rebuild the NE every cell-cycle in human cells. On the opposite end there is the completely closed mitosis of budding yeast and the fission yeast *Schizosaccharomyces pombe*, where chromosomes are segregated within an intact nuclear membrane. Regardless of the how the cell deals with the NE, every mitosis interactions between chromatin and the NE have to be remodelled to allow chromosome segregation. How chromatin tethering to the INM is controlled in interphase and mitosis and how this process contributes to subsequent mitotic NE remodelling remains unclear.

In this thesis we have probed these fundamental questions using the fission yeast *Schizosaccharomyces japonicus*, a close relative to *S. pombe*. *S. japonicus* breaks the NE during mitosis at a single defined site, leading to only a single site where the NE needs to be reformed during mitotic exit. In addition, this organism is able to re-establish nucleocytoplasmic compartmentalisation in the presence of the spindle. Thus, this organism performs a form of open mitosis, but with much reduced complexity. We show firstly that the INM complex Lem2-Nur1 together with the ESCRT-III machinery and the AAA-ATPase Vps4 regulate the establishment of nuclear compartmentalisation during mitotic exit in the presence of the spindle by maintaining the 'tail' structure. This structure consists of nuclear membrane wrapped around the mitotic spindle and provides a barrier between the nucleoplasm and the cytoplasm. We further show that attachments between heterochromatin and Lem2-Nur1 are continuously remodelled in interphase by ESCRT-III/Vps4. Failure to release Lem2-Nur1 from heterochromatin leads to persistent association of chromosomes with the INM throughout the cell cycle. At mitotic exit, this trapping of Lem2-Nur1 on heterochromatin prevents its function in re-establishment of nucleocytoplasmic compartmentalisation. Our work identifies the INM Lem2-Nur1 complex as a substrate for ESCRT-III/Vps4 to couple dynamic tethering of chromosomes to the INM with the establishment of nuclear compartmentalization.

Index

List of figures

Abbreviations

BAF	Barrier-to-autointegration-factor
CFU	colony forming unit
ChIP	chromatin immunoprecipitation
CLEM	correlative light-electron microscopy
EM	electron microscopy
ER	endoplasmic reticulum
ESCRT	endosomal sorting complex required for transport
GBP	GFP binding protein
H3K9me2	histone H3 dimethylated on lysine 9
H3K9me2	histone H3 trimethylated on lysine 9
HEH	helix-extension-helix
INM	inner nuclear membrane
MSC	Man1-Src1p-C-terminal
MTOC	microtubule organising complex
NE	nuclear envelope
NLS	nuclear localisation signal
MVB	multivesicular body
NPC	nuclear pore complex
ONM	outer nuclear membrane
LAD	lamina associated domain
LEM	LAP2-emerin-MAN1
qPRC	quantitative polymerase chain reaction
SAC	spindle assembly checkpoint
SPB	spindle pole body
TAD	topologically associated domain
WT	wild type

Chapter 1 – Introduction

1.1 The nuclear envelope

The nuclear envelope (NE) is a membranous structure that encapsulates the chromosomes in all eukaryotes. It consists of a double membrane system composed of the outer nuclear membrane (ONM), which is continuous with the endoplasmic reticulum (ER) and the inner nuclear membrane (INM), which interacts with chromatin. The membranes of the ONM and INM are continuous through the nuclear pores, channels in the membrane which contain the nuclear pore complexes (NPCs). These large protein complexes mediate the transport between the cytoplasm and the nucleoplasm. Thus, the NE forms a barrier that defines the nuclear and cytoplasmic compartments, y*et al*lows the transport of specific molecules between the two (Hetzer, 2010).

The evolution of the NE as a semi-permeable barrier has been thought to drive the complex regulation of gene expression of eukaryotes (Hetzer, 2010). Apart from maintaining a barrier and defining the nuclear and cytoplasmic compartments, the structure and integrity of the NE are vital for several nuclear functions such as genome organisation bearing on gene expression, mechano-sensing and signalling (Stewart *et al*., 2007; Mekhail and Moazed, 2010).

During the process of mitotic nuclear division, the nuclear membrane undergoes dramatic remodelling. In fact, during the open mitosis performed by human cells the NE is completely broken down to be absorbed into the ER during prophase and rebuild during telophase (Güttinger *et al*., 2009). This has to be tightly controlled in order to end up with two functional daughter nuclei after chromosome segregation.

Both the structure and the function of the NE are not defined as much by its membrane component, but primarily by its highly specialised protein composition, particularly that of the INM. The INM contains proteins that interact with chromatin and is also the site of the nuclear lamina in higher eukaryotes, a skeleton which provides structure and rigidity to the NE. It is the interaction between INM proteins and chromatin that provides the basis of the functional properties of the NE in terms of genome organisation and gene expression. Furthermore, this association has to be

regulated throughout the cell-cycle and especially during mitosis, where chromosomes segregation has to be coordinated with the remodelling of the NE.

In the following chapters I will highlight the mechanisms and players involved in the organisation of the nucleus, particularly in relation to the NE, remodelling of the NE and chromatin-NE tethering.

1.2 Organisation of chromatin within the nucleus

The genome is organised in 3D space within the nucleus. This organisation is not random (Fig. 1-2). On a larger scale, individual chromosomes occupy their own distinct chromosome territories (Cremer *et al.*, 1982, 1988). On a smaller scale, the genome is organised within discrete intra-chromosome domains delimited by boundaries (Lieberman-Aiden *et al.*, 2009). These domains are often termed topologically associated domains (TADs; Fig. 1-2; Dixon *et al.*, 2012). Loci within a domain interact primarily with other loci within this domain compared to loci outside of it. Furthermore, genes within a TAD tend to be regulated together and often exhibit similar expression levels (Dixon *et al*., 2016). In this way, two main forms of TADs have been defined: A-type TADs, largely corresponding to active euchromatin and B-type, largely corresponding to inactive heterochromatin (Fig. 1-2; Lieberman-Aiden *et al*., 2009). Another level of spatial genome organisation is provided by the fact that active and inactive chromatin, or A-type TADs and B-Type TADs, are spatially segregated from each-other into active and inactive regions (Lieberman-Aiden *et al*., 2009).

Apart from chromatin domains, the nucleus contains several functional compartments relating to the organisation, expression or regulation of the genome. These include for example the nucleolus, nuclear speckles and paraspeckles (Dundr and Misteli, 2010). These compartments are defined based on their DNA or RNA content, protein content and their function. For example, the nucleolus contains the ribosomal DNA (rDNA) loci, is enriched for RNA Pol I and RNA processing factors and is the site of ribosome biogenesis (Dundr and Misteli, 2010). The NE might be considered such a compartment as well. In metazoa, the NE organises primarily B-type or inactive chromatin. This has been found in different cell-types in *Drosophila* (Pickersgill *et al.*, 2006), *Caenorhabditis elegans* (Ikegami *et al.*, 2010) and human cultured cells. For the latter, as much as 40% of the entire genome can be associated with NE, with a large part

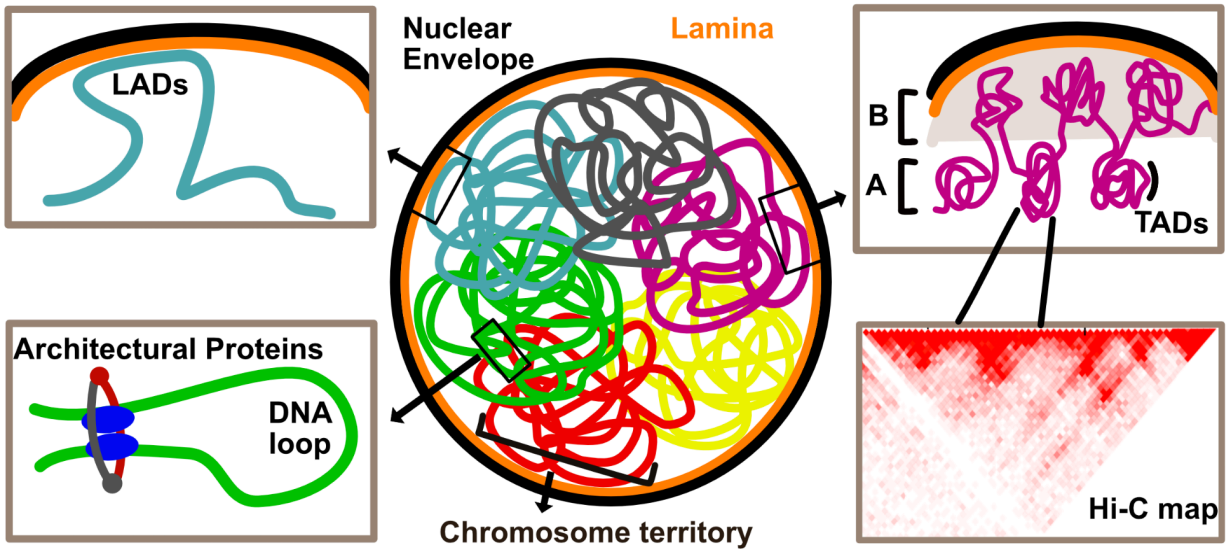

Figure 1-2. Organisation of the genome within the nucleus.

Schematic representation of the different ways in which the genome is organised within the nucleus. Figure taken from Sivakumar *et al*., 2019.

also consisting of intergenic regions (Guelen *et al.*, 2008; Peric-Hupkes *et al.*, 2010). These chromatin domains in contact with the nuclear periphery are termed lamina-associated domains (LADs) and have primarily been identified using the DamID method to identify interaction of chromatin regions to Lamin proteins, which line the INM in metazoa and are part of the nucleoskeleteon (Guelen *et al*., 2008). LADs show many similarities with TADs in that both are defined chromatin domains marked by boundaries with domain-level regulation of gene expression. In fact, many of the repressive TADs overlap with LADs, as observed primarily by the overlap of boundary sites of a subset of TADs and LADs (Kind *et al.*, 2015). Domains between LADs are looped into the nuclear interior and primarily constitute active chromatin. Using antibodies reacting specifically with either H3K9 dimethylated (H3K9me2) or trimethylated (H3K9me3) forms, both conserved epigenetic heterochromatin marks, it was shown that specifically H3K9me2 chromatin is located directly at the nuclear periphery and not in the nuclear interior in *C. elegans*, *Xenopus laevis* and mouse and human embryonic stem cells and fibroblasts. On the other hand, H3K9me3 can be found enriched at both the nuclear periphery and the interior in mouse fibroblasts (Poleshko *et al.*, 2019). Thus, a model can be suggested where the NE structurally organises silent or repressed chromatin and the nuclear interior contains actively transcribed chromatin.

However, the relationship between inactive chromatin and the NE is not so straightforward. It is not clear whether the NE provides a domain that enforces gene silencing or whether it merely organises chromatin based on its characteristics. For example, LADs are not necessarily predetermined. Some LADs can be very conserved between cell-types and even between humans and mice (Meuleman *et al.*, 2013). However, some are not inherited from cell-cycle to cell-cycle. New LADs, with the same characteristics of inactive chromatin are established and LADs from the previous cell cycle are now found in the nuclear interior (Kind *et al.*, 2013). However, it should be noted that using fluorescence *in situ* hybridisation (FISH) for specific LADs in a different system, it was found that LADs may in fact return to the nuclear periphery following mitosis (Poleshko *et al.*, 2019). Synthetically tethering chromosome loci to the NE can reduce of expression of some genes surrounding this locus (Finlan *et al.*, 2008; Reddy *et al.*, 2008). However, many genes in the same region were not transcriptionally affected and neither was complete silencing observed in these cases (Finlan *et al.*, 2008; Kumaran and Spector, 2008).

The complicated relationship between the nuclear periphery and chromatin is exemplified by the dynamic reorganisation of NE-localised chromatin during differentiation. During each step of the differentiation from mouse embryonic stem cell to neural progenitor cell to astrocyte many of the nuclear lamina-chromatin contacts are reshuffled (Peric-Hupkes *et al.*, 2010). In general, during each differentiation step the nuclear periphery remains associated with repressed chromatin. Specific genes associated with pluripotency that become downregulated during differentiation relocalize to the periphery and genes associated with neural physiology are released into the nucleoplasm. However, this was not typical for all such genes, as only a small fraction (215 out of 4052) of genes that were downregulated during differentiation became localised to the periphery. Furthermore, only one third of the genes that relocated either to or from the periphery during the embryonic stem cell to nuclear progenitor transition showed changes in expression. Interestingly, it appeared that for some of these genes, their release from the NE correlated with changes in gene expression only after the nuclear progenitor to astrocyte cell transition. Thus, it was suggested that the release from the nuclear periphery “unlocks” genes for activation rather than activates them (Peric-Hupkes *et al*., 2010). This model makes the definition

of a direct relationship between localisation to or from the nuclear periphery not straightforward. However, this is consistent with findings in the *C. elegans* embryo. Here, the CEC-4 protein specifically tethers histone H3K9 methylated heterochromatin to the NE. Removal of CEC-4 mis-localises heterochromatin to the nuclear interior, but does not directly affect the silencing of heterochromatin. What was affected however, is the ability to mount a robust muscle differentiation programme when this programme is ectopically induced. It was hypothesised that this was because *cec-4* mutants could not properly repress non-muscle programmes due to the localisation of non-muscle genes to the nuclear interior (Gonzalez-Sandoval *et al.*, 2015). This is consistent with the fact that during differentiation in *C. elegans*, the promoters of tissue-specific genes become localised to the nuclear periphery when silenced and move to the interior when activated in their specific cell types. Yet, in the undifferentiated larval cells their localisation remains random (Meister *et al.*, 2010).

Some features of chromatin organisation at the NE are conserved in lower eukaryotes. In fission yeast, lower expressed genes and repressed chromatin are also associated with the NE, also amounting to a total of around 40% of the genome being associated with the NE (Steglich *et al.*, 2012). Additionally, all heterochromatin domains in fission yeast, pericentromeric, subtelomeric and mating-type associated, are clustered at the NE as well (Allshire and Ekwall, 2015). This is conforming to what is termed the “Rabl” configuration where centromeres are associated with one pole and telomeres are attached to the NE on the opposite site of the nucleus. It was named after Carl Rabl who first described such a conformation in 1885. This configuration is also observed in plants such as wheat (Abranches *et al.*, 1998), the polytene nuclei of the *Drosophila* salivary gland cells (Hochstrasser *et al.*, 1986) and budding yeast (Jin *et al*., 2000), but not in humans (Parada and Misteli, 2002). Despite this conformation in budding yeast, some active genes are associated with NPCs at the NE in this organism. Additionally, environmentally controlled genes such as the *GAL1* promoter become localised to the NPCs when activated (Arib and Akhtar, 2011). Thus, in budding yeast the NPCs might provide local areas of active chromatin, which are interspersed with local areas of inactive chromatin between the NPCs.

In conclusion, the NE, or the nuclear periphery, as an organiser of repressed (hetero)chromatin appears to be a conserved phenomenon. Although many exceptions

for this correlation can be found for example for particular genes or during particular stages of development, the general observation holds true for many organisms.

1.3 Inner nuclear membrane proteins link genome organisation to nuclear envelope structure and function

The ability of the NE to organise chromatin is determined by specific INM proteins. The INM has a highly specialised proteome, of which not all proteins have chromatin-binding abilities. The protein composition of the INM is often termed the nuclear-lamina. In metazoa the lamina consists of transmembrane INM proteins, non-integral membrane proteins and a set of filamentous coiled-coil proteins called Lamins. Lamins line the entirety of the INM and provide a structural "nucleoskeleton" (Czapiewski *et al*., 2016). They are not conserved outside of metazoa (Mans *et al.*, 2004), although proteins with similar coiled coil structures performing similar functions can be found for example in plants (Meier *et al.*, 1996; Masuda *et al.*, 1997). Apart from the lamina, the NPCs are the major protein constituent of the NE, providing the semi-permeable barrier function of the NE.

The full extent of INM proteins that directly interact with chromatin and for that matter the full extent of INM proteins is not very well described. One difficulty with identifying such proteins is that there do not appear to be clear functional domains or even functions associated with many INM proteins, making it difficult to predict them by sequence. Additionally, INM proteins might also be found in the ER and ONM. A good example of the unappreciated amount of INM proteins was the identification of 67 previously uncharacterised INM transmembrane proteins in the rat liver, identified by a proteomic approach (Schirmer *et al.*, 2003). Many INM proteins have tissue specific expression and also tissue specific splice variants (Schirmer and Gerace, 2005; Korfali *et al.*, 2012; Capitanchik *et al.*, 2018), making it likely the INM proteomes throughout the body are very diverse. The latter might point to a potential function of this diversity, as the large range of INM transmembrane proteins might function in tethering tissue-specific genes to the silent domain of the nuclear periphery in tissues where they should not be activated or their activities reduced. Indeed, different INM transmembrane proteins can have specificities for specific chromosomes (Zuleger *et al.*, 2013). For example, NET47 has specific affinity for chromosome 5 and is mainly expressed in liver

cells, where a large part of chromosome 5 is found more often at the nuclear periphery than the interior. Knockdown of NET47 results in the release of a larger part of this chromosome into the nuclear interior (Zuleger *et al*., 2013). Many other NETs exhibit specific affinities for other chromosomes and sometimes for several chromosomes, with several NETs having affinities for the same chromosome (Zuleger *et al*., 2013).

It would be interesting to find out if indeed the parts of these specifically tethered chromosomes carry the genes that should be repressed in these tissues. One such example in which specific INM transmembrane proteins link the positioning of genes to the NE with transcriptional repression is during muscle formation (Robson *et al.*, 2016). In an *in vitro* system modelling muscle development by differentiating mouse myoblasts into myotubes, genes required for muscle function such as Titin became released from the NE and vice versa, genes related to metabolism and proliferation become localised to the NE. Roughly 2/3rd of the genes relocating to the nuclear periphery became downregulated and vice versa, roughly 2/3rd of genes relocated to the nuclear interior became upregulated (Robson *et al*., 2016). Knockdown of three muscle-specific NETs NET39, Tmem38a and WFS1 resulted in both a failure to localise genes to the nuclear periphery and to repress genes that are downregulated during the myoblast to myotube differentiation (Robson *et al*., 2016).

However, it is not yet clear for many of the proteins found in the nuclear lamina of metazoa if they have direct chromatin-tethering abilities. Genetic experiments have revealed their role in gene positioning, but what exactly they recognise on the chromatin, be it DNA sequence, histone marks or chromatin associated proteins, is not clear. Additionally, many proteins in the nuclear lamina might have functions apart from direct tethering. For example, several of the 67 novel INM proteins had enzymatic functions that are not directly related to chromatin tethering, such as phosphatase and acetyltransferase activities (Schirmer *et al.*, 2003). These proteins might for example be involved in the regulation of chromatin and chromatin associated proteins. The level of conservation of many of genes coding for these INM proteins within eukaryotes, as well as their functions remain to be elucidated.

As just described, one particular aspect in which very dynamic changes in NE-chromatin organisation are observed is differentiation. Though the processes organising the genome in single celled eukaryotes such as yeasts are by no means simple, the INM

proteome, specifically chromatin-tethering protein, of lower eukaryotes that do not undergo a differentiation process appears to be much more limited. This might in part be due to the lack of comprehensive studies attempting to identify these proteins in yeast. An attempt to identify INM proteins in budding yeast using a split-GFP system did identify 411 potential proteins with access to the INM (Smoyer *et al.*, 2016). However, due to the nature of the split-GFP system it cannot be stated categorically whether these are proteins indeed have functions at the INM, or whether they are merely retained there after having passively diffused through the NPC.

Many of the several well-described INM chromatin-tethering protein in yeast relate to the tethering of very specific chromatin domains such as telomeres, centromeres and ribosomal DNA (rDNA). In budding yeast, telomeres are anchored to the NE through the INM protein Esc1 that interacts with the heterochromatin protein Sir4 at the telomere, or through SUN-domain protein Mps3 that interacts with the yKu on telomeres through telomerase (Hediger *et al.*, 2002; Taddei *et al.*, 2004; Schober *et al.*, 2009). The Cohibin and CLIP complexes are involved in the tethering and stabilisation of rDNA repeats (Mekhail *et al.*, 2008). Cohibin links rDNA to the NE through CLIP, which consists of the INM proteins Heh1 and Nur1 (Mekhail *et al*., 2008). These complexes also maintain the stability and silencing of telomeres (Chan *et al.*, 2011). In *S. pombe*, telomeres are tethered through transmembrane proteins of the "bouquet" complex, namely Bqt3 and Bqt4, which associate with the telomere protein Rap1 (Chikashige *et al.*, 2009). Centromeres are likely tethered to the spindle pole body (SPB), the yeast microtubule-organising centre, through short microtubules in budding yeast (Jin *et al*., 2000). In *S. pombe* centromeres are tethered to the SPB through the redundant function of Csi1 and the LEM-domain protein Lem2 (Gonzalez *et al*., 2012; Barrales *et al.*, 2016). In *S. pombe* two proteins are known to tether more general chromatin to the NE. These are Ima1, homologous to human TMEM201, and the LEM-domain protein Man1 (Steglich *et al.*, 2012). Both tether repressed chromatin, with Man1 being especially enriched at sub-telomeric heterochromatin (Steglich *et al*., 2012).

In conclusion, the INM proteome responsible for the organisation of chromatin at the NE in animals is very diverse. INM transmembrane proteins with specific affinities to different chromatin domains allow for the dynamic localisation of different chromatin domains to the NE in different cell types and tissues. This aids the repression or

activation of genes that are required at specific developmental times or tissues. The INM proteome of single celled eukaryotes appears to be considerably less diverse. This is possibly related to a reduced need for dynamic transcriptional regulation.

1.4 Chromatin aids the structure and integrity of the nucleus

Over the recent years more attention has been given to the nucleus as a structural object in the cell in addition to its genetic functions (Bustin and Misteli, 2016). There are two main factors that relate to how chromatin can contribute to structural qualities of the nucleus. First is the general condensation state of the chromatin and second is the tethering of chromatin to the NE. Decreasing the chromatin compaction state by expressing a nucleosome binding protein resulted in the formation of nuclear blebs in cultured mouse embryonic fibroblasts (Furusawa *et al*., 2015). When chromatin was affected in the same way in mice which were allowed to develop to adulthood misshaped nuclei started to appear in adult cardiomyocytes. This was also associated with the development of severe cardiac hypertrophy and heart failure in these mice (Furusawa *et al.*, 2015). This last phenotype is an indicator for one of the functions of the nucleus: the response to mechanical forces. This is further exemplified by mutations in Lamins that can cause muscular dystrophy (Dahl *et al*., 2008). Another instance where nuclei are placed under a lot of stress is during cell migration. Considering that the nucleus is the largest organelle in the cell, it provides the bottleneck for cellular movement through narrow constrictions. Cells can regulate their nuclear stiffness by adjusting the ratio of different Lamins and thus affect their ability to migrate through 3D matrices (Harada *et al.*, 2014). However, another way to achieve a similar effect is the regulation of chromatin state. Cells can even regulate chromatin state as part of a developmental programme for migration. For example, T-lymphocytes when exiting the bloodstream to invade the tissue first have to attach themselves to the epithelia. As soon as they do so, a histone methyltransferase gets recruited to the NE, which is required for a nucleus wide increase in histone H3K9 methylation (Zhang *et al.*, 2015). Interestingly, analysis of the biophysical characteristics of these migration-activated nuclei showed that both their stiffness and viscoelastic properties were affected. Furthermore, cell migration speed and distance of migration depended on the chromatin state (Zhang *et al*., 2015).

A good example that not just the overall chromatin state but also its NE-tethering can affect nuclear structure comes from the fission yeast *S. pombe*, a yeast without a Lamin-based nucleoskeleton, where chromatin tethering is a main feature that gives shape and support to the nuclear envelope. In interphase *S. pombe* cells the nucleus is positioned in the middle of the cell by the microtubule network emanating several microtubule organising centres (MTOCs) on the nucleus (Tran *et al.*, 2001). This continuous repositioning provides a force on the NE that causes deformations of the NE, affecting its normally spherical shape. Untethering chromatin from the NE by the *heh1Δ heh2Δ* double deletion results in much larger nuclear shape changes (Schreiner *et al.*, 2015). Analysis of the biophysical properties of isolated fission yeast nuclei showed that chromatin tethering affects the stiffness of the nucleus and allowed it to behave as a viscous agent in response to microtubule induced forces (Schreiner *et al*., 2015).

The organisation of, in particular, silenced chromatin or heterochromatin at the NE raises a particular question: why is repressed rather than active chromatin tethered to the NE? It might be that the need to segregate inactive chromatin away from actively transcribed genes was an early adaptation occurring together with the evolution of the nuclear membrane. Alternatively, it can be hypothesised from a more mechanical point of view that the more condensed heterochromatin might provide some structural support for the nuclear membrane. Indeed, when force was applied onto the nuclear envelope by microtubules after initial depolymerisation of the microtubule network the nucleus was shown to invaginate and locally accumulate both dense chromatin and Lamin B. Interestingly, both disappeared after the microtubule network had fully restored itself and pressure was no longer applied on the nucleus (Gerlitz *et al*., 2013).

In conclusion, even though higher eukaryotes with relatively large nuclei have a nucleoskeleton that lines the inside of the nucleus, the state of the chromatin inside of the nucleus and its tethering to the NE constitute a main determinant of nuclear structure and parameters such as stiffness. Chromatin-NE tethering is a conserved feature that helps maintain the spherical shape of yeast nuclei in the absence of a nucleoskeleton in response to forces applied to the nucleus.

1.5 The evolutionarily conserved LEM-domain proteins tether chromatin to the nuclear envelope and organise chromatin regulators

There are not many known INM chromatin-interacting proteins that are conserved throughout all eukaryotic domains. One of the most conserved classes of these are LAP2-emerin-MAN1 (LEM) domain proteins. The general topology of LEM domain proteins is as follows (Fig. 1-5): A nucleoplasm localised N-terminal LEM domain is followed by a long largely disordered linker (Herrada *et al.*, 2015). Two transmembrane domains flank a lumenal cysteine-rich domain. The C-terminal domain is also nucleoplasmic. Both the lumenal and C-terminal parts comprise the so-called Man1-Src1p-C-terminal (MSC) domain (Mans *et al.*, 2004). The most conserved orthologues of LEM domain proteins throughout eukaryotes contain the "full" version containing both the LEM and MSC domains. These are all orthologues of either the human MAN1/LEMD3 or LEM2/LEMD2 proteins. Structurally similar proteins can be found in plants as well (Brachner and Foisner, 2011). In metazoa the range of LEM-domain proteins appears to have expanded beyond MAN1 and LEM2 homologues. Other LEM-domain proteins such as Emerin have appeared later throughout evolution, often losing the MSC domain and one or two of the transmembrane-domains (Brachner and Foisner, 2011). It should be noted that the actual LEM-domain is metazoan-specific as well. Other eukaryotes such as yeast instead exhibit a structurally similar helix-extension-helix (HEH) fold (Mans *et al.*, 2004). The yeast HEH domain interacts directly with chromatin (Hirano *et al.*, 2018). LEM-domain proteins on the other hand interact with chromatin through an intermediate protein called Barrier-to-auto-integration-factor (BAF; Segura-Totten and Wilson, 2004).

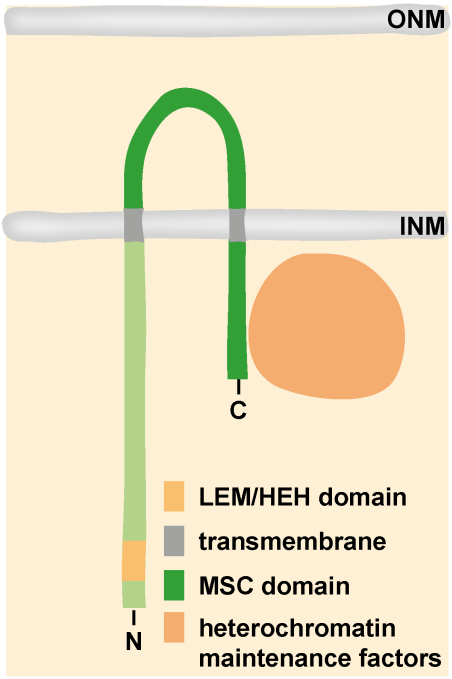

Figure 1-5. Schematic representation of the structure of LEM/MSC domain proteins.

ONM: outer nuclear membrane, INM: inner nuclear membrane (not to scale).

Due to its interaction with DNA or chromatin the LEM domain has mostly been considered the business end of LEM domain proteins. However, for the *S. pombe* LEM domain protein Lem2 several new functions were identified for the MSC domain. Whereas the HEH domain of Lem2 performs redundant functions with Csi1 in

tethering of centromeres to the SPB, the MSC domain of Lem2 is responsible for telomere anchorage at the NE (Barrales *et al.*, 2016). It should be noted that also for telomere tethering Lem2 likely is redundant, as the INM protein Bqt4 functions as a tether for telomeres. Bqt4 can interact directly with DNA and also with the telomere protein Rap1. Point mutants that affect binding to either of these release telomeres into the nucleoplasm during interphase (Hu *et al.*, 2018, 2019). Importantly, it was found that the Lem2 was not just a simple tether. The MSC domain is critical for the function of Lem2 in heterochromatic gene silencing at the telomeres. Lem2 does not mediate silencing itself, rather it interacts with the SHREC complex (Barrales *et al*., 2016), which is a heterochromatin maintenance complex (Sugiyama *et al.*, 2007; Job *et al.*, 2016). Lem2 is also required for maintenance of centromeric heterochromatin in *S. pombe*, particularly in response to a nutritional shift from rich growth medium to minimal growth medium (Tange *et al.*, 2016), although it remains to be elucidated whether this is also executed by the MSC domain. Genetic data that likely relates to heterochromatin maintenance showed that expressing just the MSC domain of Lem2 can rescue the loss minichromosomes associated with *lem2* deletion. Furthermore, expression of the MSC domain, but not the HEH domain can rescue lethality of the *lem2Δ bqt4Δ* double mutant (Tange *et al.*, 2016). From this the idea arises that the MSC domain might be a platform for interaction with different proteins to mediate events at the NE, potentially bringing chromatin maintenance factors into contact with chromatin.

1.6 Nuclear envelope remodelling during mitosis

Some form of NE remodelling is required during mitosis to end up with two functional daughter nuclei. Higher eukaryotes completely break down the NE at the onset of mitosis, therefore losing nuclear compartmentalisation, followed by NE reformation after chromosome segregation (Güttinger *et al*., 2009). This has to be followed by complete reinstatement of nuclear integrity. However, many mitotic strategies exist throughout the different domains of life. These range from the fully closed mitosis observed in many lower eukaryotes, where the nucleus divides without disrupting the nuclear membrane, to the fully open mitosis in humans. A plethora of different strategies with variant degrees of nuclear membrane disruption and loss of nucleocytoplasmic compartmentalisation are known (Makarova and Oliferenko, 2016).

Different strategies are often observed between closely related species and even during different parts of the life-cycle in the same species. When looking at all the different NE remodelling strategies found throughout life it can be considered that NE dynamics can follow a gradient of intermediates (Makarova and Oliferenko, 2016). Rather than viewing open and closed mitosis as two opposing strategies, they should be viewed as extremes on a spectrum of different possibilities that all build on the same common principles. This becomes particularly clear when also considering the formation of the spindle, which can form within an intact nucleus, a completely broken-down nucleus or in even the cytoplasm surrounding the intact nucleus (Makarova and Oliferenko, 2016). For example, the dinoflagellate *Crypthecodinium* (*Gyrodinium*) *cohnii* forms the spindle outside the mitotic nucleus, the latter then forms invaginations, resulting in channels through the nucleus through which bundles of microtubules are roped. Chromosomes within the closed nucleus somehow contact these channels. The nucleus then starts to invaginate in the middle, separating into two daughter nuclei while the spindle network is still intact (Kubai and Ris, 1969).

The process of NE breakdown in human cells is initiated in prophase when chromatin starts condensing to form the typical individual mitotic chromatin structures. The first event at the NE is that the semi-permeable barrier is broken down by the disassembly of NPCs (Güttinger *et al*., 2009). Then, the nuclear lamina breaks down and microtubules emanating from the centromeres start to deform the NE. It is unclear if discontinuities in the NE appear because of microtubule induced forces or because holes that used to be occupied by NPCs become enlarged (Güttinger *et al*., 2009). Next, chromatin is fully removed from the NE and INM proteins become redistributed through the ER, where they will reside throughout mitosis. These events are controlled by the mitotic kinases of the CDK1, Polo and Aurora families (Güttinger *et al*., 2009).

After chromosome segregation, the process of reforming the NE involves firstly the enclosure of the daughter genomes by ER membrane, mediated by chromatin tethering proteins. In an *in vitro* system for NE reformation based on *Xenopus* egg extracts it was shown that ER tubules reach to the genomes, contacting them with the tubule tips and attach themselves likely through many membrane proteins that interact with the chromatin (Anderson and Hetzer, 2007). Following this, ER tubules can attach themselves laterally onto the chromatin, thus the genomes become covered by the ER

network. These bound ER tubules are then transformed into membrane sheets by lateral expansion of the tubules. This allows membrane to spread around the chromosomes and reform the NE as the final holes are sealed through annular fusion (Anderson and Hetzer, 2007). However, fluorescence microscopy and EM data suggests that in human cultured cells NE reformation starts by the covering of the genomes by large fenestrated ER membrane sheets (Lu *et al*., 2011; Otsuka *et al.*, 2018). A large set of INM proteins with chromatin tethering abilities is required for the successful reformation of nucleus (Anderson *et al.*, 2009). Individual knockdown of Lamin B receptor (LBR), BAF, the LEM domain proteins MAN1 and Lap2β, and the transmembrane NPC components Pom121 and Ndc1 all result in a delay of the establishment of nucleocytoplasmic compartmentalisation, as measured by the nuclear enrichment of a synthetic nucleoplasmic protein GFP-NLS (Anderson *et al*., 2009). Importantly, these proteins all perform redundant functions, as double knockdown increases this delay, but overexpression of, for example, BAF combined with knockdown of Lap2β can rescue this defect (Anderson and Hetzer, 2007). Holes in the nuclear membrane where the outer and inner side are continuous are proposed to be sealed through annular fusion by the endosomal sorting complex required for transport-III (ESCRT-III) complex together with the AAA-ATPase VPS4 (Olmos *et al.*, 2015; Vietri *et al.*, 2015). The latter will be discussed in more detail in the next section. The expansion of the nuclear membrane during interphase requires intact connections with the ER network (Anderson and Hetzer, 2007). This suggests that membrane flow into the nucleus is responsible for this expansion. Only after the covering of the genomes by ER membranes has been initiated do NPCs start to reassemble (Lu *et al*., 2011; Otsuka *et al.*, 2018). Quantitative analysis by EM suggests that during telophase the NPCs are assembled in small holes in the nuclear membrane rather than needing the formation of new openings (Otsuka *et al*., 2018). Maturation of NPCs within these preformed openings is relatively fast, allowing for the many NPCs that are needed for a functional nucleus to quickly assemble during telophase (Otsuka *et al*., 2018). This is therefore markedly different from interphase NPC assembly, where during the process of NPC maturation the INM is pushed inward to form a new channel and where the maturation also takes a considerably longer time (Otsuka *et al.*, 2016).

During the closed mitosis of yeasts, cells do not have to deal with rebuilding a NE from scratch, however that does not mean that the NE is not remodelled during closed mitosis. Chromosomes have to be removed from the NE during mitotic onset, tubulins and microtubule-associated proteins have to be imported to build the spindle and the nuclear membrane has to be remodelled to form the two daughter nuclei (Zhang and Oliferenko, 2013). An important factor here is that the nuclear membrane expands during closed mitosis (Lim *et al*., 2007). This was backed up by mathematical modelling confirming that this is a requirement for chromosome segregation to occur (Lim *et al.*, 2007). Despite that most nuclear surface growth occurs during interphase, during the relatively short period of mitosis the surface expands with an additional 26% (Lim *et al.*, 2007). Furthermore, the NE has to undergo several shape changes to end up with equally sized daughter nuclei. Another mathematical model of the fission yeast nucleus predicts that the force that the chromosomes put on the NE after anaphase A dictates these shape changes (Zhu *et al.*, 2016). These shape transformations are similar for both budding yeast and *S. pombe*. First, when the spindle starts elongating during anaphase B the nucleus takes on an oblong shape, dictated by the contact of the chromosomes with the membrane, then the nucleus starts to ingress at the equator, this ingression continues until the nuclear membrane contacts the spindle, thus forming the typical "dumbbell" shape (Lim *et al.*, 2007; Zhu *et al.*, 2016). At this moment the two daughter nuclei already gain independent identities as there is no diffusion possible between them anymore (Boettcher *et al.*, 2012; Lucena *et al.*, 2015). The membrane connecting the two daughter nuclei will eventually have to be broken down, and although the

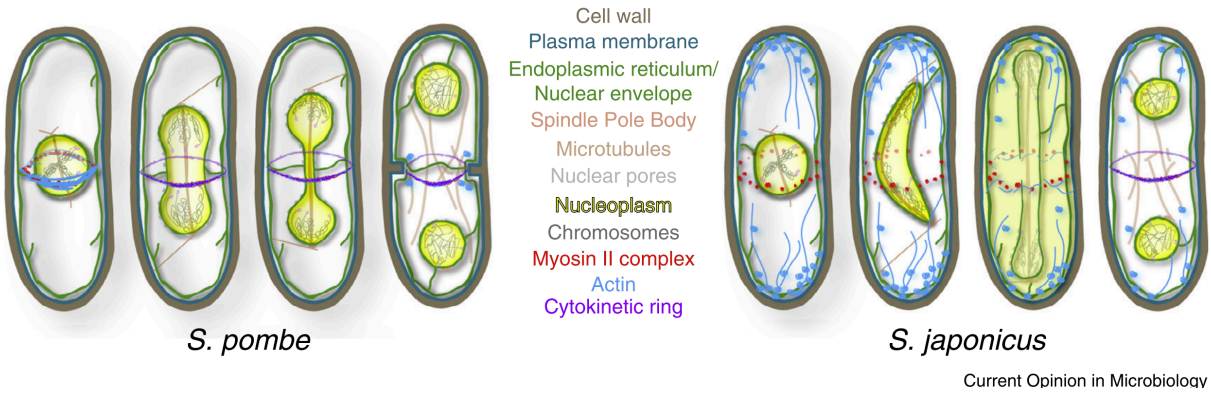

Figure 1-6. Remodelling of the nuclear envelope in fission yeasts.

Schematic overview of the different NE remodelling strategies of the fission yeasts *S. pombe* and *S. japonicus*. Taken from Gu and Oliferenko (2015).

mechanisms responsible for dissolving the spindle have been elucidated (Lucena *et al*., 2015), no factors have been described that dissolve the membrane connection. In organisms such as budding yeast and *S. pombe* the NPCs remain intact. However, in some species like the filamentous fungus *Aspergillus nidulans* some of the nucleoporins are evicted from the NPCs, which results in loss of nucleocytoplasmic compartmentalisation (De Souza *et al.*, 2004).

Even if the nuclear membrane stays largely intact during more 'closed' forms of mitosis some form of very local remodelling can occur when the SPB has to be inserted into the nuclear membrane (Zhang and Oliferenko, 2013). In budding yeast, the SPB resides in the nuclear membrane throughout the cell cycle. Duplication of the SPB starts outside of the membrane. The duplicated SPB then becomes inserted into a preformed hole adjacent to the old SPB. There is evidence that an adjacent NPC somehow aids this process, but the exact mechanism of how this is coordinated is not clear (Rüthnick and Schiebel, 2018). In *S. pombe* the SPB is located outside on the surface of the nuclear membrane throughout the entire interphase and also becomes duplicated there. Its insertion requires the combined signalling efforts of CDK1 and Polo kinases (Zhang and Oliferenko, 2013). When the SPBs become inserted the nuclear membranes first bends and then starts to accumulate electron dense material of undefined nature, followed by the appearance of discontinuities in the membrane (Ding *et al.*, 1997). However, the exact molecular mechanism that locally fenestrates the NE is not known. After mitosis, the SPB again leaves the NE (Ding *et al*., 1997). Interestingly, for the local fenestration and SPB insertion during both mitosis and meiosis intact contacts between chromosomes and the SPB are required (Fernández-Álvarez *et al.*, 2016). Thus, signalling from the centromeres or telomeres might induce fenestration. This provides another layer by which chromatin-NE contacts might aid the structure and remodelling of the nucleus.

These different ways of performing mitosis indeed point to the fact that despite many organisms using drastically different ways of remodelling the NE, many features of this process are very similar. These include mitotic regulation by kinases, breaking contacts between chromosomes and the NE and some form of NE fenestration or breakdown. This makes the study of how all of these possible options can arise through evolution and the mechanisms of these different types of mitosis very interesting. The

Oliferenko lab has been studying the related fission yeasts *Schizosaccharomyces pombe* and *Schizosaccharomyces japonicus* that exhibit markedly different dynamics of NE remodelling during mitosis despite having similar gene content (Rhind *et al.*, 2011; Yam *et al.*, 2011). Unlike *S. pombe*, *S. japonicus* does not undergo mitotic membrane expansion (Yam *et al*., 2011). The diamond shape that the nucleus takes on in the absence of membrane expansion during mitosis was predicted mathematically (Lim *et al*., 2007). Instead the NE ruptures during anaphase to allow spindle elongation and chromosome segregation (Aoki *et al.*, 2011; Yam *et al.*, 2011). Thus, these very different ways of doing mitosis might come from just slight differences in the usage of almost the same protein set (Zhang and Oliferenko, 2013). For example, mitotic regulation by CDK1 induces nuclear envelope expansion in *S. pombe* by inactivating the lipin Ned1, whereas in *S. japonicus* this regulation does not exist (Makarova *et al.*, 2016). Thus, comparative analysis of mitosis in related species might therefore be useful to identify how different mitotic programmes can arise through evolution (Russell *et al.*, 2017).

Further research into the cell biology of *S. japonicus* mitosis identified that the establishment of nucleocytoplasmic compartmentalization in *S. japonicus* begins while the spindle still connects the two daughter nuclei (Yam *et al.*, 2011). A structure is formed were nuclear membrane is tightly wrapped around the spindle (Aoki *et al.*, 2011; Yam *et al.*, 2011). This situation is similar to the situation in human cells, where microtubules perforate the reforming NE and the cutting of microtubules is coordinated with membrane resealing (Vietri *et al.*, 2015). Thus, nuclear compartmentalization is established prior to nuclear membrane resealing, which can be completed only after spindle breakdown. This mechanism appears to be separate from the establishment of compartmentalisation due to resealing of the nuclear membrane (Olmost *et al*., 2015; Vietri *et al*., 2015). It can be hypothesised that the spindle persists to keep the daughter nuclei at the cell poles when cytokinesis occurs, in order to prevent two nuclei ending up in one cell, or a nucleus being “cut” by the cytokinetic machinery. Tethering of chromatin to the NE also plays a vital role in reforming the NE in this organism. The LEM-domain protein Man1 coordinates the equal distribution of nuclear membrane with chromosome segregation (Yam *et al*., 2013), whereas the second LEM-domain protein Lem2 is involved in re-establishing nucleocytoplasmic compartmentalisation (Yam *et al*., 2011).

Although not the subject of this thesis, it is worth noting that remodelling of the NE is not just limited to mitosis. Although most cells of common research models contain spherical nuclei, this is not always the case even in our own body. Particularly neutrophils display interesting nuclear morphologies. The neutrophil nucleus contains three connected lobes, which contain extensive amounts of peripheral heterochromatin (Hoffmann *et al.*, 2007). This particular shape likely reflects its function of migrating through tissues. Indeed, mutations that affect the lobular shape of the neutrophil nucleus drastically reduce its migration speed (Hoffmann *et al.*, 2007). The giant unicellular ciliate *Stentor coeruleus* has a nucleus which is divided in multiple lobes in a linear array which are perforated by channels filled with microtubules. Interestingly, during mitosis this nucleus condenses to a single nucleus which divides, before reforming the "beads on a string" shaped nucleus (Paulin and Brooks, 1975; Raikhel *et al*., 1981).

In conclusion, even though the nucleus is the largest organelle in the eukaryotic cell in terms of a single structure and that its structure and function is built on the dynamic interplay between chromatin, the NE and many protein components and subdomains in the nucleus, cells are able to divide this complex structure every cell division. Different strategies have arisen throughout evolution to complete this feat. The study of different types of mitoses may give insight in the common principles behind this process.

1.7 The ESCRT-III/Vps4 complex functions in and outside the nucleus

The ESCRT-III/Vps4 machinery was implicated to play a role in the annular fusion of membranes that reform the NE during telophase (Olmos *et al.*, 2015; Vietri *et al.*, 2015). This section will discuss the wide variety of functions that this machinery performs in the cell, and how it is proposed to perform these functions, with a focus on the NE.

Apart from its function in NE resealing, the ESCRT-III/Vps4 machinery has been indicated to play a role NE resealing during migration induced NE rupture (Denais *et al.*, 2016; Raab *et al.*, 2016). In both instances it is thought to perform a membrane resealing event. This hypothesis is based on the described role of ESCRT-III/Vps4 in diverse cellular functions related to membrane remodelling. This machinery was first described to be the mediator of intralumenal vesicle formation during multivesicular body (MVB)

formation (Katzmann *et al*., 2001; Babst *et al.*, 2002; Babst *et al.*, 2002). Since then a long list of membrane remodelling functions has been ascribed to ESCRT-III/Vps4, such as the last step of cytokinesis (Carlton and Martin-Serrano, 2007; Morita *et al.*, 2007), viral budding from the plasma membrane (Garrus *et al.*, 2001; Martin-Serrano *et al*., 2001; Demirov *et al.*, 2002), plasma membrane and endosomal membrane repair (Jimenez *et al.*, 2014; Radulovic *et al.*, 2018; Skowyra *et al.*, 2018), the budding of viral particles from the nucleus through the nuclear membranes (Arii *et al.*, 2018) and most recently autophagosome closure (Zhen *et al.*, 2019; Zhou *et al.*, 2019).

The ESCRT-III complex consists of several core subunits (Fig. 1-7A). These core subunits all share the same structural features: They are small (221-241 amino acids) and consist of a positively charged N-terminal region comprised of a bundle of four α-helices which is thought to interact with membranes and also with other ESCRT-III subunits. This is connected to a C-terminal region comprised of two α-helices which can fold over the first four α-helices auto-inhibit the subunit or fold away to take on an active form that can assemble with other subunits (Adell and Teis, 2011). Budding yeast and fission yeast each have a single homologue of each ESCRT-III subunit. However, humans and mice have several copies of each one (Fig. 1-7A). This membrane remodelling complex is recruited to distinct cellular locations by organelle- and process-specific adaptors (Adell and Teis, 2011). For example, it is recruited to endosomal membranes by the sequential assembly of ESCRT-0, ESCRT-I and ESCRT-II complexes. The last component of ESCRT-II then recruits the ESCRT-III component Vps20, which is thought to nucleate the formation of the entire ESCRT-III complex consisting of the main component Vps32, which then recruits the capping subunits of Vps24 and Did4. These last components recruit the AAA-ATPase Vps4, which provides the energy to disassemble the complex and finalise the membrane remodelling (Adell and Teis, 2011). Thus, despite that all ESCRT-III subunits have the same overall structure, their functions within the complex as a whole are different.

ESCRT-III is recruited to the NE by the non-canonical ESCRT-III component CHMP7 (Vietri *et al*., 2015). CHMP7 bypasses the need for the earlier ESCRT complexes by mimicking the function of these complexes. It has a long extended N-terminus that bears structural resemblance to the ESCRT-II component VPS25 (Olmos *et al*., 2016).

Thus, CHMP7 might mimic the ESCRT-II-Vps20 interaction that nucleates the ESCRT-III complex.

ESCRT-III/Vps4 is thought to execute reverse membrane scission events (Fig. 1-7B; Wollert *et al.*, 2009; Wollert and Hurley, 2010; Henne *et al*., 2011). This is different from budding of endocytic vesicles into the cytoplasm from the plasma membrane. Reverse membrane scission is defined as budding away from the cytosol. The exact molecular mechanism underlying scission remains unclear. One prevailing hypothesis is that ESCRT-III forms a filament on the inside of membrane necks, rather than on the outside like for example Dynamin, and that the constriction of this filament with the help of the ATPase Vps4 can sever the membrane neck, resulting in an intralumenal vesicle (Fig. 1-7B; Schöneberg *et al.*, 2016).

The spiral hypothesis of ESCRT-III function is most based on the *in vitro* behaviour of this complex. CHMP2A together with CHMP3 form large tubular structures *in vitro*, composed of helical filaments of ESCRT-III, which can be disassembled by VPS4 (Lata *et al*., 2008). CHMP1B together with IST1 can form large helical tubes consisting of a single filament. When overexpressed in cultured cells CHMP1B induced inward tubulation of the plasma membrane by forming filaments on the outside of these membrane tubes (Lata *et al*., 2008). A large advancement in the understanding of these structures was the observation of the live formation of filament-based spirals of budding yeast Snf7 on supported lipid membranes using a combination of fluorescence microscopy and atomic force microscopy. When these filaments were formed on membrane vesicles they were able to deform and disrupt the membrane (Chiaruttini *et al.*, 2015). However, such structures have not been observed yet under endogenous conditions in live cells. Overexpression of human CHMP4 in cultured cells results in the accumulation of many helical structures at the plasma membrane as observed by deep-etch EM (Hanson *et al.*, 2008). The structures can interact with VPS4 and when both CHMP4 and the dominant negative VPS4^{EQ} are overexpressed they can deform the plasma membrane and induce the formation of membrane buds and tubules (Hanson *et al*., 2008). Similar spiral structures were also found to surround HIV budding sites on the plasma membrane upon VPS4 knockdown (Cashikar *et al.*, 2014). Similarly, overexpression of CHMP2B or knockdown of VPS4 result in the formation of large CHMP2B tubules that also deform the plasma membrane. When purified from cells and analysed by cryo-EM these tubules

were found to consists of long rigid helical tubes (Bodon *et al.*, 2011). Thus, the overexpressed CHMP2B behaves the same in cells as ESCRT-III subunits do *in vitro*, that is forming large helical tubules (Lata *et al.*, 2008). However, these filaments and tubes are outside of the context of normal regulation of this complex due to massive overexpression that is often used to study them. It is unclear what their physiological relevance is or how these large structures relate to ESCRT-III complexes that are formed during intralumenal vesicle budding where due to the small size of organelles involved, such giant assemblies could not exist. Using super resolution STORM imaging it was observed that at the cytokinetic midbody, the largest ESCRT-III assembly known, a large spiral structure is formed (Goliand *et al.*, 2018). However, it was not possible to determine the organisation of individual subunits or to detect any smaller filaments within this spiral. Using EM, regularly spaced filaments were detected at the cytokinetic bridge, however these completely disappeared in most cells after knockdown of VPS4, whereas with fluorescence microscopy some ESCRT-III was still visible after VPS4 knockdown (Mierzwa *et al*., 2017). This makes it unclear if these filaments indeed correspond to ESCRT-III assemblies.

Recent studies show that ESCRT-III/Vps4 is highly dynamic at endosomes (Adell *et al.*, 2017; Wenzel *et al.*, 2018), during cytokinesis (Mierzwa *et al.*, 2017) and during HIV budding (Bleck *et al.*, 2014; Johnson *et al*., 2018). Thus, the ESCRT-III complex likely functions not in the form of a single static filament. Indeed, based on *in vitro* data it appears that exchange of different subunits is required for the remodelling and function

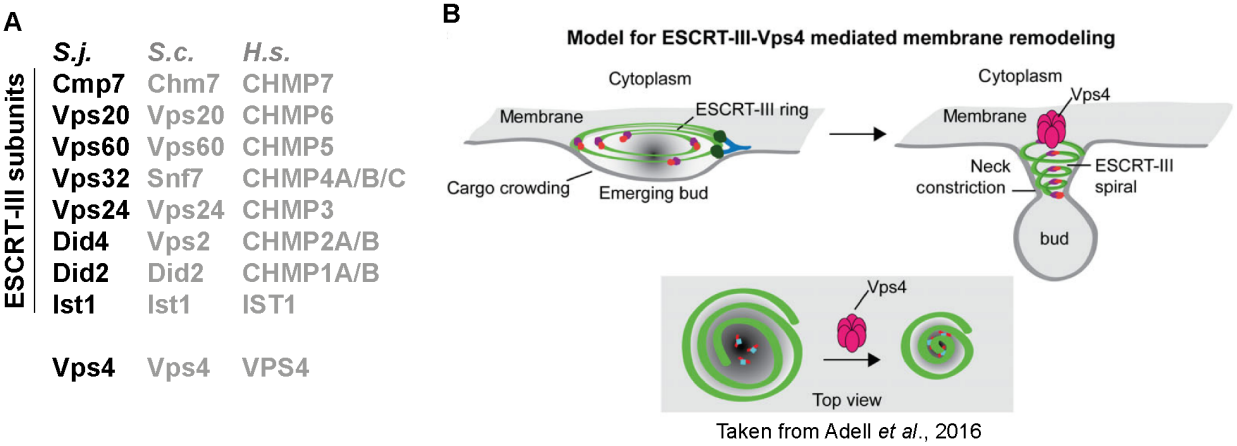

Taken from Adell *et al*., 2016

Figure 1-7. ESCRT-III/Vps4 subunits and function.

A) All orthologues of the ESCRT-III subunits of the following species: *S.j.*: *S. japonicus*, *S.c.*: *S. cerevisiae* and *H.s.*: *Homo sapiens*. **B)** The spiral model of ESCRT-III/Vps4 function in membrane remodelling. Taken from Adell *et al*. 2016.

of the complex (Mierzwa *et al*., 2017). It is thought that remodelling of the complex can somehow drive membrane deformation, but how exactly this is achieved is not clear. In fact, close analysis of the molecular events of HIV budding of the plasma membrane has revealed that ESCRT-III/Vps4 leaves the membrane neck before the scission event has occurred (Johnson *et al*., 2018). It is also not clear at what stage exactly the complex is recruited to the membrane, as during viral budding ESCRT-III only comes in after the membrane is already mostly deformed (Johnson *et al*., 2018), but ESCRT-III has also been observed to form on flat membranes (Hanson *et al.*, 2008). Based on live imaging data it has been hypothesised that multiple Vps4 hexamers might bring several small ESCRT-III filaments together, which may induce protein crowding and inward membrane buckling, followed by membrane constriction and fission (Adell *et al.*, 2017).

Although this model explains ESCRT-III/Vps4 function in the case of protein sorting during MVB formation or viral budding, it cannot be straightforwardly applied to the NE associated functions of this complex, as it is not clear what the cargo is in this case. For its other nuclear functions, the ESCRT-III/Vps4 complex interacts with LEM-domain proteins, specifically, the LEM domain proteins that also contain the MSC-domain. In human cells, LEM2 is thought serve as a recruiter of the ESCRT-III/Vps4 machinery to the resealing NE (Gu *et al.*, 2017). The budding yeast Heh1 and Heh2 proteins interact physically and genetically with ESCRT-III, recruiting it to the NE to mediate the proper assembly of nuclear pore complexes (NPCs; Webster *et al.*, 2014, 2016). Finally, in the fission yeast *Schizosaccharomyces pombe*, genetic interaction between *lem2*, *cmp7* and *vps4* maintain the integrity of the NE (Gu *et al.*, 2017). Thus, more insight into the network of proteins that interact with ESCRT-III/Vps4 at the NE might help us gain a better understanding of the molecular mechanisms by which this complex could perform its distinct functions in different organism.

1.8 Aims of this work

In this thesis I aimed to use a simple eukaryote that performs a “stripped bare” variant of open mitosis, *i.e.* not disassembling NPCs and having only a single defined site of rupture, to investigate the dynamics of nuclear membrane remodelling during mitosis. This would allow us to investigate the genetic, regulatory and molecular components that evolved to accommodate a semi-open mitosis. Specifically, we hoped to learn how

the regulation of NE-chromatin tethering aids NE dynamics. Also, we hoped to gain insights into the mechanisms of establishment of nucleocytoplasmic compartmentalisation, considering that data has suggested that *S. japonicus* can compartmentalise the nucleus in the presence of the spindle, but human cells rely on an ESCRT-III/Vps4 mediated mechanism to reseal the membrane. The direct focus of this PhD project was to gain insight into the regulatory and functional network around Lem2 in *S. japonicus*. We aimed to use the convenience and power of haploid genetics in this unusual yeast system and perform genetic, biochemical and cell biological experiments. By comparing what we learned to *S. pombe* we hoped to analyse how LEM-domain proteins evolved to support different types of nuclear division. We further hypothesised that abrogation of NE-chromatin interactions may allow Lem2 to perform its function at the timing of anaphase NE rupture. This function may be independent of chromatin tethering, as at this stage all chromosomes are already partitioned to the spindle poles.

The main aims of this thesis were the following:

1. How does Lem2 mediate the establishment of nucleocytoplasmic compartmentalisation during mitotic exit?
2. Is there a role for the ESCRT-III/Vps4 machinery in supporting this process?
3. How does NE-chromatin tethering aid NE dynamics during mitosis?

Chapter 2 – Materials and Methods

2.1 Method details

2.1 Culturing of yeast strains

Standard fission yeast methods and culturing media were used (Moreno, Klar and Nurse, 1991; Furuya and Niki, 2009; Aoki *et al.*, 2010; Petersen and Russell, 2016). *S. japonicus* and *S. pombe* cells were typically maintained on yeast extract with supplements (YES) rich medium 2% agar plates at 30°C. For experiments, cells were grown until exponential growth phase (OD_{595} ~0.2-0.4) in liquid YES in baffled flasks in a shaker incubator at 30°C, at 200 RPM. For ChIP experiments cells were grown in non-baffled flasks due to the need for larger cultures. *S. japonicus* cells were mated on SPA and dissected using a micro-dissector (Singer Instruments).

2.1.2 Generation of fission yeast mutants

All tagged proteins were tagged at their endogenous loci, under control of the endogenous promoters, except when noted. Partial open reading frames (ORFs) and 3'UTR regions directly downstream of genes of interest were cloned into pJK210-based integration vectors containing either mCherry (pSO730 for *S. japonicus*) or eGFP (pSO729 for *S. japonicus*; pSO32 for *S. pombe*) and the full-length *S. japonicus* or *S. pombe ura4*$^+$ gene. The *S. japonicus* Lem2-GFP construct was cloned into a pJK210-based plasmid carrying the *kanMX* resistance cassette (pSO820). Gene deletions were obtained using either a plasmid-based or a PCR-based method. Targeting constructs were made by cloning the 5'UTR and 3'UTR regions flanking the gene of interest into pJK210-based plasmids containing *kanR* (pSO820 for *S. japonicus*) or *natR* (pSO893 for *S. japonicus*) resistance cassettes, or the respective *ura4*$^+$ genes (pSO550 for *S. japonicus*; pSO13 for *S. pombe*). PCR-based knockouts were obtained by amplifying the *hygR* resistance cassette flanked by 80 base pairs flanking the target gene. Plasmids were linearized before transformation. Transformation of *S. japonicus* was done by electroporation based on the protocol of Aoki *et al.*, (2010). *S. pombe* cells were transformed using lithium acetate and heat shock (Moreno, Klar and Nurse, 1991). Selection for both species was performed on YES agar plates containing G418 (Sigma),

nourseothricin (HKI Jena), hygromycin B (Roche) or minimal media (EMM) agar plates lacking uracil.

2.1.3 Generation of Vps24, Vps4 and Cmp7 functional tagged constructs

The following constructs were designed with restriction sites flanking the 3'overlap region, endogenous promoter-ORF, tag and terminator: *Xho*I-3'UTR-*Srf*I-promoter-Vps4-*Asc*I-3xHA-eGFP-PacI-terminator-*Sac*II, *Xho*I-3'UTR-*Eco*RV-promoter-Vps24-*Asc*I-LAP-eGFP-*Pac*I-terminator-*Xba*I, *Eco*RV-3'UTR-*Srf*I-promoter-Cmp7-*Asc*I-LAP-eGFP-*Pac*I-terminator-*Xba*I. Constructs were synthesised by Eurofins. The eGFP of the Cmp7 construct was exchanged with mNeonGreen using Gibson assembly (NEB). Each construct was cloned into a pJK210-based integration vector for transformation into. Plasmids were linearized with *Srf*I or *Eco*RV respectively and transformed into *S. japonicus*, replacing the endogenous allele. The $vps4^{EQ}$ and $vps4^{ts}$ alleles were constructed by site-directed mutagenesis PCR based on the corresponding budding yeast mutations (Babst *et al.*, 1997).

2.1.4 Canavanine sensitivity assay for functionality of ESCRT-III/Vps4 constructs

ESCRT mutants show inhibited growth in the presence of the arginine analogue canavanine (Lin *et al.*, 2008). To test if our fluorescently tagged Vps24 and Vps4 constructs were functional we assessed growth of these tagged strains on canavanine. We titrated canavanine concentration in EMM plates with full supplements from 0-10 µg ml^{-1} and determined the optimal working concentration for *S. japonicus* to be around the 4-4.5 µg ml^{-1} level (data not shown). Note that this is significantly higher than the working concentration for *S. cerevisiae* (Adell *et al*., 2017).

2.1.5 FM4-64 staining

Cells were grown to early exponential growth phase (OD_{595} 0.2). 10 ml of cells were spun down at 3000 RPM for 1 min and resuspended in 100 µl YES media. 1 µl of FM4-64 (Thermo Fisher, stock 1 mg/ml in DMSO) was added to the cells and incubated for 5 min at 30°C. Subsequently, the cells were washed twice with YES and resuspended in 10 ml

of YES. Cells were grown for 1 hr at 30°C in a shaking incubator before imaging to allow the dye to be taken up and transported to the vacuoles.

2.1.6 Vps4 inactivation using a temperature-sensitive allele

Cells were grown in liquid culture overnight at 25°C in a shaking incubator to early exponential growth phase (OD_{595} 0.2). The culture was shifted to 36°C and samples were taken at time point 0 (before switch) and then after 1 hour, 2 hours and 4 hours. Samples were transformed to pre-heated tubes. Slides for imaging were prepared on a heat block at 36°C. Imaging was performed in a pre-heated chamber at 36°C.

2.1.7 Colony-forming unit (CFU) assay

Cells were grown overnight at 30°C in a shaking incubator. The next day, cells with an OD_{595} of 0.2-0.3 were diluted to 0.1. Next, three serial dilutions of 10x, 100x and 1000x were prepared. Of these dilutions, 50 µl of cells were plated in triplicate on YES plates and spread using glass beads. Plates were incubated for two days at 30°C. Plates were scanned using an Epson Perfection V700 Photo scanner and Epson Scan software. CFU count and size were analysed using ImageJ.

2.1.8 Microscopy

For imaging, cells grown overnight in liquid YES media to early exponential growth phase (OD595 0.2-0.4) were placed on a thin YES 2% agarose strip and immobilised by a cover slip sealed with wax. This slide was first rested for 30 min at the 30°C. During imaging cells were kept at 30°C in an environmental control chamber. Imaging was performed on a Nikon Eclipse Ti-E inverted system equipped with CSU-X1 spinning disk confocal unit and 600 series SS 488nm, SS 561nm lasers. Images were obtained with an Andor iXon Ultra U3-888-BV monochrome EMCCD camera using a Nikon CFI Plan Apo Lambda 100x/1.45NA objective lens. Pixel length was 0.0695 µM. All images presented in this report are Z-projections unless noted otherwise. For microscopy images contrast and brightness were adjusted for each individual image for optimal visibility unless noted otherwise. For time-lapse imaging, laser power and exposure time were adjusted to minimise photobleaching.

2.1.9 Protein expression and purification

Expression of proteins was performed as previously described (Babst *et al.*, 1998; Teis *et al*., 2008). Recombinant proteins were expressed in C41 (DE3) pLysS *E. coli* (Lucigen) and induced at 37°C for 4 hours in 1mM IPTG (Thermo R0392). GST-tagged proteins were purified with Glutathione Sepharose 4B (GE Healthcare, GE17-0756-01), the washed and either eluted with glutathione or cleaved with PreScission protease (GE Healthcare, 27084301) overnight at 4°C. Recombinant proteins were dialyzed in a Slide-a-lyzer (VWR, 514-0172) overnight in ATPase buffer (100 mM potassium acetate, 5 mM magnesium acetate, 20 mM Hepes 7.4) and were additionally purified via a Superdex 2000 column (GE Healthcare). Proteins were flash frozen in liquid nitrogen and stored at -80°C until further usage.

2.1.10 Plasmids used for in vitro experiments

Name	Insert	Backbone
pSS76	GST-Lem2$^{564-673}$	pGex 6P1
pSS98	GST-Did4	pGex 6P1
pSS113	GST-Cmp7$^{242-436}$	pGex 6P1
pSS114	GST-Cmp7$^{242-436}$-3xFLAG	pGex-6P1
pSS115	Vps4-3xHA	pGex 6P1
pSS116	Vps4^{E233Q}-3xHA	pGex 6P1
pSS117	Vps32-3xMyc	pGex 6P1

2.1.11 GST pulldown assays

GST pulldown assays were performed as previously described (Shestakova *et al.*, 2010; Adell *et al.*, 2014). Pierce magnetic glutathione beads (Thermo, 78602) were incubated in 0.1% BSA in ATPase buffer overnight. 5 µg of GST tagged proteins were bound to beads for 2 hours at 4°C, washed and optionally incubated with 500 ng of Cmp7-3xFLAG and/or Vps32-3xMyc for 1 hour at 4°C. 500ng of Vps4^{E233Q} -3xHA or Vps4-3xHA was added in the presence or absence of 1 mM ATP for 10 minutes at room temperature. Proteins were washed five times in ATPase buffer with 600 mM NaCl. Then, proteins were eluted from beads using sample buffer (2% SDS, 100 mM Tris 6.8, 10% glycerol, 5% beta-mercaptoethanol, 0.01% bromophenol blue) at 96°C for 10 minutes. Samples were

separated on a 12.5% SDS Page gel. Proteins were either stained by Brilliant Blue Coomassie or subjected to Western blotting.

2.1.12 Antibodies and Reagents used for pull-down assays

Anti-FLAG (3165) and anti-Myc (4439) antibodies were purchased from Sigma. Anti-HA antibody was purchased from Cell Signalling (C29F4). ATP was purchased from Sigma (A-2383).

2.1.13 Chromatin-immunoprecipitation and qPCR

Chromatin-immunoprecipitation (ChIP) was performed according to the protocol of (Barrales *et al.*, 2016).

Buffers:

ChIP lysis buffer	50 mM HEPES/KOH pH 7.5 140 mM NaCl (500 mM in high salt lysis buffer) 1 mM EDTA 1% Triton X-100 0.1% Na-deoxycholate
Wash buffer	10 mM Tris-HCl pH 8.0 250 mM LiCl 1 mM EDTA 0.5% NP-40 0.5% Na-deoxycholate
Elution buffer	50 mM Tris/HCl, pH 8 10 mM EDTA 0.8% Na-deoxycholate
TE	10 mM Tris/HCl pH 7.5 1 mM EDTA

Reagents

Name	Brand	catalogue number
Formaldehyde (FA)	Fisher Scientific	BP531-25
AEBSF	Melford	A20010-50
Leupeptin	Generon	103476-89-7
Protease inhibitor mix	Roche	25178600
Zirconium beads	MP biomedicals	6960-500

α-GFP antibody	Sigma-Aldrich	11814460001
α-H3K9me2 antibody	Abcam	ab1220-100ug
Protein-G dynabeads	Invitrogen	10003D
Proteinase K	New England Biolabs	P8107S
ChIP DNA cleanup kit	Zymo Research	#D5201
SyGreen Blue Mix Hi-ROX	PCR Biosystems	PB20.16-20
Powerup SYBR Green mastermix	Applied Biosystems	A25742
MicroAmp Plate Optical 384-Well	Applied Biosystems	4483315
MicroAmp Optical Adhesive Film	Applied Biosystems	4360954

Cell culturing and cross linking:

Cells were grown in YES rich media overnight at 30°C until an OD_{595} of 0.3-0.4 was reached. For Lem2-GFP 60 ODs of cells were and for H3K9me2 ChIP 15 ODs of cells were used. Cells were crosslinked with fresh 37% FA for 10 minutes at room temperature: 2.7 ml of FA per 100 ml cells for Lem2-GFP ChIP and 1.35 ml of FA per 50 ml cells for H3K9me2 ChIP. FA was quenched by adding 2.5M glycine: 5 ml for Lem2-GFP ChIP and 2.5 ml for H3K9me2 ChIP. Cells were spun down at 3000 RPM for 1 min and washed twice with 25 ml of ice-cold phosphate-buffered saline (PBS). Cells were resuspended in 800 µl ice cold PBS and transferred to a 1.5 ml tube and spun down at 3000 RPM for 1 min. Supernatant was removed and cells were snap-frozen in liquid nitrogen. From here, cell pellets were either stored at -80°C or used for IP.

Lysis, sonication and IP:

Cell pellets were thawed on ice. From here on until reverse crosslinking all steps are at 4°C. Note that for Lem2-GFP two pellets of 30 ODs were used throughout the protocol and combined during DNA purification as the Lem2 extraction protocol was optimised for these amounts of cells. 10 ml of ChIP lysis buffer was chilled and prepared with final concentrations of 1 mM AEBSF, 100 µg/ml leupeptin and Roche complete protease inhibitor cocktail. 500 ml of lysis buffer with inhibitors was added to each cell pellet. Pellets were dissolved and added to screw-cap tubes with zirconium beads. Cells were disrupted in a MP biomedicals cell disruptor for 2 cycles of 15 seconds with 150 seconds on ice in between. Using a hot needle, a hole was poked in each tube and tubes were spun down for 3 min at 1500 RPM, while resting on a pipette tip to isolate the lysate. The lysate was sonicated in a digenotide bioruptor plus (55 cycles of 30 seconds on/off for Lem2-GFP and 45 cycles of 30 seconds on/off for H3K9me2). Cells were spun down

at 16.000 RCF for 10 min. The supernatant was transferred to a new pre-chilled tube. Volumes were adjusted to 540 µl with lysis buffer plus inhibitors.

For Lem2-GFP ChIP 5 µgr of α-GFP antibodies was added to each tube. For H3K9me2 ChIP 2 µl of α-H3K9me2 antibody was added to each sample. Samples were incubated overnight on a rotator at 10 RPM. Following day, 60 µl of each sample was taken to be used as input (Lem2-GFP samples were combined first and divided in two again after). To each input sample 140 µl of TE-1% SDS was added. Next, 15 µl of protein-G dynabeads were added and incubated for another 4 hours.

IP wash, reverse crosslinking, protease K treatment and DNA purification:

Beads were washed 2x with 500 µl lysis buffer, 2x with 500 µl high salt lysis buffer, 2x with 500 µl wash buffer and transferred to a new tube in 150 µl TE. Beads were washed a final time and resuspended in 200 µl elution buffer. Washed IP samples and input samples were eluted for 10 min at 95°C in a shaking heat block at 1400 RPM. Then samples were spun down to remove condensation from the lid. Removal of crosslinking was performed for 3 hours at 65°C. Samples were incubated for 1 hour with 4 mg/ml Proteinase K at 55°C, samples were spun down to remove condensation from the lid, resuspended and incubated for another hour. Samples were spun down to collect the beads and the supernatant was transferred to a new tube. DNA purification was performed using the Zymo Research, ChIP DNA Clean & Concentrator™ kit. DNA was collected in 17 µl water.

qPCR

For qPCR each IP and input sample were diluted 100x. qPCR on Lem2-GFP samples was performed using SyGreen Blue Mix Hi-ROX mastermix and qPRC on H3K9me2 were performed using Powerup SYBR Green mastermix according to manufacturer's protocol. qPCR was performed in 384 well plates with two technical repeats per primer pair per strain. For each experiment centromeric loci and telomeric loci were tested in individual plates. Plates were run on an Applied Bioscience Quantstudio 6 Flex real-time PCR system and data was extracted and analysed with associated software.

2.1.14 qPCR primer list

Tel 1 R

name	seq	name	seq
Sj Tel1 1 fwd	CTACCTTTTTGACCGCTGGA	Sj Tel1 1 rev	CCGAGATAGCCCACGTAGAA
Sj Tel1 2 fwd	AGCCTGACAGTGATCCCAAG	Sj Tel1 2 rev	GATGGAAGCGAAACTCTGGA
Sj Tel1 3 fwd	GACGGATGCAGCTCCAGTAT	Sj Tel1 3 rev	CTTGGCAAGTTGCTGATGAA
Sj Tel1 4 fwd	AGGTGTTTGTCAGCGTTGTG	Sj Tel1 4 rev	CCGATGTATTCGCAGAGCTT
Sj Tel1 5 fwd	ATCGGAAGTGCCTTGGAGTA	Sj Tel1 5 rev	GCTTTGCCCATCATGATTTC
Sj Tel1 6 fwd	CGTACGTTCGGTTGTACACG	Sj Tel1 6 rev	AAGAGCGTACCCCTCATCAA
Sj Tel1 7 fwd	ACGCTTAAACTCGGCTACCA	Sj Tel1 7 rev	CCTGCCTGCTCGTCTAATTC
Sj Tel1 8 fwd	TTGTGCTACGACCAACAAGC	Sj Tel1 8 rev	AGGATCGCGTGACCATATCT
Sj Tel1 9 fwd	TATCGGTGTGCTGTGATGGT	Sj Tel1 9 rev	CGGAAGAAGCAGAGTGGAAG
Sj Tel1 10 fwd	CCCGCTTCCTAGTTTTCTCC	Sj Tel1 10 rev	GTTCATAGGCGTCGATGGTT
Sj Tel1 11 fwd n	GACGGGTCTTTGGAAATTGA	Sj Tel1 11 rev n	GTGTCCCAGCAATCTTGGTC

Cen 1 L

name	seq	name	seq
Sj Cen1 1 fwd	CTTGGGCTCGTATCCGTAAG	Sj Cen1 1 rev	CATCTTTCCACCCACAAACC
Sj Cen1 2 fwd	CAGTAAAGTCCCCGACTGGA	Sj Cen1 2 rev	CCGCTTCCTTGTAGTTCGTC
Sj Cen1 3 fwd	TTGGTGTGTGAGCATCAGGT	Sj Cen1 3 rev	CGCAGTCTCCCGAACATACT
Sj Cen1 4 fwd	GCCAAAGGTTGCAGCATAAC	Sj Cen1 4 rev	CTTGTGCCGTACAAAAGCAA
Sj Cen1 5 fwd	ATTGGATCACCGAGTGGAAG	Sj Cen1 5 rev	AATGCGGGTACTTTCCCTTT
Sj Cen1 7 fwd	TTGACAAGCATTCCAGGTTG	Sj Cen1 7 rev	CGCTAGCAAGGGCTACAATC
Sj Cen1 8 fwd	CACCGACAAGGACATGCTAA	Sj Cen1 8 rev	CGAAGTTCGAACCAGGAGAG

Cen 1 R

name	seq	name	seq
Sj Cen1 10 fwd	ATACGCGAAACACCACCTTC	Sj Cen1 10 rev	TCCAATCCTCGGTCAACTTC
Sj Cen1 12 fwd	GCAATCATCCATGCAGTCAC	Sj Cen1 12 rev	CTGCCACTGGGTTGTCTCTT
Sj Cen1 13 fwd	GCAACACTGGGAGAGATTCC	Sj Cen1 13 rev	AAGGAGCTGCACTACGAAGC
Sj Cen1 14 fwd	ACGTCGCTCAAGGTTTCAAT	Sj Cen1 14 rev	CGACATTGGCTAATCCCTGT
Sj Cen1 15 fwd	TAAATCGGGTGAACGGAAAG	Sj Cen1 15 rev	GAACTGCCCGATGGAGAATA
Sj Cen1 16 fwd	TTCGGCTTCTCTCGGTTAGA	Sj Cen1 17 rev	CTTCAAACGGTGTCAGAGCA

act1

name	seq	name	seq
Sj act1 1 fwd	AGGACCTGTACGGCAACATC	Sj act1 1 rev	TTTGTTGGAAGGTGGAGAGG
Sj act1 2 fwd	GAGCACGGTATTGTCACGAA	Sj act1 2 rev	GCCTGGATGGAGACGTAGAA

2.2.15 Yeast strain list

***S. japonicus* strains**		
All strains derived from:		
SOJ11	*ura4sj-D3 ade6sj-domE*	h-
SOJ88	*ura4sj-D3 ade6sj-domE*	h+
***S. japonicus* strains constructed in this work unless noted otherwise**		
SOJ88	*ura4sj-D3 ade6sj-domE* (Yam *et al*., 2011)	
SOJ359	*ura4::GFP-atb2 nhp6-mCherry:ura4* (Yam *et al*., 2011)	h+
SOJ2001	*ura4::GFP-GST-NLS-GFP pcp1-mCherry:ura4:kanR*	h+
SOJ2003	*lem2Δ:kanR ura4::GFP-GST-NLS-GFP pcp1-mCherry:ura4:kanR*	
SOJ2251	*did4Δ:kanR*	h-
SOJ2370	*cmp7Δ:kanR*	h-
SOJ2615	*lem2-GFP:kanR*	h+
SOJ2664	*did4Δ:kanR ura4::GFP-GST-NLS-GFP pcp1-mCherry:ura4:kanR*	h+
SOJ2668	*cmp7Δ:kanR ura4::GFP-GST-NLS-GFP pcp1-mCherry:ura4:kanR*	h+
SOJ2748	*cmp7Δ:kanR lem2-GFP:kanR pcp1-mCherry:ura4:kanR*	
SOJ2775	*vps24Δ:kanR*	h+
SOJ2778	*vps20Δ:kanR*	h+
SOJ2782	*vps4Δ:kanR*	h+
SOJ2788	*vps4Δ:kanR ura4::GFP-GST-NLS-GFP pcp1-mCherry:ura4:kanR*	h-
SOJ2791	*vps24Δ:kanR ura4::GFP-GST-NLS-GFP pcp1-mCherry:ura4:kanR*	h-
SOJ2824	*vps4Δ:kanR lem2-GFP:kanR*	h-
SOJ2841	*vps24Δ:kanR lem2-GFP:kanR pcp1-mCherry:ura4:kanR*	
SOJ2842	*vps4Δ:kanR lem2-GFP:kanR pcp1-mCherry:ura4:kanR*	
SOJ2843	*lem2Δ:natR*	h+
SOJ2845	*lem2-GFP:kanR taz1-mCherry:ura4*	h-
SOJ2863	*lem2-GFP:kanR pcp1-mCherry:ura4:kanR*	
SOJ2867	*vps4Δ:kanR lem2-GFP:kanR taz1-mCherry:ura4*	
SOJ2883	*vps25Δ:kanR*	h+
SOJ2885	*vps27Δ:kanR*	h+
SOJ2890	*vps28Δ:kanR*	h+
SOJ2895	*vps27Δ:kanR lem2-GFP:kanR*	
SOJ2896	*vps25Δ:kanR lem2-GFP:kanR*	
SOJ2927	*vps28Δ:kanR lem2-GFP:kanR*	
SOJ2976	*lem2-GFP:kanR swi6-mCherry:ura4*	
SOJ2977	*vps4Δ:kanR lem2-GFP:kanR swi6-mCherry:ura4*	
SOJ2981	*vps4-3xHA-GFP:ura4*	h+
SOJ2982	*lem2Δ:natR vps4-3xHA-GFP:ura4*	h+
SOJ2983	*cmp7Δ:kanR vps4-3xHA-GFP:ura4*	h+
SOJ2984	*vps24Δ:kanR vps4-3xHA-GFP:ura4*	h+
SOJ3000	*nur1-mCherry:ura4 lem2Δ:natR*	
SOJ3018	*vps24-LAP-GFP:kanR*	h+
SOJ3034	*vps25Δ:kanR vps4-3xHA-GFP:ura4*	h+
SOJ3057	*vps4-3xHA-GFP:ura4 nup189-mCherry:ura4*	h-

SOJ3062	*vps25Δ:kanR vps24-LAP-GFP:kanR nup189-mCherry:ura4*	h+
SOJ3065	*lem2-GFP:kanR nur1-mCherry:ura4*	h-
SOJ3079	*vps27Δ:kanR vps24-LAP-GFP:ura4*	
SOJ3080	*vps27Δ:kanR vps4-3xHA-GFP:ura4*	
SOJ3081	*vps28Δ:kanR vps4-3xHA-GFP:ura4*	
SOJ3097	*did4Δ:kanR vps4-3xHA-GFP:ura4*	
SOJ3099	*did4Δ:kanR vps24-LAP-GFP:ura4*	
SOJ3132	*cmp7Δ:kanR vps24-LAP-GFP:ura4*	h+
SOJ3233	*vps25Δ:kanR vps4-3xHA-GFP:ura4 nup189-mCherry:ura4*	h-
SOJ3237	*lem2Δ:natR vps25Δ:kanR vps4-3xHA-GFP:ura4 lem2-mCherry:ura4*	h+
SOJ3244	*lem2Δ:natR vps25Δ:kanR vps24-LAP-GFP:ura4 nup189-mCherry:ura4*	
SOJ3263	*vps4-3xHA-GFP:ura4 lem2-mCherry:ura4*	
SOJ3267	*lem2Δ:natR vps24-LAP-GFP:ura4*	
SOJ3268	*vps25Δ:kanR vps24-LAP-GFP:ura4*	
SOJ3284	*lem2-GFP:kanR ura4::adh1pro-GST-NLS-mCherry*	
SOJ3291	*vps4(E233Q)-3xHA-GFP:kanR lem2-mCherry*	h+
SOJ3293	*vps28Δ:kanR vps24-LAP-GFP:ura4*	
SOJ3294	*vps4Δ:kanR vps24-LAP-GFP:ura4*	
SOJ3305	*did4Δ:kanR vps4-3xHA-GFP:ura4 lem2-mCherry*	
SOJ3322	*vps25Δ:kanR ura4::GFP-GST-NLS-GFP pcp1-mCherry:ura4:kanR*	
SOJ3341	*vps24Δ:kanR vps4-3xHA-GFP:ura4 lem2-mCherry*	
SOJ3355	*lem2Δ:natR vps4Δ:natR ura4::GFP-GST-NLS-GFP pcp1-mCherry:ura4:kanR*	
SOJ3444	*vps24Δ:kanR lem2-GFP:kanR swi6-mCherry:ura4*	h-
SOJ3477	*vps4Δ:natR ura4::GFP-atb2 nhp6-mCherry:ura4*	
SOJ3478	*vps24Δ:natR ura4::GFP-atb2 nhp6-mCherry:ura4*	
SOJ3481	*lem2Δ:natR ura4::GFP-atb2 nhp6-mCherry:ura4*	
SOJ3500	*cmp7Δ:kanR lem2-GFP:kanR swi6-mCherry:ura4*	
SOJ3514	*cmp7Δ:kanR vps25Δ:kanR vps4-3xHA-GFP:ura4 lem2-mCherry:ura4*	h-
SOJ3578	*taz1-GFP:ura4 nup189-mCherry:ura4 pcp1-mCherry:ura4:kanR*	
SOJ3592	*vps24Δ:hygR did4Δ:kanR ura4::GFP-GST-NLS-GFP pcp1-mCherry:ura4:kanR*	h+
SOJ3596	*nur1Δ:hygR*	h-
SOJ3623	*mad2-GFP:ura4 pcp1-mChery:ura4:kanR*	h-
SOJ3638	*mis6-GFP:ura4 nup189-mCherry:ura4 pcp1-mCherry:ura4:kanR*	h+
SOJ3640	*vps4Δ:kanR taz1-GFP:ura4 nup189-mCherry:ura4 pcp1-mCherry:ura4:kanR*	
SOJ3650	*vps4Δ:kanR mad2-GFP:ura4 pcp1-mChery:ura4:kanR*	
SOJ3697	*vps32Δ:hygR ura4::GFP-GST-NLS-GFP pcp1-mCherry:ura4:kanR*	
SOJ3700	*vps32Δ:kanR lem2-GFP:kanR pcp1-mCherry:ura4:kanR*	
SOJ3701	*vps32Δ:kanR lem2-GFP:kanR swi6-mCherry:ura4*	
SOJ3728	*vps4Δ:kanR mis6-GFP:ura4 nup189-mCherry:ura4 pcp1-mCherry:ura4:kanR*	
SOJ3748	*cmp7-LAP-mNeonGreen:kanR lem2-mCherry:ura4*	h+
SOJ3756	*nur1Δ:hygR vps4Δ:kanR lem2-GFP:kanR swi6-mCherry:ura4*	

SOJ3762	*vps32Δ:hygR vps4-3xHA-GFP:ura4 nup189-mCherry:ura4*	
SOJ3764	*nur1Δ:hygR lem2-GFP:kanR swi6-mCherry:ura4*	
SOJ3765	*nur1Δ:hygR vps4Δ:kanR*	h+
SOJ3770	*nur1Δ:hygR ura4::GFP-GST-NLS-GFP pcp1-mCherry:ura4:kanR*	h+
SOJ3774	*nur1Δ:hygR vps32Δ:hygR ura4::GFP-GST-NLS-GFP pcp1-mCherry:ura4:kanR*	
SOJ3799	*vps4Δ:kanR cmp7-LAP-mNeonGreen:kanR lem2-mCherry:ura4*	
SOJ3800	*vps4Δ:kanR nur1-mCherry:ura4 lem2-GFP:kanR*	
SOJ3803	*nur1Δ:hygR vps4Δ:kanR ura4::GFP-GST-NLS-GFP pcp1-mCherry:ura4:kanR*	
SOJ3812	*nur1Δ:hygR vps25Δ:kanR vps4-3xHA-GFP:ura4 nup189-mCherry*	
SOJ3940	*vps25Δ:kanR vps4-3xHA-GFP:ura4 lem2-mCherry:ura4*	h-
SOJ3989	*lem2-mCherry-TEV-GBP:ura4 nup189-GFP:ura4 ura4::atb2pro:NLS-GST-mCherry*	
SOJ3990	*lem2-mCherry-TEV-GBP:ura4 nup189-GFP:ura4 ura4::atb2pro:NLS-GST-mCherry*	
SOJ3992	*nup189-GFP:ura4 lem2-mCherry-TEV-GBP:ura4*	
SOJ4001	*lem2-mCherry-TEV-GBP:ura4 nup189-GFP:ura4 ura4::atb2pro:NLS-GST-mCherry*	
SOJ4092	*nur1Δ:hygR vps32Δ:hygR*	h+
SOJ4097	*nur1Δ:hygR mis6-GFP nup189-mCherry:ura4 pcp1-mCherry:ura4:kanR*	
SOJ4098	*nur1Δ:hygR vps4Δ:kanR mis6-GFP nup189-mCherry:ura4 pcp1-mCherry:ura4:kanR*	
SOJ4117	*lem2-Δ136(lumen)-GFP:kanR nur1-mCherry*	
SOJ4119	*cmp7Δ:hygR vps4-3xHA-GFP:ura4 lem2-mCherry*	
SOJ4171	*vps4ts-I307T-L327S-3xHA-GFP:ura4 lem2-mCherry:ura4 nup189-GFP:ura4 sad1-mNeonGreen:kanR*	
SOJ4172	*vps4ts-I307T-L327S-3xHA-GFP:ura4 lem2-mCherry:ura4 nup189-GFP:ura4 sad1-mNeonGreen:kanR*	
SOJ4173	*vps4ts-I307T-L327S-3xHA-GFP:ura4 lem2-mCherry:ura4 nup189-GFP:ura4 sad1-mNeonGreen:kanR*	
SOJ4178	*nur1Δ:hygR taz1-GFP:ura4 nup189-mCherry:ura4 pcp1-mCherry:ura4:kanR*	
SOJ4227	*vps4Δ:kanR lem2-GFP:kanR nup184-mCherry:ura4*	
SOJ4252	*vps4Δ:kanR lem2-GFP:kanR nup85-mCherry:ura4*	
SOJ4254	*nur1Δ:hygR lem2-GFP:kanR*	
SOJ4255	*vps4Δ:kanR nur1Δ:hygR lem2-GFP:kanR*	
SOJ4288	*vps4Δ:kanR nur1Δ:hygR taz1-GFP:ura4 nup189-mCherry:ura4 pcp1-mCherry:ura4:kanR*	
SOJ4332	*vps4Δ:kanR lem2-mCherry nup189-GFP:ura4 sad1-mneonGreen:kanR*	
SOJ4340	*vps24Δ:kanR lem2-mCherry nup189-GFP:ura4 sad1-mneonGreen:kanR*	
SOJ4359	*did4Δ:kanR lem2-mCherry nup189-GFP:ura4 sad1-mneonGreen:kanR*	
SOJ4387	*cmp7Δ:kanR lem2-mCherry nup189-GFP:ura4 sad1-mneonGreen:kanR*	
SOJ4447	*vps32Δ:kanR lem2-mCherry nup189-GFP:ura4 sad1-mneonGreen:kanR*	

***S. pombe* strains**

All strains derived from:		
SO1082	*ade6-M210 ura4-D18 leu1-32*	h-
SO1083	*ade6-M210 ura4-D18 leu1-32*	h+
SO2865	*ade6-210 ura4-D18 leu1-32*	h+
SO2866	*ade6-216 ura4-D18 leu1-32*	h-
***S. pombe* strains constructed in this work**		
SO8284	*lem2-GFP:ura4 pcp1-mCherry:ura4*	h-
SO8355	*vps4Δ:ura4 lem2-GFP:ura4 pcp1-mCherry:ura4*	

2.2 Quantification and data analysis

2.2.1 Analysis software

All imaging data was analysed and imaging data figures were prepared in ImageJ (Schindelin *et al.*, 2012, 2017). Data was analysed using Microsoft Excel. Statistics was performed in Graphpad Prism or in R (R Core Team, 2019). Graphs were prepared in Graphpad Prism. Figures were prepared in Adobe Indesign or Adobe Illustrator.

2.2.2 Establishment of nuclear compartmentalisation during mitotic exit assay

For imaging the establishment of nucleocytoplasmic compartmentalisation, cells undergoing mitosis were imaged every 30 seconds for a maximum duration of 40 min (n=15 cells). Z-stacks of slices with 0.5 µm distance (total stack 6.0 µm) were obtained for each time point. To measure the GFP intensity in the nucleus maximum Z-projections were made. Before rupture, average intensity was measured in a circle selection with a diameter of 0.695 µm (10 pixels) within the centre of the nucleus (Fig. 2-2-2). For each cell, a background measurement was taken which was subtracted from the measurement. After rupture, a similar circular selection was used adjacent to the SPB. Here, the SPB was used as a spatial cue for the location of the nucleus. Of note, it was not possible to measure the intensity in the entire nucleus, as directly post-rupture and for nuclei exhibiting a compartmentalisation phenotype the nucleus was not visible. For each measurement the background was subtracted. Each timepoint was normalised to timepoint 0. For plotting the quantification, the individual traces of the mother nucleus before rupture and the traces of each of the daughter was shown.

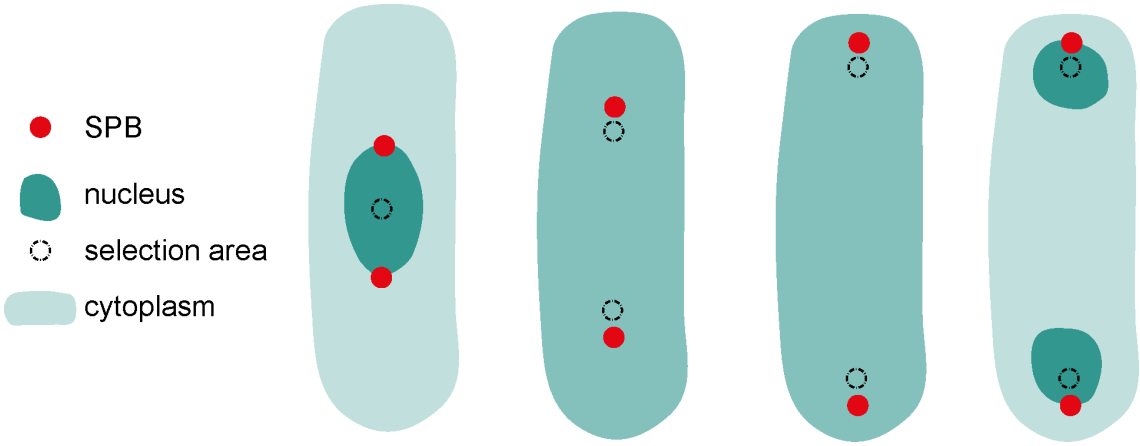

Figure 2-2-3. Analysis of the establishment of nucleocytoplasmic compartmentalisation.

Schematic overview of the analysis of the data presented in Fig. 3-3 and Fig. 3-4.

2.2.3 Measurement of mitotic spindle breakdown

Time-lapse imaging of cells expressing GFP-Atb2 and Nhp6-mCherry was performed at intervals of 1 minute. Z-stacks of confocal plains with 0.5 µm distance (total stack 4.5 µm) were obtained for each time point. The point of spindle breakdown was defined as the point at which the spindle either broke or started to retract. The data was normally distributed (Shapiro-Wilk p = 0.16). The WT was compared to each other genotype by one-way ANOVA and Dunnet's post-hoc test.

2.2.4 Analysis of recruitment of Vps4 to distal NE tails

For time-lapse imaging, cells were imaged every 60 seconds for a maximum duration of 30 minutes. Z-stacks of slices with 0.5 µm distance (total stack 4.5 µm) were obtained for each time point. Maximum Z-projections were made and a line selection was drawn of 8 pixels wide and 80 pixels long starting from the SPB to the end of the tail structure. Fluorescence intensity was extracted using the plot-profile function for 10 cells (Fig. 4-2C). For Fig. 4-2D 13 cells were followed from NE rupture to spindle breakdown and every time frame with Vps4 on the tail was quantified.

2.2.5 Recruitment of ESCRT-III/Vps4 to the NE during interphase

For imaging of persistent recruitment of Vps4-GFP to the NE (Fig. 5-3A), cells were imaged every 10 seconds for 5 minutes. Z-stacks of slices with 0.5 µm distance (total stack 4.5 µm) were obtained for each time point. One replicate experiment constituted

imaging several fields of view for a total period of 1 hour. This was repeated three times with different biological replicates. For analysis, single confocal slices of each cell at each time-point were screened for fluorescence signal on the NE. The ImageJ line-plot tool was used to confirm if the fluorescent signal was an ESCRT-III/Vps4 focus directly on the Nup189-mCherry marked NE. If so then the event was counted as one event. Persistent events were defined as events that lasted for the full duration of each 5-minute time-lapse.

2.2.6 Measurement of distance between Taz1 or Mis6 and the NE

Z-stacks of with high Z-resolution in Z with 0.25 µm distance between each plane (total stack 4.5 µm) were obtained. To measure the distance of a Taz1 or Mis6 focus to the NE in single confocal planes a line selection was drawn from the centroid of Taz1/Mis6 signal to the centre of the NE signal (Fig. 2-2-6A). The length in pixels was measured and amplified by the pixel length of 0.0695 to obtain the physical distance. In many cases the focus was nearer to the NE in Z than in X or Y based on analysing each confocal plane in the stack. In this case the orthogonal view function of ImageJ was used to count the number of Z-steps from the centre of the focus to the centre of the NE signal as the distance (Fig. 2-2-6B). For each focus, the number of Z-steps was used as the readout for the distance to the NE. For example, if a Taz1 or Mis6 focus was located in a confocal plane three planes from the confocal plane that contained the NE signal, the distance was quantified as 3 x 0.25µM (Fig. 2-2-6B). Note that this resulted in a lot of data points having 0.25, 0.5, 0.75 µm etc. as the quantified distance. The statistical differences between genotypes were analysed separately for prophase and metaphase. For both Taz1 and Mis6 the data was not normally distributed for both mitotic phases (Shapiro-Wilk test $p < 1.0E-4$ for each data set). Therefore, a Kruskal-Wallis test and Dunn's post-hoc test were used to separately analyse the difference between the genotypes for prophase and metaphase measurements.

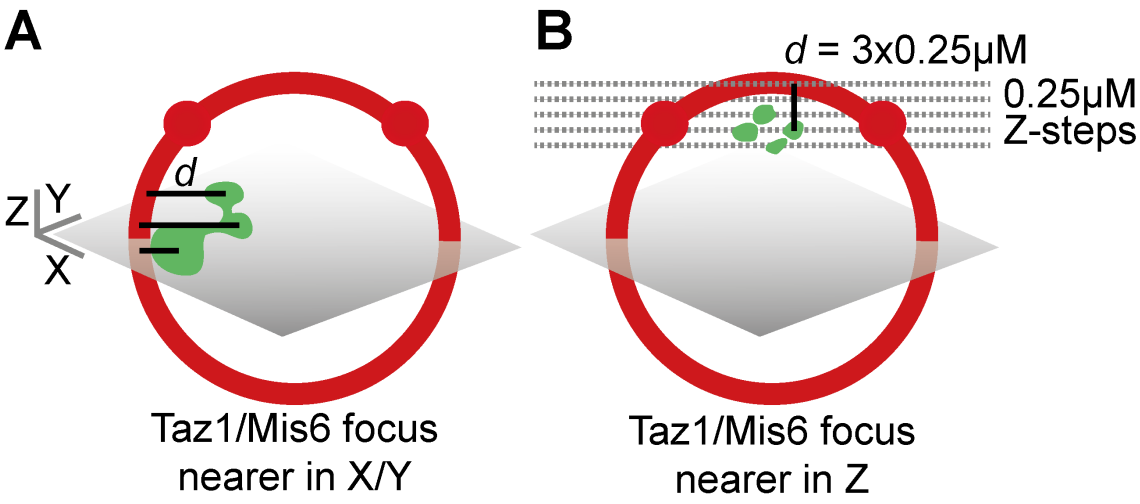

Figure 2-2-6. Measurement of the distance between Taz1, Mis6 and the nuclear envelope.

A) Schematic overview of the analysis of the experiment presented in Fig. 6-4. The NE and SPB are represented in red, the Taz1-GFP or Mis6-GFP signal are represented in green, the gray plane represents a single confocal plan through the centre of the nucleus in which the Taz1/Mis6 signal is observed. The distance of the centre of each focus to the NE was measured using the line selection tool in ImageJ **B)** Same as in (A). Each gray dotted line represents confocal planes that were imaged and which were used to quantify the distance from Taz1/Mis6 foci to the NE in the Z dimension as described in section 2.2.6.

2.2.7 CFU analysis

For analysis in ImageJ, a circle selection was drawn around the circumference of the plate. Using the "clear outside" function the surrounding area was removed. The "threshold" was set from 0-166. "Make binary" and "watershed" functions were used to isolate clustered colonies. The "analyse particles" function was used to analyse the colonies. Each identified particle was inspected manually and background was removed. Clustered colonies were quantified manually using the circle selection. The Kruskal-Wallis test and Dunn's post-hoc test were used to analyse the difference between the colony size of each genotype. The data points for the CFU amount for each genotype followed a normal distribution according to the Shapiro-Wilk ($p = 0.65$) test. Therefore, a one-way ANOVA was used to analyse the difference in CFUs between each genotype.

2.2.8 Quantification of Mad2-GFP on kinetochores

Time-lapse imaging was performed with a frequency of 1.5 minutes. Mad2-GFP occupation of kinetochores was assessed by eye. Neither the WT (Shapiro-Wilk $p = 6.0E-$

4) nor *vps4Δ* (Shapiro-Wilk p = 7.0E-3) datasets were normally distributed. Therefore, to test if there was a statistically significant difference between the two genotypes the Mann-Whitney U test was used, however a difference was not found (p = 0.69). We did note that the dataset for the *vps4Δ* appeared to have a much larger variation or spread. To test if this was true we used the Fligner-Killeen test, which is a non-parametric test to detect differences in variance (p = 1.3E-3).

2.2.9 Quantification and analysis of ChIP-qPCR data

Data was exported from the Applied Bioscience Quantstudio 6-7 Flex Studio software to Excel. Technical repeats were averaged. IP was corrected as percentage of input for each biological repeat (N=3). For the input samples the adjusted cycle-threshold (CT) value was calculated using the following function: adjustedΔCT = CT - $\log_2$(dilution factor). Next, the % of input was calculated with the following function: % of input = 100*2^(deltaCT), where deltaCT is the CT value of the test sample minus the adjusted CT value.

R was used to generate the data of figures 6-2D, E, F, G and 6-3B, C, D. Fig 6-D was generated by comparing the mean of the biological repeats for each genomic locus of the Lem2-GFP ChIP in the *vps4Δ* background to the H3K9me2 ChIP in the WT background. Correlation analysis was performed with the Pearson's correlation test and a graph was generated with each data point, the linear trendline and the 95% confidence interval. For figures 6-2E, F, G only the genomic loci were analysed with higher than median levels of H3K9me2 signal. For each of these loci the mean Lem2-GFP signal in each of the genetic backgrounds was pooled globally and also specifically for centromeric and telomeric loci. On each of these pooled data sets a Kruskal-Wallis test was performed followed by a Dunn’s post-hoc test and Benjamini-Hochberg false discovery rate correction. The same method was applied on the H3K9me2 samples of figures 6-3B, C, D.

Chapter 3 – The establishment of nucleocytoplasmic compartmentalisation during mitotic exit in *S. japonicus*

3.1 Nur1 stabilises the Lem2 on the inner nuclear membrane

The establishment of nucleocytoplasmic compartmentalisation in *S. japonicus* begins while the spindle is still connecting the two daughter nuclei (Yam *et al.*, 2011). After the full extension of the mitotic spindle during anaphase B, the nuclear membrane wraps around the intersecting spindle microtubules (Aoki *et al.*, 2011; Yam *et al.*, 2011). This structure is able to form a barrier between the nucleoplasm and the cytoplasm. In this way, nucleocytoplasmic compartmentalisation is established before the resealing of the nuclear membrane, which can only be completed after the breakdown of the spindle.

The LEM-domain protein Lem2 was identified to be vital for the establishment of compartmentalisation during mitotic exit (Yam *et al*., 2011). During anaphase, Lem2 has a similar localisation pattern as during interphase. It is enriched at the SPBs and distributed homogeneously around the NE (Yam *et al*., 2011; Fig. 3-1A). After NE rupture, Lem2 enriches at the membrane wrapped around the spindle. We termed these structures 'tails' (Yam *et al.*, 2011; Fig. 3-1A). The appearance of Lem2 on the tails occurs at the same time that nucleocytoplasmic compartmentalisation is established, as was visualised by the stable transport of a nucleoplasmic protein back into the nucleus from the cytoplasm (Fig. 3-1A).

For its interphase function in heterochromatin maintenance Lem2 works in a complex together with another INM transmembrane protein: Nur1 (Banday *et al.*, 2016). We found that both Lem2 and Nur1 localise together throughout the cell-cycle, including at the tails (Fig. 3-1B). This suggests that Lem2 and Nur1 work together both for their interphase and mitotic exit functions.

We wondered if either Lem2 or Nur1 determined the specific localisation pattern of the Lem2-Nur1 complex to the SPB, NE and tails. Analysing the localisation of Nur1 in the absence of Lem2, we observed that Nur1 redistributed throughout the ER in *lem2Δ* cells and was no longer enriched at the nucleus (Fig. 3-1C). Conversely, in cells lacking Nur1, less Lem2 signal was detected at the SPBs and the NE (Fig. 3-1D). This suggested a reciprocal requirement for each protein for the proper nuclear localisation of the

complex. Since Lem2 was still present in the nucleus in the absence of Nur1, albeit at lower levels, we wondered how the deletion of *nur1* affected the localisation of Lem2 to the tails. We found that the residence time of Lem2 at the 'tails' was significantly reduced in Nur1-deficient cells (Fig. 3-1E).

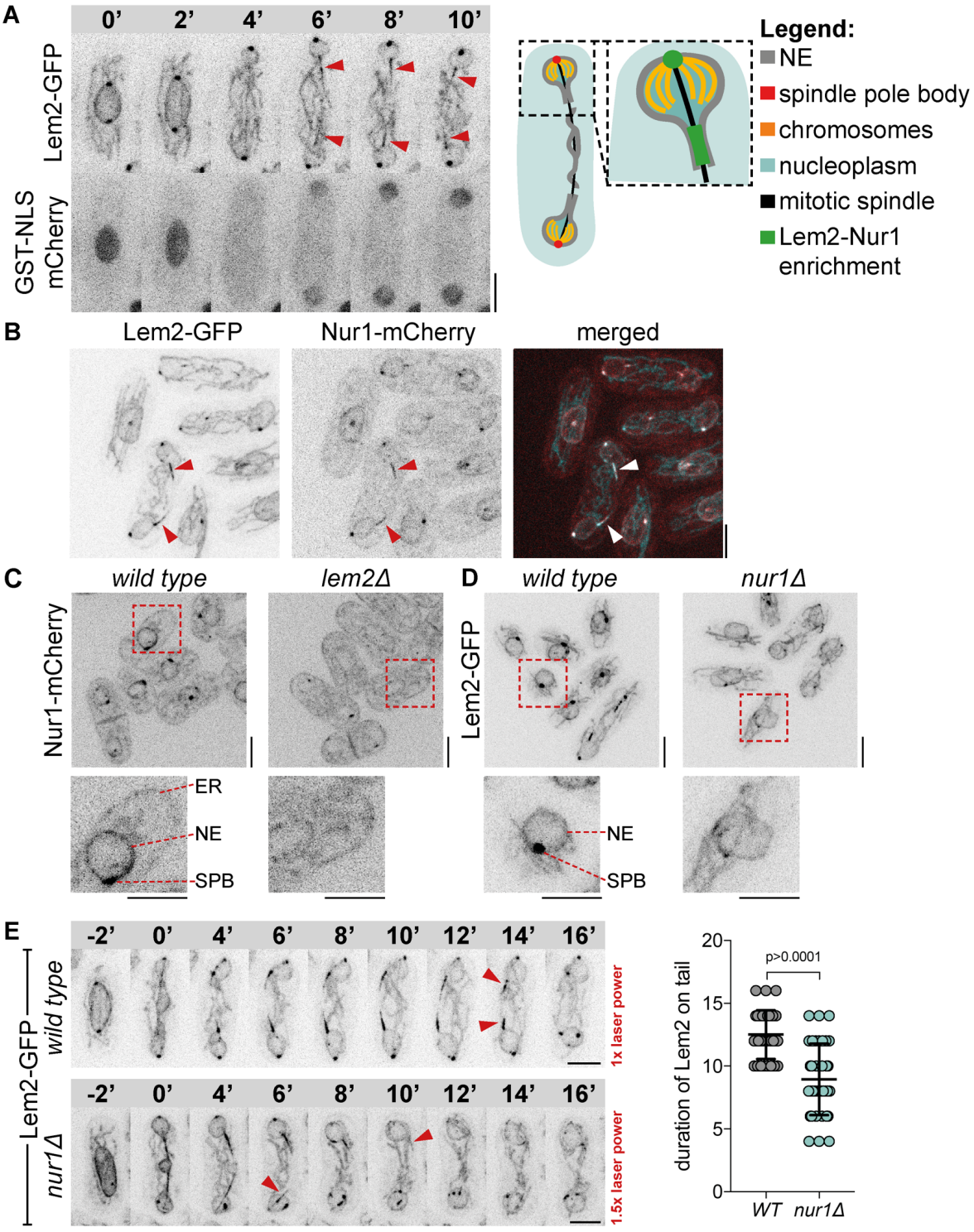

Figure 3-1. Localisation of the inner nuclear membrane complex Lem2-Nur1.

A) Time-lapse sequence of a representative WT *S. japonicus* cell expressing Lem2-GFP and GST-NLS-mCherry that is undergoing mitosis. Time-point 0' is from early anaphase B. Arrows indicate the enrichment of Lem2 at the 'tails'. Note that this coincides with the establishment of nucleocytoplasmic compartmentalisation. The scheme in the right panel is a representation of the 8-minute time point based on the data presented here and in Yam *et al*. (2011) and Yam *et al*. (2013) **B)** Cells co-expressing Lem2-GFP and Nur1-mCherry. Arrows indicate their enrichment at the tail structures. **C)** Nur1-mCherry expressing cells of indicated genotypes imaged and presented with the same settings for comparison of fluorescent signal strength. See magnified images below. Shown are Z-projections of the middle 8 (out of 10) Z-slices of the nucleus over a distance of 3.5 μm. **D)** Z-projections of images of Lem2-GFP expressing cells of indicated genotypes imaged and presented at the same settings for comparison of signal strength. **E)** Representative cells of indicated genotypes expressing Lem2-GFP used for quantification of the duration of Lem2 presence on the tail. The *nur1Δ* mutants were imaged using higher laser power (1.5x) as compared to the WT due to the fact that Lem2 was less more difficult to visualise on the tail structure in this mutant. Arrows indicate the last time point before Lem2 disappeared from the tail. On the right is presented a graph of the quantification of the duration of Lem2 presence on the tails. NB: Scale bars represent here and from here on represent 5 μm.

Thus, Lem2 and Nur1 appear to co-depend on each other for proper localisation to the nucleus throughout the cell cycle. Lem2 is the main determinant for the localisation of the Lem2-Nur1 complex, with Nur1 depending on Lem2 for being retained in the nucleus. We hypothesised that Nur1 is required for the stabilisation of Lem2 at the tail structures. Other NE proteins such as components of the NPCs and the second fission yeast LEM-domain protein Man1 are largely excluded from the 'tails' due to their interactions with segregating chromosomes at this stage of mitosis (Aoki *et al.*, 2011; Yam *et al.*, 2011; Yam *et al*., 2013). Thus, the 'tail' is a specialised membrane domain, spatially segregated and partitioned away from the rest of the NE during mitotic exit (Fig. 3-1A, right panel).

3.2 Exclusion of Lem2 from the nuclear poles enriches it at the nuclear equator

We noted that before the NE rupture occurred during anaphase, Lem2 became enriched at the nuclear equator (Fig. 3-2). We wondered if this was due to an active enrichment process, or perhaps due to a passive mechanism. At this stage of mitosis chromosomes are tethered to the NE by the second LEM-domain protein Man1, which in turn is

associated with NPCs (Yam *et al.*, 2013). During anaphase A chromosomes are segregated to the nuclear poles. Therefore, this area becomes locally very enriched with NPCs (Yam *et al.*, 2013). We asked if the local high concentration of Man1 and NPCs could exclude Lem2 from the nuclear poles. Indeed, in *man1Δ* cells, Lem2 was no longer enriched at the nuclear equator and was distributed homogeneously around the NE (Fig. 3-2).

We hypothesise Lem2 is released from chromatin already during early mitosis. This allows Lem2 to enrich at the nuclear equator during anaphase due to it being excluded from the NPC rich nuclear pole region associated with chromosomes. Then, after the NE rupture occurs, Lem2 is already in close proximity to the future tail site, allowing it to quickly enrich here. This data also suggests that during anaphase the bulk of all chromatin tethering is purely mediated by Man1. We speculate that this state continues also during mitotic exit and early G1/S-phase, when Lem2 is enriched at the tail and SPB and only a small fraction of Lem2 is localised to the nuclear periphery proper.

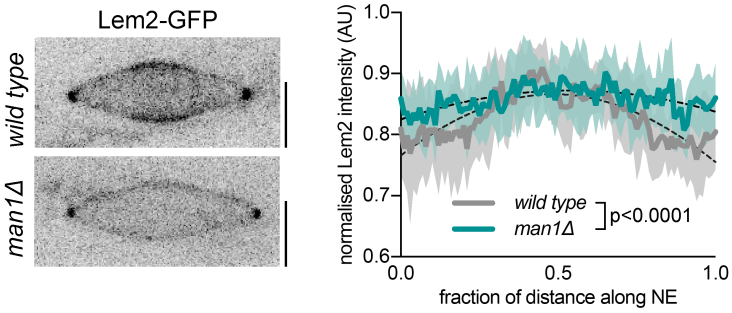

Figure 3-2. Enrichment dynamics of Lem2 during mitosis.

Representative images of anaphase nuclei of cells expressing Lem2-GFP of indicated genotypes are shown. To the right is shown a quantification of the intensity of Lem2 along the NE between the SPBs during anaphase. Intensities were normalised for intensity and length of nucleus. Shown are mean (coloured lines) and standard deviation (shaded) of the two genotypes. N=9 for WT and N=10 for *man1Δ*. Black dashed lines represent fitted Gaussian distributions with the following parameters for WT: amplitude 0.8692, mean 0.4929 standard deviation 0.9583 and the following parameters for *man1Δ*: amplitude 0.8692, mean 0.4929 standard deviation 1.73. R^2 values for fitted distributions are 0.6988 for WT and 0.4126 for *man1Δ*. An extra sum of squares F-test was used to determine if the fitted curves were different.

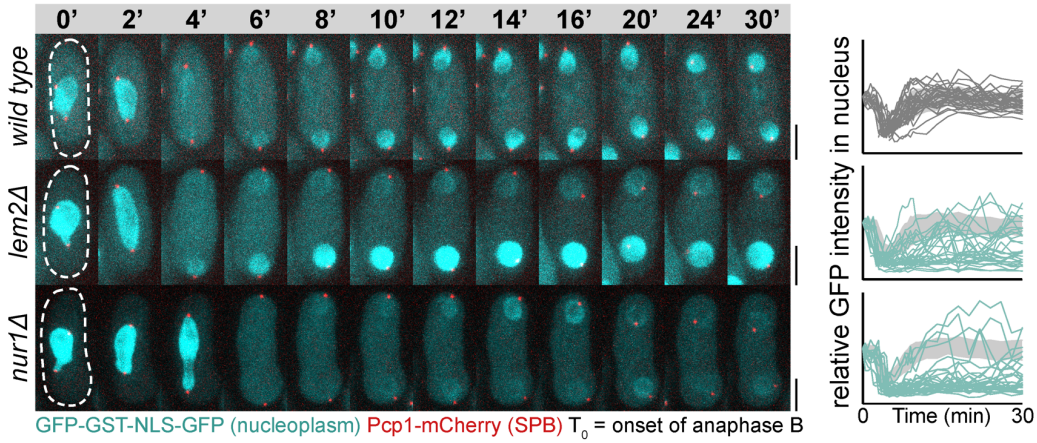

Figure 3-3. Lem2-Nur1 establishes nucleocytoplasmic compartmentalisation during mitotic exit.
NE resealing assay in cells of indicated genotypes co-expressing GFP-NLS and Pcp1-mCherry. Time-lapse sequences were obtained throughout mitosis and for around 30 min after mitosis. For quantification of the GFP fluorescence intensity in the nucleus the onset of anaphase B spindle elongation was used as time point 0, prior to NE breakage (n= 15 cells / 30 nuclei). The standard deviation of the WT quantification for each time-point (light grey) is shown together with the quantification of each mutant to aid in the comparison.

3.3 Lem2-Nur1 establishes nucleocytoplasmic compartmentalisation during mitotic exit in *S. japonicus*

The Oliferenko lab has previously shown that proper establishment of nucleocytoplasmic compartmentalisation during mitotic-exit fails in the absence of Lem2 (Yam *et al*., 2011). The previous study used the nucleoplasmic protein Nhp6 as a marker for compartmentalisation. Nhp6 interacts with chromatin, specifically with the rDNA locus (Yam *et al.*, 2011; Yam *et al*., 2013), which might affect the dynamics of its shuttling between the cytoplasm and nucleoplasm. Here, we used a synthetic nucleoplasmic reporter protein GFP-GST-NLS-GFP (referred to as GFP-NLS) to analyse the defect in establishment of compartmentalisation associated with *lem2* deletion in more detail. Compared to wild type (WT) cells, where nucleocytoplasmic compartmentalisation was re-established typically 4-6 minutes after NE rupture in anaphase, *lem2Δ* mutants achieved this state considerably later. Daughter nuclei in the same cell often behaved in a desynchronised manner, with one nucleus establising comparmentalisation faster than the other (Fig. 3-3). Mutants of *lem2* also frequently lost nuclear integrity after an initial, seemingly successful, recovery event (Fig. 3-3).

Following an extended delay, most mutant cells eventually recovered nuclear integrity. Consistent with the role of Nur1 in stabilising Lem2 at the tail structure, we discovered that *nur1Δ* cells displayed a similar compartmentalisation phenotype to *lem2Δ* mutants.

From this, we concluded that the enrichment of the Lem2-Nur1 complex at the sites where the NE wraps around the mitotic spindle is a determinant for the timely re-establishment of nucleocytoplasmic compartmentalisation. We hypothesise that this complex is essential for the maintance of this structure.

3.4 Lem2-Nur1 mediates the establishment of compartmentalisation together with the ESCRT-III/Vps4 complex

As discussed before, LEM-domains have been linked to the ESCRT-III complex at the NE. We wondered if ESCRT-III/Vps4 might be involved in the resealing of nuclear membrane in *S. japonicus*, similar to its proposed function in cultured human cells (Olmos *et al.*, 2015; Vietri *et al.*, 2015), or if it would function in the establishment of compartmentalisation in the presence of the spindle before the resealing of the nuclear membrane. We addressed this question by systematically analysing post-mitotic establishment of nucleocytoplasmic compartmentalisation in individual deletion mutants of all ESCRT-III subunits: the adaptor protein Cmp7 (Vietri *et al*., 2015), the major ESCRT-III subunit Vps32, the capping subunit Vps24, the Vps4 recruiter Did4 (Teis *et al*., 2008) and the AAA-ATPase Vps4 (Babst *et al*., 1997). See Fig. 3-4A for a list of the nomenclature of the fission yeast, budding yeast and human orthologues of these ESCRT-III subunits. Similar to *lem2Δ* and *nur1Δ* cells *cmp7Δ*, *vps32Δ* and *vps4Δ* mutants exhibited defects in re-establishing nucleocytoplasmic compartmentalisation following mitosis (Fig. 3-4B). Surprisingly, two of the ESCRT-III core subunits, Vps24 and Did4, which are essential for the endosomal ESCRT functions (Babst *et al.*, 2002), did not appear to be involved in this process (Fig. 3-4B). Notably, the *vps24Δ did4Δ* double mutant compartmentalised like WT. To test if the compartmentalisation phenotype was specific to a nuclear-specific function of ESCRT-III we also deleted the ESCRT-II subunit Vps25, which is the endosome-specific adaptor for ESCRT-III (Teis *et al.*, 2010). We found that it was not required for establishing compartmentalisation (Fig. 3-4C). Double mutants of *nur1Δ vps32Δ*, *lem2Δ vps4Δ* and *nur1Δ vps4Δ* exhibited similar phenotypes

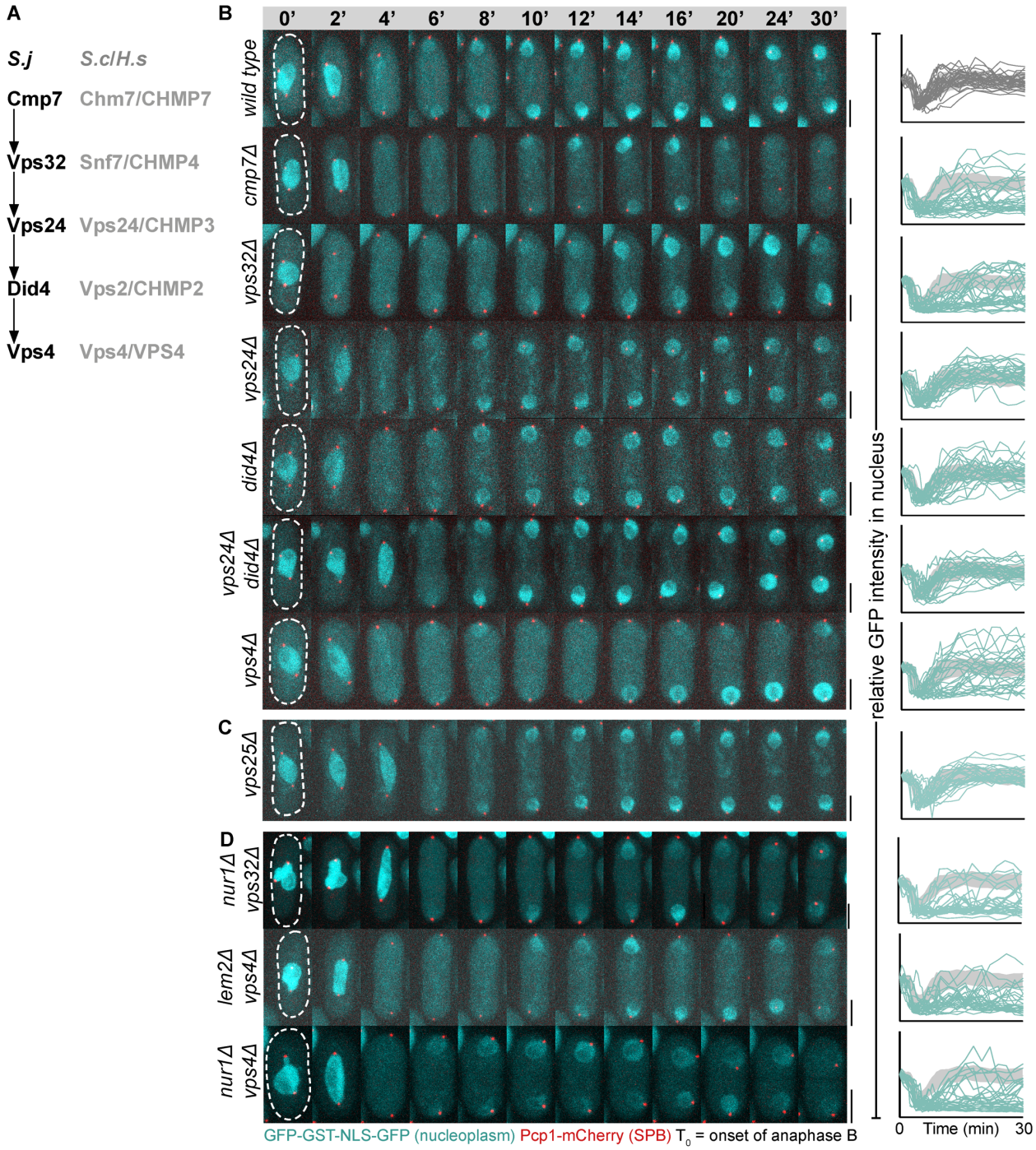

Figure 3-4. ESCRT-III/Vps4 together with Lem2-Nur1 mediate compartmentalisation during mitotic exit.
A) Schematic overview of the hypothesised order of assembly of the ESCRT-III/Vps4 complex on the nucleus based on its assembly on endosomes (Teis *et al.*, 2008; Olmos *et al.*, 2015; Vietri *et al.*, 2015). Orthologues of *S. japonicus*, *S. cerevisiae* and humans are listed. **B-D)** NE resealing assay similar to Fig 3-3 for the indicated ESCRT-III/Vps4 mutants. The WT data is the same as presented in Fig. 3-3.

to that of the single mutants (Fig. 3-4D), suggesting that the Lem2-Nur1 complex and ESCRT-III/Vps4 appeared to function in the same pathway.

Thus, a non-canonical ESCRT-III/Vps4 complex, consisting of Cmp7, Vps32 and Vps4 together with Lem2-Nur1 is involved in mediating nucleocytoplasmic compartmentalisation in the presence of the spindle. This is before the actual resealing of the membrane and therefore suggests a different mechanism from other reports regarding ESCRT-III/Vps4 on the NE.

3.5 Spindle breakdown and establishment of compartmentalisation are uncoupled in *S. japonicus*

In cultured human cells the breakdown of the mitotic spindle microtubules is temporally connected to NE resealing and establishment of compartmentalisation. ESCRT-III recruits the AAA-ATPase Spastin to sever microtubules during mitotic exit (Vietri *et al*., 2015). However, in *S. japonicus* compartmentalisation is established in the presence of the spindle. Notably, the *S. japonicus* genome does not appear to encode a Spastin homologue. We therefore asked if ESCRT-III/Vps4 plays a role in dismantling the mitotic spindle in this organism. We used an N-terminally GFP tagged Tubulin (Atb2) expressed as a second copy to analyse spindle dynamics. We defined "breakdown" of the spindle as the first point in which either the spindle fractured or was no longer connecting the two daughter nuclei. We observed that the persistence of the mitotic spindle was not affected by the lack of Lem2, Vps24 or Vps4 (Fig. 3-5), suggesting that ESCRT-III/Vps4-mediated establishment of nuclear compartmentalisation and spindle breakdown are not coupled in *S. japonicus*.

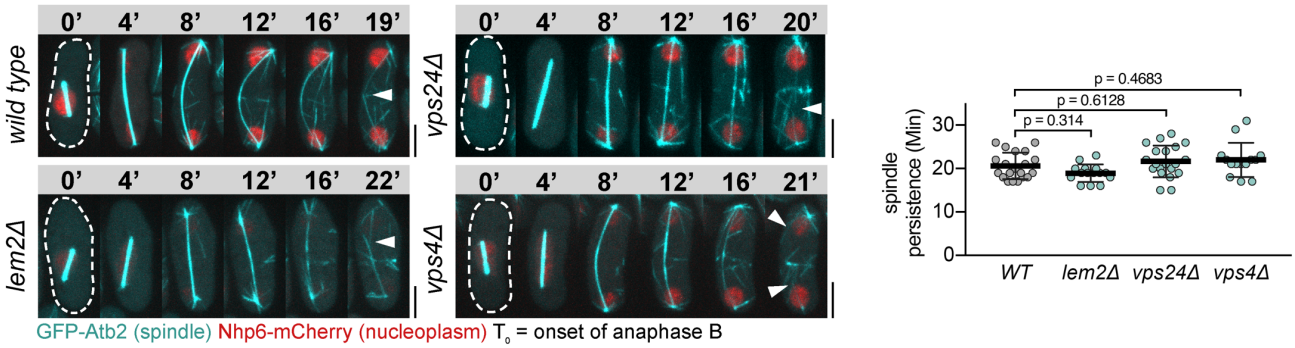

Figure 3-5. Uncoupling of spindle breakdown and establishment of compartmentalisation.

Time-lapse maximum projection sequences of cells expressing GFP-Atb2 and Nhp6-mCherry of indicated genotypes. The onset of anaphase B was defined as the abrupt elongation of the mitotic spindle towards the cell poles. Arrows indicate the breakage of the spindle. Quantification of time

between anaphase B onset and breakage of the spindle is presented on the *right* (n≥14 cells; one-way ANOVA followed by Dunnett's comparison test; multiplicity-adjusted p-values are presented).

3.6 Precocious loss of nuclear integrity during anaphase spindle elongation in *lem2Δ* and ESCRT-III mutants

Previously it was reported that a premature loss of nucleocytoplasmic integrity occurred in Lem2-deficient mitotic cells during the elongation of the anaphase spindle (Yam *et al*., 2011). It was suggested that Lem2 played a role in maintaining NE rigidity and integrity during mitosis (Yam *et al.*, 2011; Gu *et al*., 2012). We observed a similar leakage from the nucleus using GFP-NLS in *lem2Δ* mutants and also in a subset of ESCRT-III/Vps4 mutants already at the onset of anaphase spindle elongation (Fig 3-6). Interestingly, this leakage was observed in a different set of ESCRT-III mutants than those exhibiting mitotic-exit compartmentalisation phenotypes (Fig. 3-3). In WT cells, loss of comparmentalisation was always very abrupt, occuring from one 30 second time-point to the next or over the course of 60 seconds (Fig 3-6). Using the same cells that were quantified in Fig. 3-2 and Fig. 3-3 we classified this leakage in two types: early rupture and gradual leakage, by quantifying the time during which a nucleus was losing GFP-NLS. "Gradual leakage" was only observed in *lem2Δ* and *cmp7Δ* mutants and was defined as the continuous loss of GFP-NLS from the nucleus over several minutes. "Early rupture" was observed in *lem2Δ*, *cmp7Δ* and *vps24Δ* mutants and was defined as a rupture event that was resealed again during anaphase before the main anaphase B rupture event (Fig 3-6; For example in the *vps24Δ* mutant one can observe an initial loss of compartmentalisation followed by in increase in nuclear GFP before the main rupture event). Interestingly, we did not observe a significant difference in GFP-NLS loss for *vps32Δ* and *vps4Δ* mutants, both of which had strong phenotypes during mitotic exit.

Thus, in the absence of some ESCRT-III subunits, the timing of NE rupture during anaphase is deregulated. Additionally, cells lacking Lem2 or Cmp7 also exhibit a slow leakage of nuclear protein already from the onset of anaphase B spindle elongatation. The latter might be attributed to a more "brittle" membrane that is more prone to rupturing. The enrichment of Lem2 at the nuclear equator is likely not required for the stabilisation of the membrane. In *man1Δ* cells Lem2 is not enriched at the equator (Fig. 3-2), yet no precocious loss of compartmentalisation is observed in these cells (Yam *et*

al., 2013). Absence of chromatin-NE tethering by LEM-domain proteins in *S. pombe* leads to a more deformable interphase nuclear membrane (Schreiner *et al.*, 2015). However, the loss of chromatin-tethering is not likely to be responsible for the loss of compartmentalisation as it is likely that Lem2 has already been released from chromatin at this stage (Fig. 3-2) and chromatin is tethered through Man1 from anaphase B (Yam *et al*., 2013). This makes it possible that the "brittle" membrane phenotype might be ascribed to another role of Lem2. It likely requires at least the ESCRT-III subunit Cmp7 for this, as *cmp7Δ* mutants exhibit similar phenotypes to *lem2Δ* (Fig. 3-6). Notably, the main anaphase rupture event is not affected, suggesting that the rupturing is not mediated by ESCRT-III, which is something that might be hypothesised due to its membrane remodelling ability.

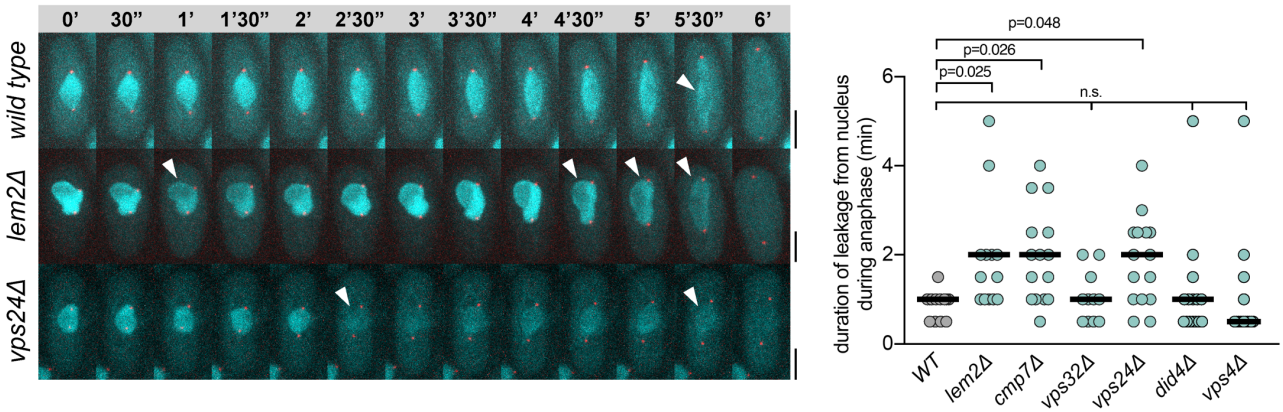

Figure 3-6. Precocious loss of nuclear integrity during anaphase spindle elongation.

The same cells used for quantifcation of establishment of compartmentalisation during mitotic exit in Fig. 3-3 and Fig. 3-4 are used for quantification of loss of nuclear integrity during anaphase. Arrows indicate loss of nuclear integrity. Note the single abrupt rupture in WT versus the repeated rupture versus the slow leaking of the nucleoplasm or the deregulated timing of rupture in the mutants. For quantification, The duration in which nuclei were losing GFP-NLS was quantified. Medians are indicated. Kruskal-Wallis multiple comparison test and Dunn's post-hoc test were used for statistical comparison, multiplicity-adjusted p-values are presented.

3.7 Conclusions

In this chapter we have shown that the localisation of the Lem2-Nur1 complex is a main determinant for proper establishment of nucleocytoplasmic compartmentalisation during mitotic exit. During interphase Lem2-Nur1 is involved in chromatin-tethering to the NE. At the beginning of mitosis, chromatin releases from the NE (Yam *et al*., 2013).

During anaphase, the second LEM-domain protein Man1 becomes responsible for all chromatin-NE associations, allowing the equal segregation of chromosomes, membrane and NPCs. Through the exclusion of Lem2 from the nuclear poles, it becomes enriched at the nuclear equator during anaphase. When the rupture occurs, this allows Lem2-Nur1 to enrich at the tail structures and establish compartmentalisation.

We have also shown that a non-canonical version of the membrane remodelling complex ESCRT-III/Vps4 is also required for establishing compartmentalisation during mitotic exit, functioning in the same pathway as Lem2-Nur1. Importantly, it is involved in establishing compartmentalisation while the spindle is still penetrating the nuclear membrane. This indicates that it is performing an additional function related to the tail structure separate from a potential role in resealing the nuclear membrane, which can only occur after spindle breakdown. We hypothesise that Lem2-Nur1 and ESCRT-III/Vps4 are involved in the maintenance of the tail structure. Specifically, this likely means enforcing the strict association between membrane and the spindle, allowing a strong barrier between the nucleoplasm and the cytoplasm.

Chapter 4 – The localisation of ESCRT-III/Vps4 to the nuclear envelope during interphase and mitosis

4.1 The construction of functional fluorescent tags for ESCRT-III/Vps4 in *S. japonicus*

Due to the function of ESCRT-III/Vps4 together with Lem2-Nur1 at the tails we set out to visualise this complex and determine if it could localise specifically to this structure. It has been observed that simple C-terminal fusions to fluorescent tags such as GFP interferes with the function of ESCRT-III. For example, C-terminally tagging all the ESCRT-III subunits in budding yeast blocked MVB formation (Teis *et al*., 2008). Working together with the Teis lab we set out to generate functionally tagged ESCRT-III subunits in *S. japonicus*, using the strategy reported in Adell *et al*. (2017) and Mierzwa *et al.* (2017).

We created a fluorescent Vps24 construct by using a LAP tag as a linker between Vps24 and eGFP. Similarly, we created a fluorescent Vps4 construct by using a 3xHA tag linker between Vps4 and eGFP (Adell *et al.*, 2017; From here on termed Vps24-GFP and Vps4-GFP in the main text). We integrated both into the *S. japonicus* genome at their ndogenous loci and under the control of their endogenous promoters. We tested the functionality of these constructs by testing the sensitivity of the tagged yeast strains to canavanine. Canavanine is an arginine analogue. ESCRT deficient cells are sensitive to this drug and when plated on plates containing canavanine ESCRT mutants show severe growth defects (Lin *et al.*, 2008; Teis *et al.*, 2010). We titrated the functional concentration of canavanine for *S. japonicus* and determined it be around 4-4.5 μgr/ml (data now shown). This is notably higher for the functional concentration for budding yeast (Teis *et al*., 2010). We confirmed that all ESCRT mutants in *S. japonicus*, including ESCRT-0, -I and -II, were indeed deficient to canavanine by using a spot assay (Fig. 4-1A). Of note, *cmp7Δ* cells did not show any growth defect on canavanine, suggesting that it does not function in the MVB pathway. Next, we compared the growth of the Vps24-GFP and Vps4-GFP strains to their respective deletion mutants and found that the tags did not confer sensitivity to canavanine (Fig. 4-1B). This suggests that the MVB pathway is not affect and that the ESCRT machinery is functional in these cells and our tagged constructs function like the WT alleles.

Both constructs also localised as could be expected for their role in MVB formation. The vast majority of Vps24-GFP and Vps4-GFP localised to cytoplasmic foci adjacent to FM4-64-marked vacuoles (Fig. 4-1C), resembling the localisation of ESCRT-III/Vps4 to perivacuolar MVBs in budding yeast (Adell *et al* 2017). As expected, deletion of *vps27* (ESCRT-0), *vps28* (ESCRT-I) and *vps25* (ESCRT-II) resulted in failure to recruit Vps24 and Vps4 to endosomes. In these mutants, both were mainly detected in the cytosol (Fig. 4-1C). Confirming the sequential formation of the ESCRT-III complex (Teis *et al*., 2010), deletion of either *vps24* or *did4* also delocalised Vps4 from endosomes. Notably, we observed bright foci of Vps4 in these mutants, which appeared to be peri-nuclear. This will be discussed further later. Confirming that in the absence of Vps4, ESCRT-III complexes cannot be resolved (Babst *et al.*, 1998), we found that in *vps4Δ* cells Vps24 becomes enriched onto endosomes, and most of the cytoplasmic Vps24 pool is locked onto endosomes as well (Fig. 4-1C).

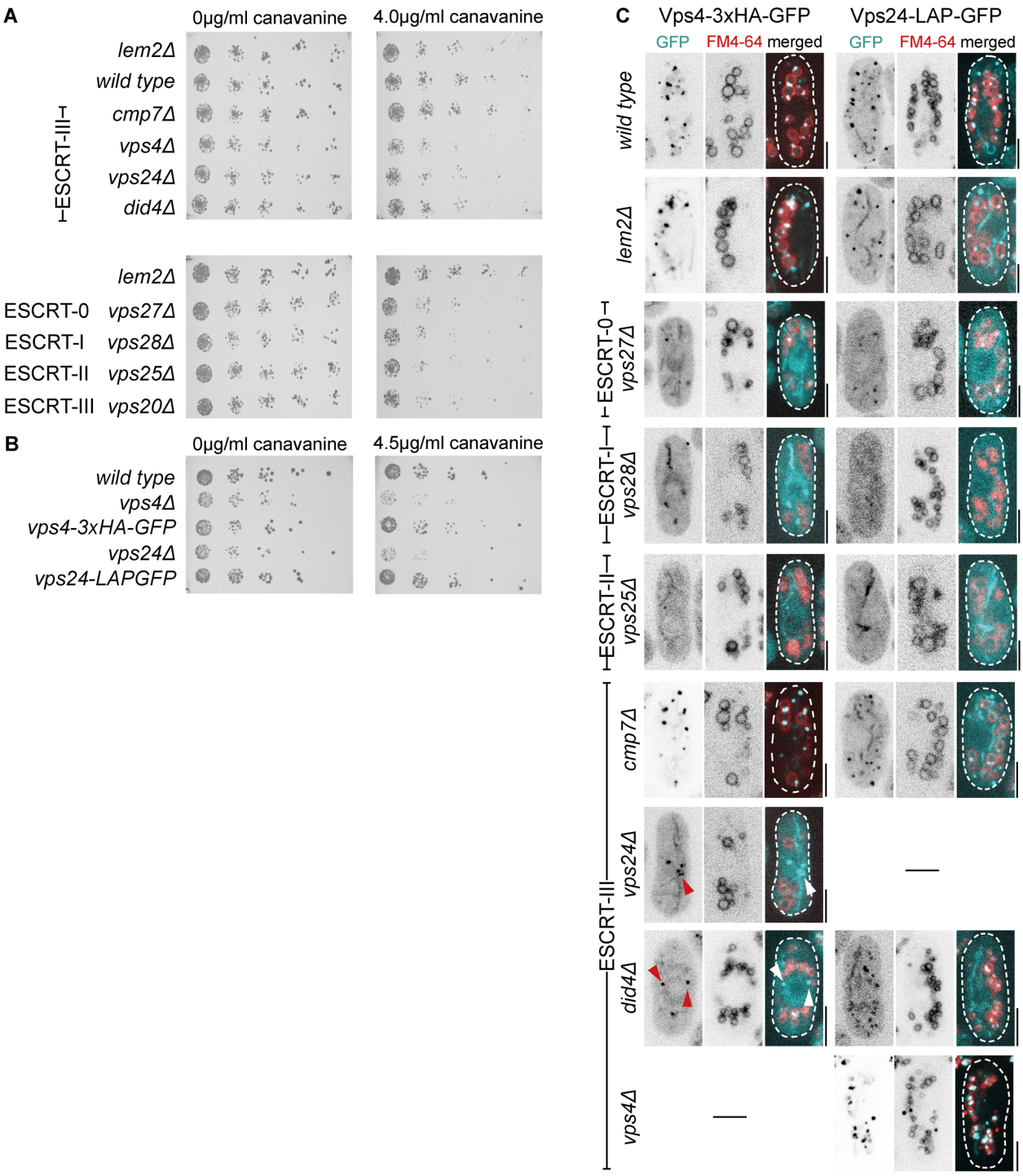

Figure 4-1. Functionally tagged Vps24 and Vps4 constructs.

A) Canavanine assay of ESCRT-0, -I, -II and -III complexes showing the sensitivity of ESCRT mutants except for *cmp7Δ* to canavanine. **B)** Canavanine assay showing that Vps24-LAP-GFP and Vps4-3xHA-GFP tagged strains do not show any growth defect on canavanine. **C)** Shown are single confocal slices of cells expressing Vps24-LAP-GFP or Vps4-3xHA-GFP that were incubated with FM4-64 for 5 minutes followed by washout of the drug and recovery for 1 hour before imaging. Note that in early ESCRT mutants Vps4 and Vps24 are no longer recruited to FM4-64 marked structures. Arrows indicate bright perinuclear Vps4 foci in *vps24Δ* and *did4Δ* mutants.

We also attempted to construct a functional Vps32-LAP-GFP construct. In budding yeast the tagged Snf7-LAP-GFP construct was expressed as a second copy, as a single tagged construct was not functional (Adell *et al*., 2017). We integrated the Vps32-LAP-GFP construct as a second copy into the *ura4* locus. However, we found that it likely was not functional. We observed many very bright foci in the cytoplasm. Aditionally, when combining the Vps32-LAP-GFP construct with the *vps25* deletion, Vps32 formed very bright "bubble-like" structures in the cytoplasm (data not shown). We concludedthat the extra tagged copy formed unfunctional aggregates, perhaps similar to overexpressed CHMP2 in cultured human cells that forms tubular helical structure in human cells (Bodon *et al.*, 2011). Therefore we did not continue with this construct for further analysis.

In conclusion, we were able to construct functionally tagged constructs of Vps24 and Vps4. Both constructs localised to ubiquitous structures likely corresponding to peri-vacuolar endosomes in a fashion depending on early ESCRT complexes and did not interfere with the MVB pathway.

4.2 Lem2-Nur1 dependent recruitment of ESCRT-III/Vps4 to the tail structures

Next, we aimed to see if ESCRT-III/Vps4 localised to the tails. Using Lem2-mCherry as a marker for the NE and the tails we detected a small pool of Vps4-GFP, specifically localising both to the post-mitotic tail structures and the SPBs during mitotic exit (Fig. 4-2A). The SPB localisation is likely due to the extrusion of the SPB from the NE at this stage (Ding *et al.*, 1997; Horio *et al.*, 2002). The high intensity of the fluorescent signal of endosomal Vps4 made visualising events at the NE challenging, and it was difficult to definitely determine NE localisation of Vps4. Therefore, we further assessed the recruitment of Vps4 to the NE using the ESCRT-II mutant *vps25Δ*, which disrupts the MVB pathway and removes all ESCRT-III components from endosomes, without causing defects in NE resealing (Fig. 3-4C). Using this system, we established that Vps4-GFP was primarily recruited dynamically to the distal ends of the Lem2-mCherry-labelled tails (Fig. 4-2B). Interestingly, Vps4 did not exactly correlate to Lem2, as Vps4 localised slightly distal to Lem2 on the tail, where Lem2 signal had already tailed off (Fig. 4-2C). Peak Vps4-GFP recruitment occurred around 7 min after NE rupture (Fig. 4-2D). This was

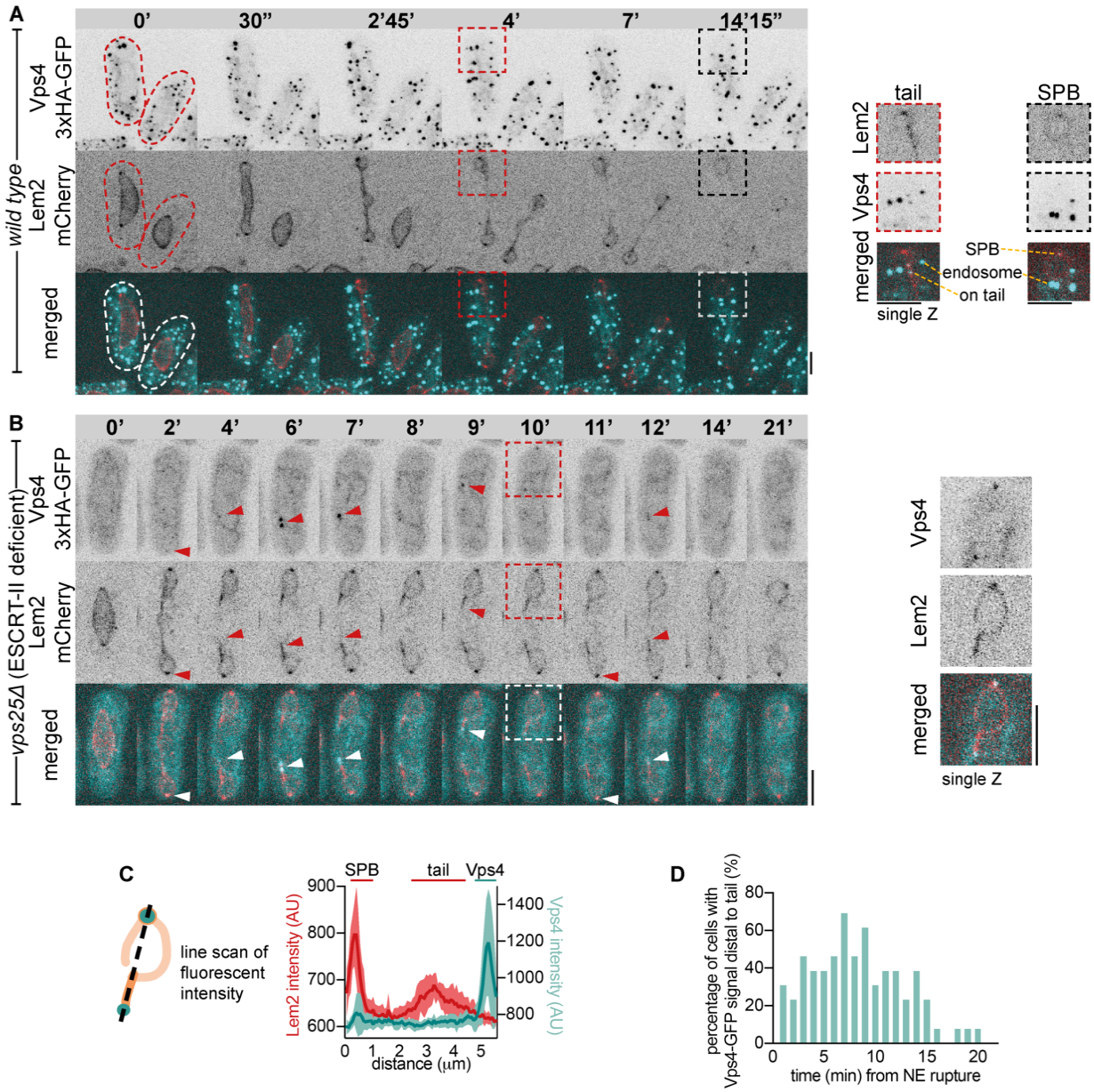

Figure 4-2. Vps4 is recruited to the tail structure in a dynamic fashion throughout mitotic exit.

A) Time-lapse maximum projection sequences of cells expressing Vps4-GFP and Lem2-mCherry starting from prior to NE breakage. Magnified images focus on a single confocal slice showing Vps4 localisation to the SPB and to the tail. Note that the endosomal Vps4 signal drowns out the NE-localized Vps4. **B)** A time-lapse Z-projected sequence of a *vps25Δ* Vps4-GFP- Lem2-mCherry-expressing cell starting prior to NE rupture (n=21 cells). Arrows indicate Vps4 localisation to the SPBs and to the distal end of the tail structure. A single Z-slice of an area outlined at the 10-minute time point is shown as a magnified image on the right to show the localisation of Vps4 and Lem2 in the same Z-plane. **C)** Quantification of Vps4 enrichment at the distal end of the Lem2 tail (n=10) using a line-scan measurement of intensity of both markers. The schematic represents the enlarged image of Fig. 4-2B. **D)** Quantification of the timing of Vps4 recruitment to the tails, shown as the percentage of cells exhibiting Vps4-GFP signal on at least one of the two tails. Cells were followed between NE rupture and spindle breakdown (n=13).

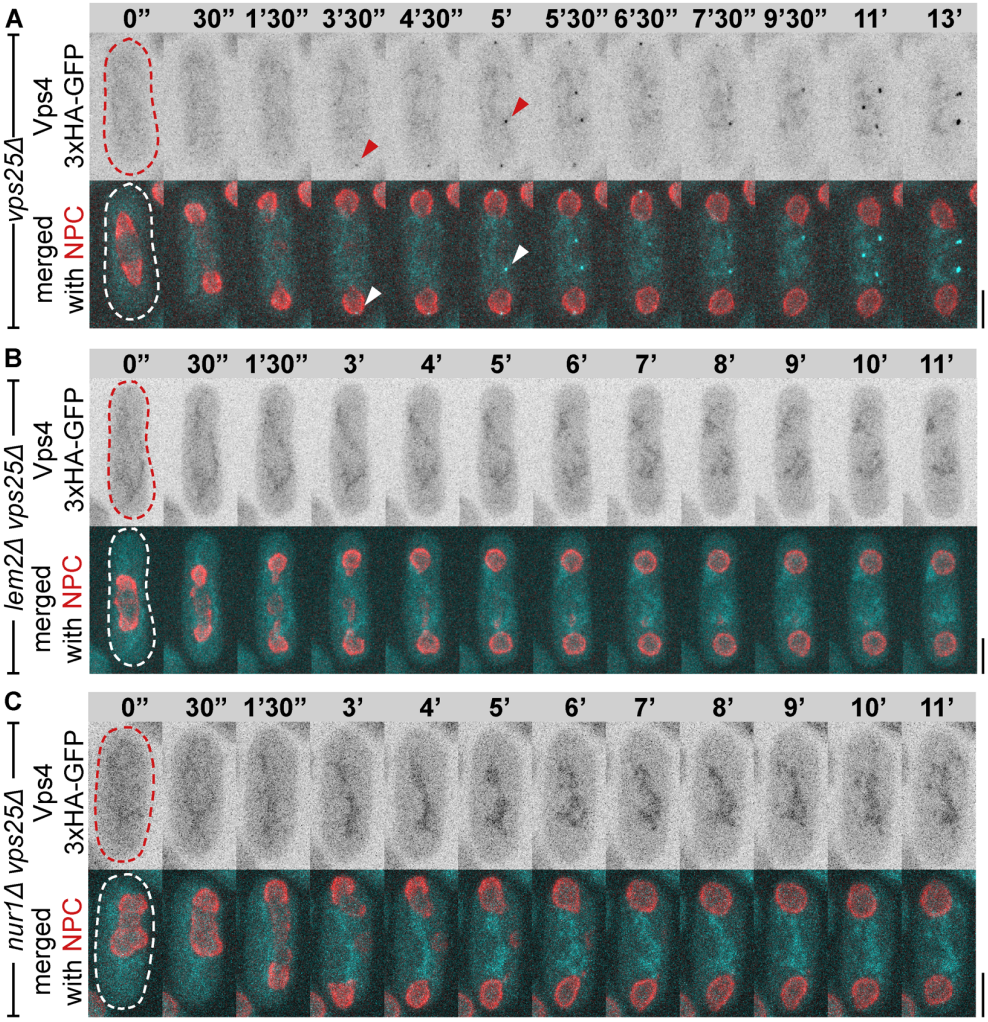

Figure 4-3. Tail localisation of Vps4 depends on Lem2-Nur1.

A) A time-lapse sequence of a *vps25Δ* Vps4-GFP Nup189-mCherry cell starting prior to NE rupture (n=12). Arrows indicate Vps4 localisation to the tails and SPBs. Note that the NPCs are excluded from the ‘tails’. **B)** A time-lapse sequence of a *lem2Δ vps25Δ* Vps4-GFP Nup189-mCherry cell starting prior to NE rupture (n=11). **C)** A time-lapse sequence of a *nur1Δ vps25Δ* Vps4-GFP Nup189-mCherry cell starting prior to NE rupture (n=17).

concurrent with the timing of the re-establishment of nuclear compartmentalisation before the breakdown of the spindle (Fig. 3-1A, Fig. 3-5).

We wondered if Lem2-Nur1 was responsible for the recruitment of Vps4 to the tails. We therefore used NPC component Nup189-mCherry as a marker for the NE. Note that tails are not visible using the Nup189-mCherry marker as NPCs do not extend along the tail region. Because of this, we had difficulties observing Vps4 on the tails in WT cells using the Nup189 marker (not shown). However, we confirmed transient recruitment of

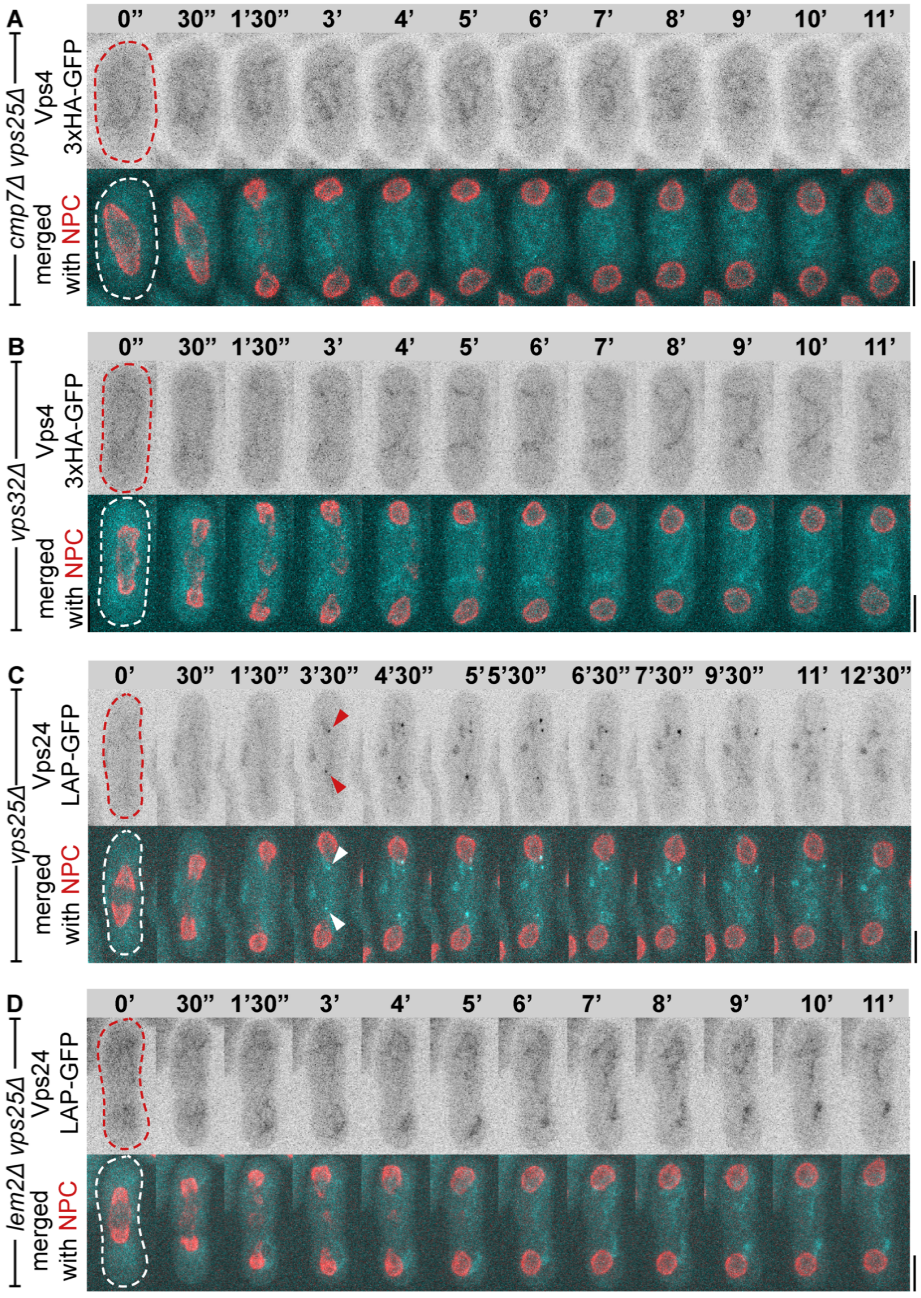

Figure 4-4. Tail localisation of Vps4 depends on ESCRT-III and localisation of Vps24.

A) A time-lapse sequence of a *cmp7Δ vps25Δ* Vps4-GFP Nup189-mCherry cell starting prior to NE rupture (n=15). **B)** A time-lapse sequence of a *vps32Δ* Vps4-GFP Nup189-mCherry cell starting prior to NE rupture (n=12). **C)** A time-lapse sequence of a *vps25Δ* Vps24-GFP Nup189-mCherry cell starting prior to NE rupture (n=12). Note that Vps24 also localizes to the ‘tails’ despite not being required for re-establishment of nucleocytoplasmic compartmentalisation. **D)** A time-lapse sequence of a *lem2Δ vps25Δ* Vps24-GFP Nup189-mCherry cell starting prior to NE rupture (n=8) shows the dependency of Vps24 on Lem2 for NE recruitment.

Vps4-GFP to both SPBs and tails using the *vps25* deletion (Fig. 4-3A). In the absence of either Lem2 or Nur1 Vps4 was no longer detected at the tails or SPBs during mitotic exit (Fig. 4-3B, C), suggesting that Lem2-Nur1 is upstream of Vps4.

We next asked if the recruitment of Vps4 followed the normal order of assembly of the ESCRT-III/Vps4 complex. Indeed, deletion of the upstream components *cmp7* or *vps32* completely abrogated the recruitment of Vps4 to either the SPBs or tail (Fig. 4-4A, B), similar to *lem2Δ* or *nur1Δ* mutants (Fig. 4-3B, C).

We also analysed the behaviour of Vps24 during mitotic exit, which is not involved in the establishment of compartmentalisation (Fig. 3-4B). Strikingly, we observed that Vps24 exhibited the same localisation pattern as Vps4 in the *vps25Δ* background (Fig. 4-4C). All Vps24 recruitment was abolished in the absence of Lem2 (Fig. 4-4D), suggesting the same mode of recruitment as for Vps4.

4.3 Conclusions

In conclusion, we show that Vps4 is recruited to the tail structure during mitotic exit in a Lem2-Nur1 and ESCRT-III dependant manner. Strikingly, Vps24 is also recruited to the tails, despite not being required for establishing compartmentalisation. We hypothesise that it can be recruited to the tail together with the non-canonical ESCRT-III/Vps4 complex that is required for compartmentalisation (Cmp7, Vps32 and Vps4), but that its recruitment is not essential for the function of this complex. It is interesting to note that despite that Vps24 and Vps4 only appear were the Lem2 signal starts to disappear, meaning that the signals do not overlap, both Lem2 and Nur1 are still required for its recruitment there. It appears that ESCRT-III/Vps4 is not able to penetrate into the tail structure. This suggests that the membrane is indeed tightly wrapped around microtubules, potentially excluding ESCRT-III/Vps4. Potentially only a small amount of Lem2-Nur1 is available at the distal end of the tail and required to recruit ESCRT-III/Vps4, potentially "activating" the complex. Due the fact that this recruitment happens primarily during the persistence of the spindle, we hypothesise that the recruitment of ESCRT-III/Vps4 is functioning to maintain the tail structure, and not necessarily to reseal the nuclear membrane. We hypothesise that ESCRT-III/Vps4 might regulate membrane proteins at this structure, specifically Lem2-Nur1, rather than working directly on the membrane, and in this way establish and maintain compartmentalisation.

Chapter 5 – Vps4 disassembles Lem2-ESCRT-III complexes and controls the localisation of Lem2-Nur1 at the nuclear envelope

5.1 Vps4 disassembles Lem2-Cmp7 complexes *in vitro*

Since we hypothesised that ESCRT-III/Vps4 might regulate the Lem2-Nur1 complex at the tails, we wondered if we could detect any direct interaction between these complexes. To this end, we set up an *in vitro* binding assay using *S. japonicus* proteins purified from *Escherichia coli* to analyse the interactions between Lem2 and the non-canonical ESCRT-III/Vps4 complex that were essential for establishment of nucleocytoplasmic compartmentalisation. In human cells, the C-terminal part of LEM2 was shown to interact with CHMP7 (Gu *et al.*, 2017). In budding yeast the N-terminal nucleoplasmic linker of Heh2 interacted with the C-terminal ESCRT-III-like domain of Chm7 (Webster *et al.*, 2016). However, our genetic data presented later in this chapter suggested that any interaction between Lem2 and ESCRT-III was likely mediated through the MSC domain. As these reports suggested an interaction between Lem2 orthologues and ESCRT-III and not through Nur1, we focussed our analysis on Lem2. Therefore, we decided to purify the C-terminal nucleoplasmic domain (aa564-673) of Lem2 (GST-Lem2$^{C\text{-}term}$) encompassing the MSC domain. We also purified the C-terminal ESCRT-III-like domain (aa 242-436) of Cmp7 (Cmp7$^{242\text{-}436}$-3xFLAG), full-length Vps32 (Vps32-3xMYC) as well as full-length Vps4 (Vps4-3xHA) and an ATP hydrolysis deficient mutant of Vps4 (Vps4^{E233Q}3xHA). This mutant functions as a substrate trap mutant that binds ATP but cannot hydrolyse it. Similarly, it can bind its substrates, but not disassemble and release them (Babst *et al.*, 1997). Did4 orthologues are known to strongly bind to Vps4 (Obita *et al.*, 2007; Adell *et al.*, 2014). Therefore, we also purified Did4 (GST-Did4) as a positive control for Vps4 binding.

First, we confirmed the binding of ESCRT-III subunits to Vps4. We used the Vps4^{EQ} mutant, as the interaction between ESCRT-III and WT Vps4 is very transient and cannot be detected by Western blot. We incubated GST-tagged proteins of our interest

with Vps4^{EQ}. Firstly, we observed strong interaction between Did4 and Vps4^{EQ} as predicted (Fig. 5-1A). We also observed weaker interaction between Vps32 and Vps4^{EQ}. We for the first time observed that the C-terminus of Cmp7 can interact directly with Vps4, binding to Vps4^{EQ} with an affinity lower than Did4 (Fig. 5-1A). Notably, we did not observe any direct binding between Lem2 and Vps4^{EQ}. This confirms our genetic data that recruitment of Vps4 to the NE depends on Vps32 and Cmp7 (Fig. 4-4A,B) and suggests that these two factors are in between Lem2 and Vps4.

Next, to analyse the interaction between Lem2 and ESCRT-III we set up *in vitro* binding experiments as follows: GST-Lem2$^{C\text{-}term}$ was bound to glutathione beads. Then, we added the purified ESCRT-III/Vps4 components to the beads either individually or in different combinations. ATP was present in all reactions. Next, we pulled down Lem2 and observed which proteins interacted with Lem2 by Western blotting. First, we added just Cmp7$^{242\text{-}436}$ to Lem2$^{564\text{-}673}$ and observed a stable interaction between the two (Fig. 5-1B, lane 8). Thus, the C-terminal MSC domain of Lem2 is sufficient for binding to the C-terminal ESCRT-III-like domain of Cmp7. Direct binding of Vps32 to Lem2$^{564\text{-}673}$ was not detected (Fig. 5-1B, lane 10). Yet, Vps32 was capable of associating with preformed Lem2$^{564\text{-}673}$ - Cmp7$^{242\text{-}436}$ complexes (Fig. 5-1B, lane 11). Notably, we only observed very minimal direct interaction between Vps32 and Cmp7 in the absence of Lem2 (Fig. 5-1C), suggesting a dual requirement for Vps32 binding between Lem2 and Cmp7.

Next, we tested the interaction with Vps4. We added Vps4 to Lem2$^{564\text{-}673}$ alone, or to preformed Lem2-Cmp7 and Lem2-Cmp7-Vps32 complexes. Interestingly, when Vps4 was added to these preformed complexes, it released Vps32 and Cmp7$^{242\text{-}436}$ from Lem2$^{564\text{-}673}$ (Fig. 5-1B; lanes 9 and 12), as observed by the fact that these proteins were no longer pulled down with Lem2. This suggested that Vps4 was able to disassemble the interaction specifically between Lem2 and Cmp7.

To confirm that this was because of the ATPase activity of Vps4, we repeated the same experiment, but using the mutant Vps4^{EQ} instead of the WT version. The substrate trap mutant Vps4^{EQ} failed to disassemble Lem2$^{564\text{-}673}$-Cmp7$^{242\text{-}436}$ interaction and instead, was retained on these complexes (Fig. 5-1D; lane 9). Notably, significantly more Vps4^{EQ} was trapped in complexes containing Vps32 in addition to Cmp7$^{242\text{-}436}$ as compared to Cmp7 alone (Fig. 5-1D; lane 12). To further confirm that the ATPase activity of Vps4 is required to disassemble Lem2-Cmp7 complexes we added WT Vps4 to

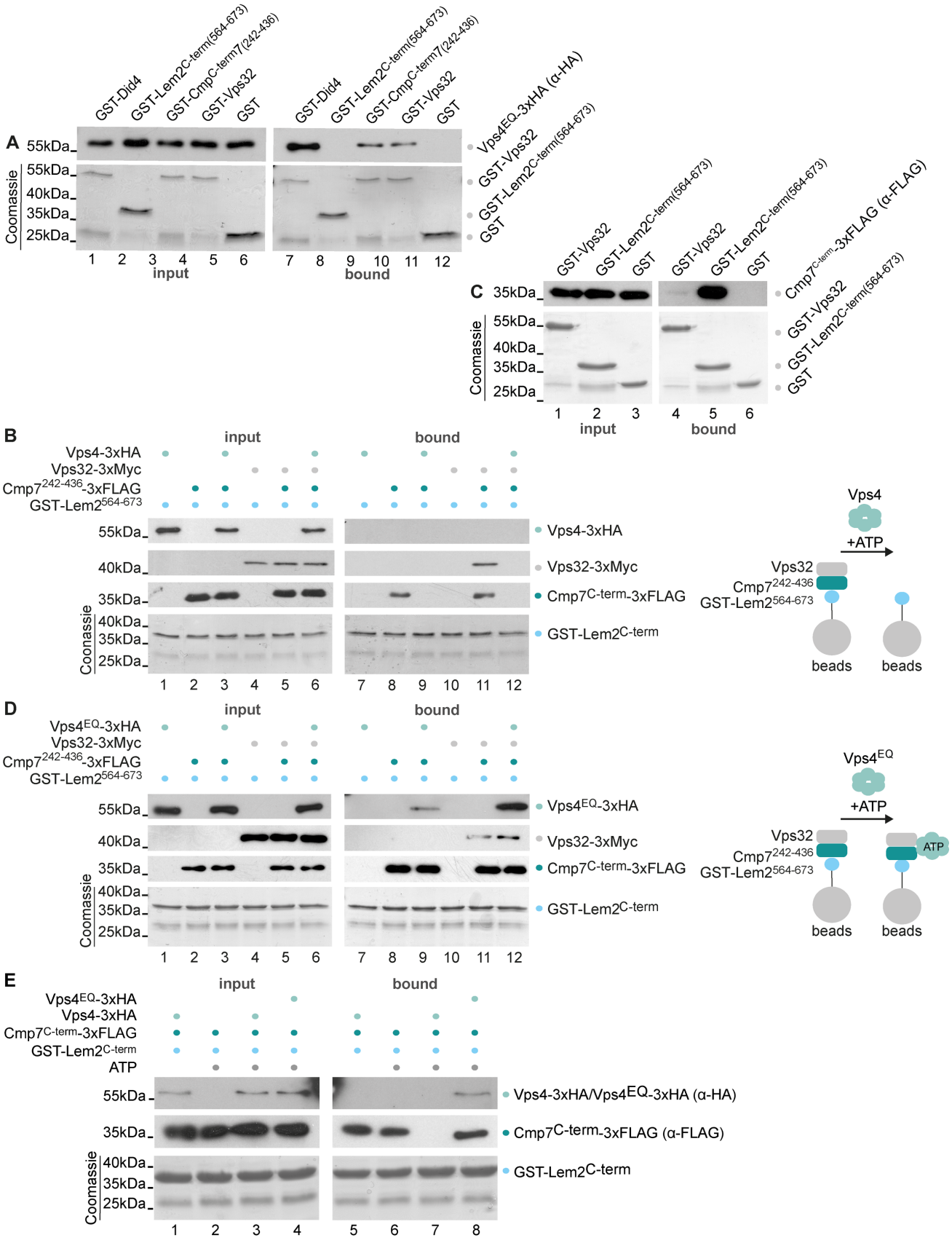

Figure 5-1. Vps4 disassembles a Lem2-Cmp7 complex.

A) *In vitro* binding experiment. An ATPase dead Vps4^{EQ} that can bind to its substrates but cannot hydrolyse ATP was added to glutathione beads coated with GST-Did4, GST-Lem2^{Cterm}, GST-Cmp7^{Cterm}, GST-Vps32 or just GST. Vps4^{EQ} bound strongly to Did4 and less strong to Cmp7$^{C\text{-}term}$ and Vps32. No binding of Vps4^{EQ} to Lem2$^{C\text{-}term}$ could be detected. **B)** *In vitro* binding assay. GST-Lem2$^{C\text{-}term}$ captured at glutathione beads was first incubated with Cmp7$^{C\text{-}term}$ with or without Vps32 followed by wash-out of the unbound protein. This complex was then incubated with Vps4. Binding experiments were performed in the presence of ATP. The left panel shows the protein input with Coomassie staining for Lem2$^{C\text{-}term}$ and by Western-blotting for ESCRT-III/Vps4. The right panel shows the proteins recovered from Lem2-C-term-bound beads after the binding reactions. A schematic overview of experimental setup and results the experiment is presented to the right **C)** *In vitro* binding experiment similar to Fig. 5-1A. Cmp7$^{C\text{-}term}$ was added to glutathione beads coated with GST-Vps32, Lem2^{Cterm} or GST. **D)** *In vitro* binding experiment similar to Fig. 5-1C except that Vps4^{EQ} was added instead of WT Vps4. **E)** *In vitro* binding assay. WT Vps4 or Vps4^{EQ} was added to preformed Lem2-Cmp7 complexes in the presence or absence of ATP.

preformed Lem2-Cmp7 complexes in the absence of ATP. We observed that in this scenario Vps4 was no longer able to disassemble the Lem2-Cmp7 complex (Fig. 5-1E; compare lane 5 to lane 7).

In conclusion, these results suggest that Vps4 can disassemble the interaction specifically between Cmp7 and Lem2 *in vitro*. This also confirmed our genetic data that Lem2 is upstream of ESCRT-III and that recruitment of Vps4 requires ESCRT-III to bind to Lem2. Of note, we did not include Nur1 in this experiment. However, ESCRT-III/Vps4 is no longer recruited to the tail in *nur1Δ* cells (Fig. 4-3C). This suggests that in living cells Lem2 does require Nur1 for its functions. This is confirmed by our data showing that Nur1 stabilises Nur1 for example at the tails (Fig. 3-1E).

The fact that Vps32 binds stronger to Cmp7 in the presence of Lem2 suggests that binding of Cmp7 to Lem2 might induce some sort of conformational change that is recognised by Vps32, similar to the “open” or “activated” form of ESCRT-III subunits which can polymerise and associate with membranes (Schöneberg *et al.*, 2016). Alternatively, Vps32 might recognise a binding interface consisting of both Lem2 and Cmp7. Our data also for the first time shows the *in vitro* reconstitution of a functional ESCRT-III/Vps4 system with non-canonical components. Notably, this *in vitro* system is in the absence of any lipid membranes, suggesting that the function of ESCRT-III/Vps4

in associating with and remodelling transmembrane proteins does not depend on association with membranes.

5.2 Lem2 and ESCRT-III form nuclear envelope clusters in the absence of Vps4

We wanted to test if our *in vitro* model also applied to live cells. We asked if the absence of Vps4 would also cause Lem2-Cmp7 interaction to be maintained in cells and what the consequences of this would be. We therefore constructed a GFP tagged Vps4^{EQ} mutant and introduced it into *S. japonicus*, replacing the original allele under the control of the endogenous Vps4 promoter. Vps4^{EQ}-GFP endosomal foci were much brighter and appeared to be bigger in this mutant, consisting with its substrate trapping ability (Fig. 5-2A). It also became trapped onto large NE clusters together with Lem2 (Fig. 5-2A). Suggesting that Vps4^{EQ}-GFP was trapped onto Lem2-ESCRT-III complexes, similar to the *in vitro* system.

We next asked if we could also observe Lem2-Cmp7 association in live cells. We constructed strains expressing Cmp7-LAP-mNeonGreen and Lem2-mCherry. In WT cells, Cmp7-LAP-mNeonGreen around the cell cortex and not really around the NE (Fig. 5-2B), indicating ER localisation as previously observed for the budding yeast and human Cmp7 orthologues (Bauer *et al.*, 2015; Olmos *et al.*, 2016). Of note, in yeasts most ER is anchored to the plasma membrane through plasma membrane-ER specific tethers (Voeltz *et al*., 2002). However, in cells lacking Vps4 function Cmp7 and Lem2 were found together in big clusters on the NE (Fig. 5-2B), similar to their strong association *in vitro* in the absence of Vps4. Notably, these clusters contained the entire Lem2-Nur1 complex (Fig. 5-2C).

All core ESCRT-III mutants exhibited Lem2 clustering, however not all to the same extend (Fig. 5-2D). Some residual Lem2 was found on the NE in *cmp7Δ*, *vps24Δ* and *did4Δ* mutants, whereas the clustering phenotype was strongest in *vps32Δ* and *vps4Δ* mutants (Fig. 5-2D). Thus, the severity of this clustering phenotype did not directly correlate to failed nucleocytoplasmic compartmentalisation. However, the compartmentalisation phenotype did correlate to whether Vps4 was found in these clusters, as *cmp7Δ* and *vps32Δ* clusters were devoid of Vps4 and naturally in *vps4Δ* mutants there is also no Vps4 in these clusters (Fig. 5-2E). Of note, this suggested that *in vivo*, unlike *in vitro*, Vps32 was essential to recruit Vps4 to Lem2 and Cmp7. In the

absence of Vps24 and Did4, Lem2 clusters were smaller in size and contained Vps4 (Fig. 5-2E). Thus, in these mutants Vps4 could be at least partially functional and disassemble Lem2-Cmp7-Vps32 complexes at the NE. Lem2 localisation was not affected by the loss of ESCRT-0, -I and –II function (Fig. 5F), further proving that only ESCRT-III functions on the NE in a Cmp7 dependant fashion.

To analyse how Lem2 cluster arise we constructed a temperature sensitive Vps4 mutant, Vps4^{ts}-GFP (*vps4*-^{I307T,L327S};Babst *et al.*, 1997), and combined it with the Lem2-mCherry marker. We used this mutant to acutely inactive Vps4 and used the NE marker Nup189-GFP and SPB marker Sad1-mNeonGreen as guides to quantify Lem2 fluorescent intensity on the NE. At the permissive temperature of 25°C, Lem2 remained largely distributed around the NE and the SPBs, although we detected a few Lem2 clusters at the NE, suggesting that Vps4^{ts}-GFP behaved as a hypomorph (Fig. 5-2G). When shifted to the restrictive temperature of 36°C, Lem2 progressively incorporated into NE clusters (Fig. 5-2G). Over time, Lem2 around the NE disappeared, whereas the Lem2 level in clusters increased (Fig. 5-2G). This suggested that continuous Vps4 activity is required to prevent the formation of persistent Lem2 clusters at the INM during interphase.

In conclusion, using an *in vitro* system we identified that Vps4 can specifically disassemble the interaction between Lem2 and Cmp7. In the absence of Vps4 these two proteins can form a stable complex. We observed a similar phenomenon in living cells, were in the absence of Vps4 function Lem2-Nur1 and ESCRT-III formed large aggregates on the NE. We found that different ESCRT-III subunits were differentially required for the formation of these aggregates. In the absence of Vps24 and Did4 Lem2 was still largely distributed around the NE. NE clusters in these mutants did contain Vps4. In the absence of Vps32 and Vps4 Lem2 form very large clusters, with almost no free Lem2 found on the NE. In the absence of Cmp7 we found smaller clusters and also free Lem2 on the NE, however these clusters contained no Vps4. We interpret these results as evidence that Cmp7 plays an integral role in driving the formation of these strong clusters. Thus, in the absence of Cmp7 large clusters cannot be formed anymore. This is consistent with our *in vitro* data that places Cmp7 upstream of all the ESCRT-III/Vps4 components. Indeed, when we did add not Cmp7 to our *in vitro* reaction, or when we deleted *cmp7* from cells, we observed no ESCRT-III complexes formed on Lem2.

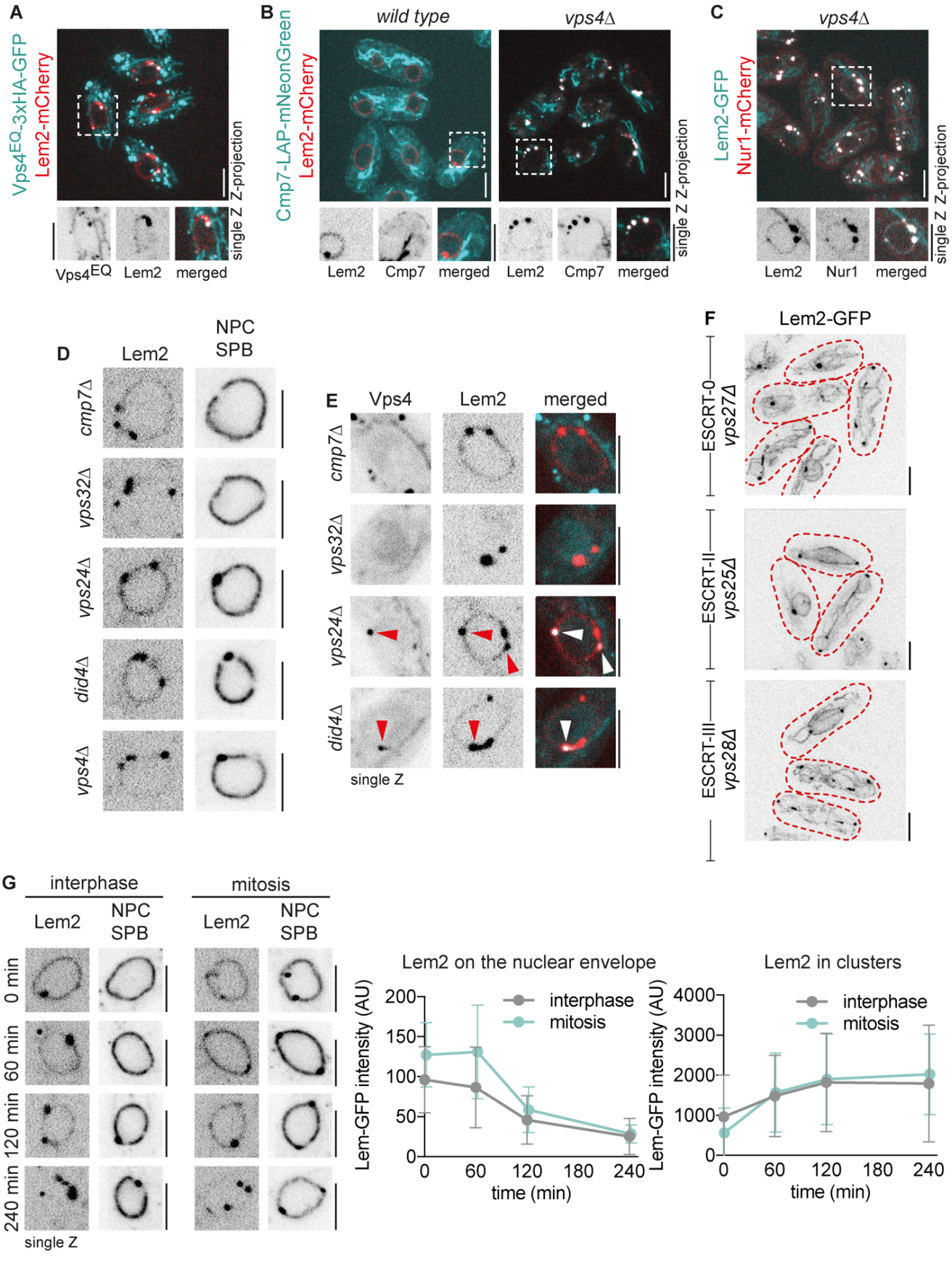
A
Vps4EQ-3xHA-GFP
Lem2-mCherry
single Z Z-projection
Vps4EQ
Lem2
merged
B
wild type
vps4Δ
Cmp7-LAP-mNeonGreen
Lem2-mCherry
single Z Z-projection
Lem2
Cmp7
merged
C
vps4Δ
Lem2-GFP
Nur1-mCherry
single Z Z-projection
Lem2
Nur1
merged
D
Lem2
NPC SPB
cmp7Δ
vps32Δ
vps24Δ
did4Δ
vps4Δ
E
Vps4
Lem2
merged
single Z
F
Lem2-GFP
ESCRT-0 vps27Δ
ESCRT-II vps25Δ
ESCRT-III vps28Δ
G
interphase
mitosis
Lem2
NPC SPB
0 min
60 min
120 min
240 min
single Z
Lem2 on the nuclear envelope
Lem-GFP intensity (AU)
interphase
mitosis
time (min)
Lem2 in clusters
Lem-GFP intensity (AU)
interphase
mitosis
time (min)

Figure 5-2. Lem2 and ESCRT-III form nuclear envelope clusters in the absence of Vps4.

A) A maximum projection of a spinning disk confocal Z-stack of interphase cells expressing Vps4^{EQ}-GFP and Lem2-mCherry. Magnified single Z-slice images focus on colocalisation of Vps4^{EQ} with Lem2 in clusters at the NE. **B)** Maximum projections of spinning disk confocal Z-stacks of WT and *vps4Δ* cells expressing Cmp7-LAP-mNeonGreen and Lem2-mCherry. Magnified single Z-slices show ER localisation of Cmp7 and NE/SPB localisation of Lem2. Note that Cmp7 could only be faintly detected on the cortical ER. High mitochondrial autofluorescence is visible because of weak specific signal. **C)** Maximum projection of a spinning disk confocal Z-stack of *vps4Δ* cells expressing Lem2-GFP and Nur1-mCherry. **D)** Nuclei of cells expressing Lem2-mCherry Nup189-GFP Sad1-mNeonGreen of indicated genotypes. **E)** Nuclei of cells expressing Vps4-GFP and Lem2-mCherry of indicated genotypes. Arrows represent Lem2 NE clusters overlapping with Vps4 signal. **F)** Maximum projection images of spinning disk confocal Z-stacks of early ESCRT mutants expressing Lem2-GFP. **G)** Time course experiment of cells expressing Lem2-mCherry Nup189-GFP Sad1-mNeonGreen in the temperature sensitive Vps4ts-GFP background. Cells grown at 25°C were shifted to 36°C to inactivate Vps4ts and samples were taken at 0, 1, 2 and 4 hours. Quantification of Lem2 fluorescence intensity at the NE and in clusters is presented for interphase and mitotic cells (n=2 experiments, at least 30 cells for each experiment per time-point).

5.3 Dynamic and persistent localisation of ESCRT-III/Vps4 to the nuclear envelope during interphase

We asked if we could also observe ESCRT-III/Vps4 at the NE when the machinery was fully functional. We observed persistent NE-associated foci of Vps4-GFP in 16.6% of WT interphase cells (Fig. 5-3A; typically one Vps4-GFP object per nucleus). The frequency of these foci was not affected by the deletion of *vps25* but they were no longer present when *lem2* or *cmp7* were deleted (Fig. 5-3A), suggesting that they follow the same recruitment rules and biogenesis as in our *in vitro* system and the large Lem2-ESCRT-III aggregates observed in ESCRT-II/Vps4 mutants (Fig. 5-2). We hypothesise that these clusters are indeed similar to those observed in ESCRT-III/Vps4 mutants. Thus, in WT cells we also could observe unresolved Lem2-ESCRT-III interactions which are also bound by Vps4.

We next used the *vps25Δ* background to attempt to visualise ESCRT-III/Vps4 events at the NE that do not result into unresolved clusters. We used very short shutter times and confocal Z-sectioning to scan entire interphase nuclei over a period of 5 minutes. Using this method, we were able observe very transient enrichments of Vps4

at the NE (Fig. 5-3B, C). These likely represented real events, as they colocalised directly with the NE and their intensity was notably higher compared to the free cytosolic Vps4 and the green channel intensity on another part of the same NE (Fig. 5-3B, D). We were also able to observe these events for Vps24 (not shown). It is unlikely that these numbers reflect the true amount of Vps4 events on the NE. We only scanned each nucleus every 10 seconds, therefore we lack some temporal information related to frequency and duration of these events. As we analysed this data by eye we likely missed many events with weaker intensity. Additionally, we excluded many potential enrichment events when their intensity was only marginally above background. Considering that functional ESCRT-III/Vps4 events require hexameric Vps4, and cytosolic Vps4 is usually monomeric (Adell *et al*., 2017), we suggest using for example fluores

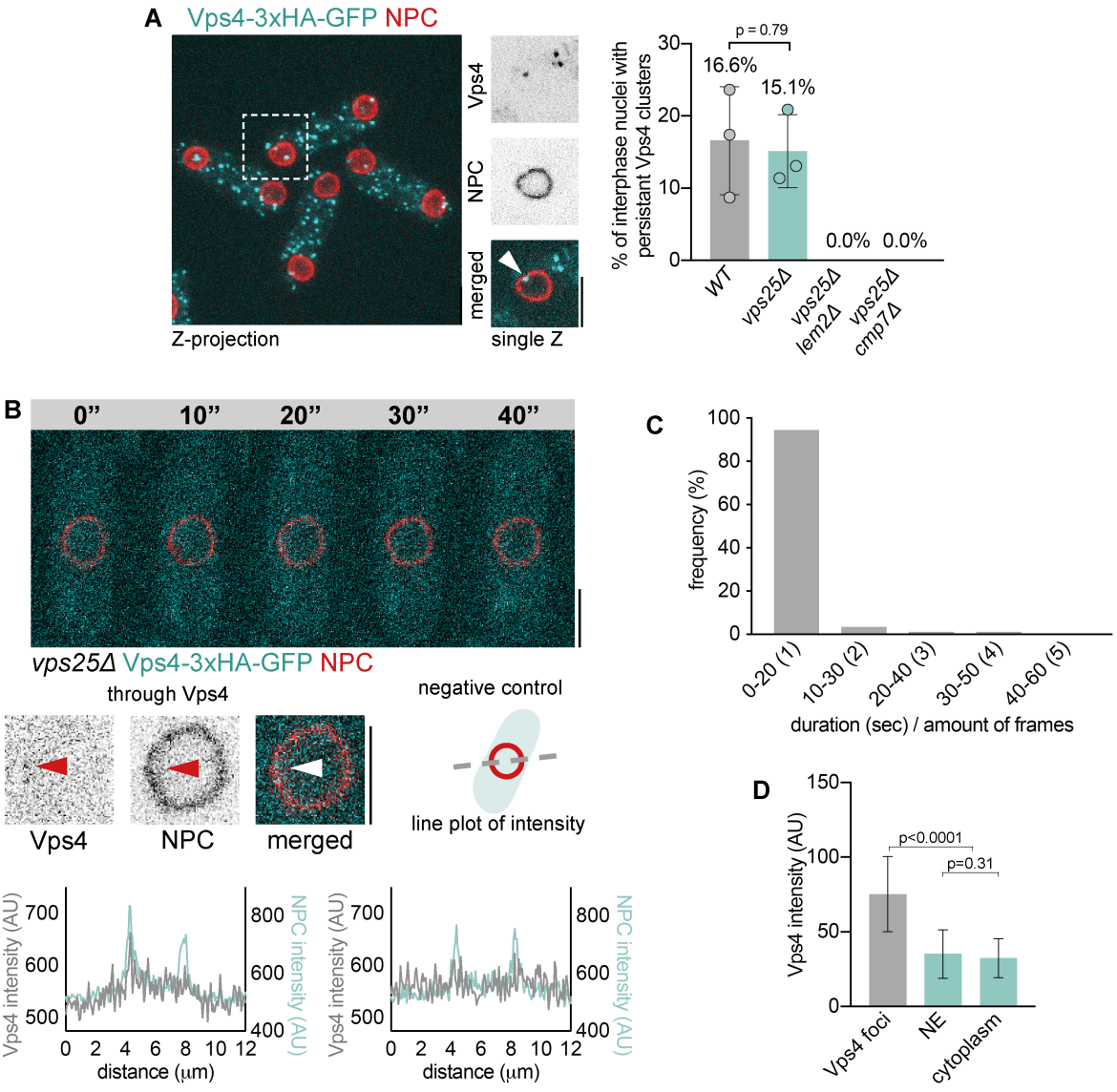

Figure 5-3. Dynamic and persistent localisation of ESCRT-III/Vps4 to the nuclear envelope during interphase.

A) Z-projection spinning disk confocal image of cells expressing Vps4-GFP and Nup189-mCherry. Magnified image below of a nucleus exhibiting a persistent Vps4 focus on the NE. Presented is a graph showing the percentage of interphase cells of indicated genotypes harbouring a persistent Vps4 focus at the NE (n=3 experiments with at least 40 cells counted for each experiment; error bars indicate standard deviation; T-test). Note that no persistent clusters were observed in *lem2Δ vps25Δ* or *cmp7Δ vps25Δ* mutants. **B)** Time lapse sequence of a single confocal Z-slice of a cell expressing Vps4-GFP Nup189-mCherry in the *vps25Δ* genetic background. Magnified image of the 20" timepoint is presented below. Quantification of the fluorescent intensity of the Vps4 and Nup189-GFP signals with a line-scan through the Vps4 cluster is presented. A similar line scan through a different region of the same nucleus is presented as a negative control. **C)** Quantification of the frequency of transient Vps4 foci on the NE. Data represents 93 nuclei imaged for 5 min each. **D)** Quantification of the fluorescent intensity of the Vps4 signal at indicated locations of the 93 nuclei of (C).

fluorescence correlation spectroscopy (FCS) or other methods of single molecule counting to assess physiological ESCRT-III/Vps4 function at the NE. Nonetheless, we have shown that transient Vps4 recruitment occurs on the NE, suggesting constant monitoring of the NE by the ESCRT-III/Vps4 system. We hypothesise that these transient events, when not resolved, can result in the formation of persistent Lem2-ESCRT-III/Vps4 aggregates on the NE.

5.4 The C-terminal MSC domain of Lem2 likely interacts with ESCRT-III

Our *in vitro* data suggested that Lem2 interacts directly with Cmp7. We set out to identify what region of Lem2 is responsible for this interaction. We created C-terminally tagged truncations of the HEH-domain (Lem2$^{\Delta HEH}$-GFP) and the nucleoplasmic part of the MSC domain (Lem2$^{\Delta MSC}$-GFP) and analysed their localisation pattern using live-cell time-lapse microscopy. Lem2$^{\Delta HEH}$-GFP localised like WT, although the nuclear Lem2 signal appeared slightly lower (Fig. 5-4A). However, the localisation of Lem2$^{\Delta MSC}$-GFP was very similar to that of Lem2 in the *cmp7Δ* mutant (Fig. 5-4A). Lem2 appeared clustered throughout interphase, but these clusters disappeared during mitosis. Immediately after mitosis, these Lem2 clusters returned (Fig. 5-4A). This suggested that

the nucleoplasmic MSC-domain of Lem2 is responsible for interaction with Cmp7 and this interaction is required for the proper localisation of Lem2.

We aimed to pinpoint the amino-acid residues responsible for this interaction. The Lem2 MSC domain contains several residues that are highly conserved throughout eukaryotes (Mans *et al.*, 2004). We noted that a short stretch containing several highly conserved residues bore striking resemblance to the MIM1 motif found on ESCRT-III subunits that is responsible for interaction with Vps4 (Fig. 5-4B; Obita *et al.*, 2007). Based on the structural model of the human MAN1 nucleoplasmic MSC domain we determined that these residues were part of an α-helix (Caputo *et al*., 2006). When we disrupted this α-helix by making a nine amino acid truncation (Lem2$^{\Delta aHEL}$-GFP) or by mutating the four conserved residues L626, R629, L630 and L633 to aspartic acid (Lem2$^{aHEL\text{-}4D}$-GFP), we observed a similar localisation pattern as the full MSC truncation (Fig. 5-4A). The single mutant of Lem2^{L630D}-GFP also phenocopied the full MSC deletion, however the Lem2^{L629D}-GFP mutant did not, suggesting that the latter did not destabilise this α-helix (Fig. 5-4A).

We combined the Lem2$^{aHEL\text{-}4D}$-GFP mutant with a synthetic nucleoplasmic fluorescent marker GST-NLS-mCherry to assess whether the clustering phenotype of Lem2 is correlated to defects in establishing nucleocytoplasmic compartmentalisation. Indeed, we found that Lem2$^{aHEL\text{-}4D}$-GFP cells had a similar compartmentalisation phenotype to deletion mutants of Lem2-Nur1 and ESCRT-III/Vps4 (Fig. 5-4C).

In conclusion, mutants affecting an α-helix in the C-terminal domain of Lem2 phenocopy ESCRT-III mutants in both Lem2 localisation and establishment of compartmentalisation. Of note, despite similarity of this α-helix to the MIM1 motif of ESCRT-III, we do not think that Lem2 contains a true MIM1 motif since Lem2 does not interact directly with Vps4 (Fig. 5-1). Instead, we suggest that Lem2 interacts with Cmp7 through this α-helix. When Lem2 fails to interact with ESCRT-III, either through deletion of *cmp7* or by disruption of the α-helix on Lem2 that is responsible for interaction with Cmp7, Lem2 forms clusters on the NE. This further proves that Lem2 needs constant interaction with ESCRT-III/Vps4 to maintain its proper localisation around the NE.

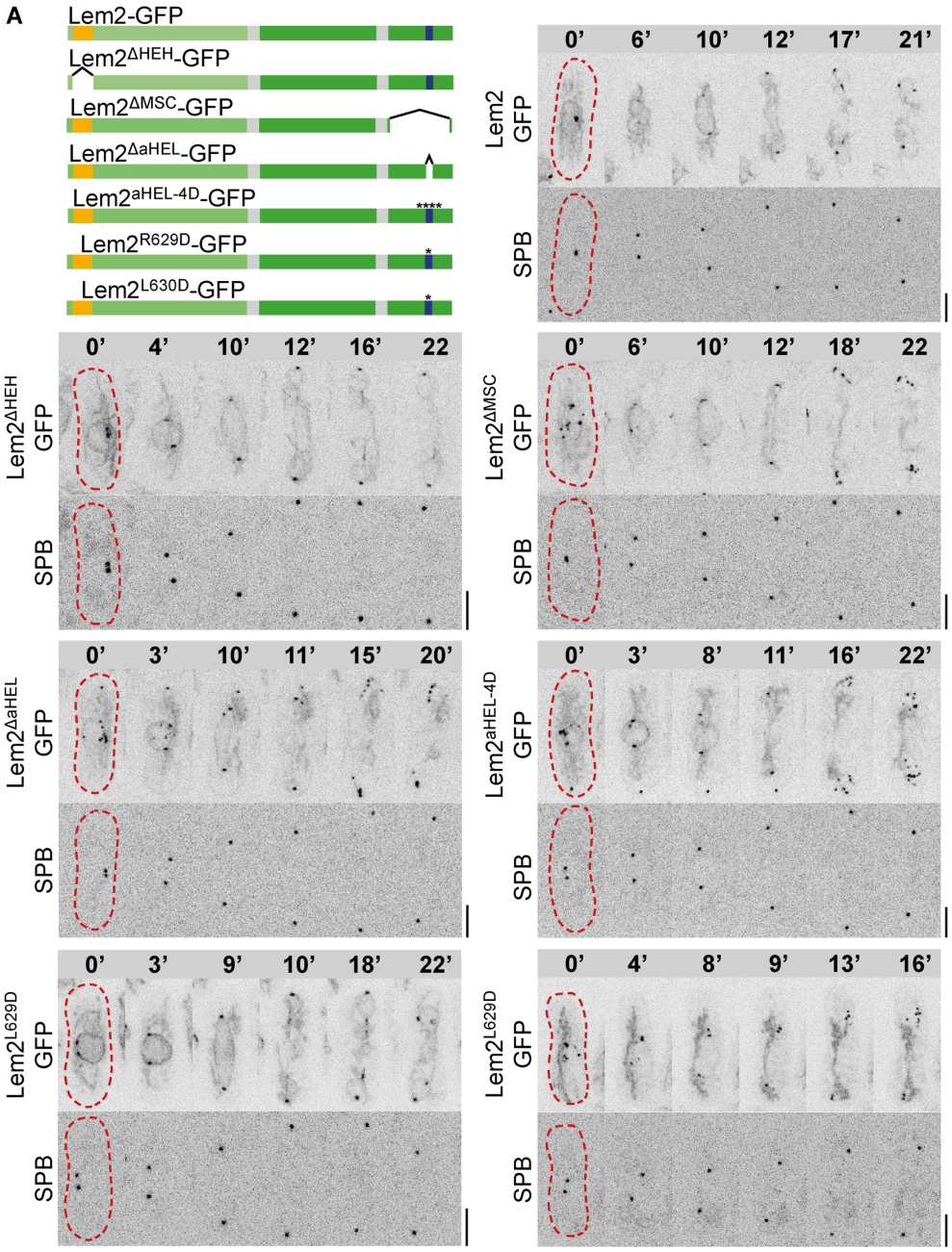

B

S.japonicus	lem2	623	.SKHLENRLWSLVVNK.	627
S.pombe	lem2	627	.TKATARTLWEAIVER.	641
S.japonicus	did4	194	.TISSGLNLEDLAHIR	208
S.pombe	did4	198	.EDNLQARLDELAKR	210
S.cerevisiae	vps2	218	.DDDLQARLNTLKKQ	231
H.sapiens	CHMP2A	210	.DADLEERLKNLRRD	222
S.japonicus	vps24	225	.ILDIRGRLDALKS	237
S.pombe	vps24	219	.LLDIRDKLDALKS	231
S.cerevisiae	vps24	212	.VNEMRERLRALQN	224
S.cerevisiae	chm7	413	.SEDLLKRLNNLKINT.	425
MIM1 consensus			DxxLxxRLxxLR	
			E K	

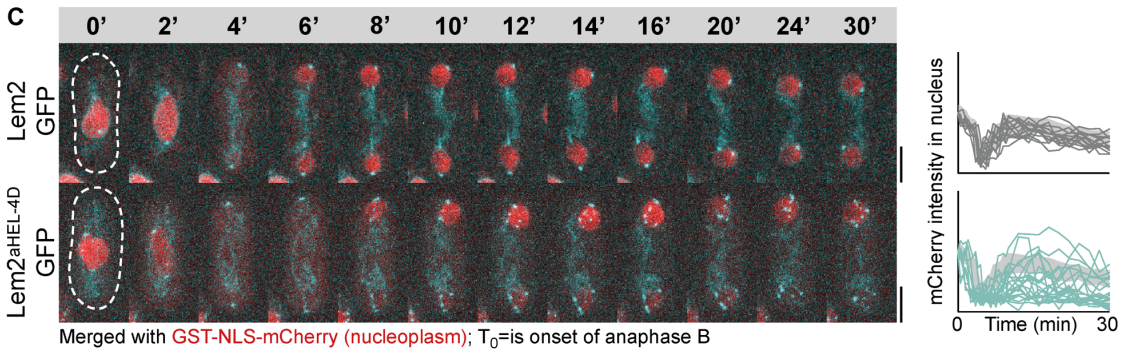

Merged with GST-NLS-mCherry (nucleoplasm); T_0=is onset of anaphase B

Figure 5.4. Mutants of the C-terminal domain of Lem2 mimic ESCRT-III deletions.

A) Time-lapse images of representative cells expressing Lem2-GFP and GFP tagged Lem2 mutants and Pcp1-mCherry (SPB). **B)** Alignment of a stretch of the C-terminal MSC-domain of Lem2 and the MIM1 motif of ESCRT-III subunits. **C)** NE sealing assay, similar to Fig. 3.3 but using GST-NLS-mCherry as a marker for nuclear integrity. N=7 for WT and N=11 for Lem2$^{MIM1\text{-}4D}$-GFP.

5.5 Lem2 and Nur1 interact through their lumenal domains

Next, we wondered which domain of Lem2 is responsible for interaction with Nur1. We hypothesised that any truncation mutant of Lem2 that does not interact with Nur1 should abolish Nur1 localisation to the nucleus, similar to what we observed in *lem2Δ* mutants (Fig. 3.1C). The budding yeast LEM-domain protein Heh1 was shown to interact with NPC component Pom152 through its lumenal domain (Yewdell *et al.*, 2011), we therefore additionally created a C-terminally tagged truncation mutant of Lem2 lacking the lumenal domain. We combined the Lem2$^{\Delta LUMEN}$-GFP mutant with Nur1-mCherry. Indeed, in this mutant we observed that Nur1 was excluded from the nucleus, becoming primarily localised to the ER (Fig. 5-5A). Likewise, the localisation of Lem2$^{\Delta LUMEN}$-GFP was affected. We observed asymmetric localisation of Lem2 to the tails and also observed that the distribution of Lem2 around the NE became less homogeneous (Fig. 5-5A).

Using co-IP it was shown that in *S. pombe* Lem2 and Nur1 directly interact (Banday *et al.*, 2016), although the domains responsible for this interaction were not identified. Interestingly, a computational transmembrane helix prediction method, predicts that *S. japonicus* only has three transmembrane domains, as compared to the four domains predicted for *S. pombe* and *S. octosporus* (Fig. 5-5B). This potentially translocates the most C-terminal lumenal domain to the nucleoplasm. Additionally, the budding yeast Nur1 was predicted to only have two transmembrane helices (Godfrey *et al*., 2015). We conclude that at least in *S. japonicus* Lem2 and Nur1 likely interact through their lumenal domains. Apart from the lumenal interaction between Heh1 and Pom152 in budding yeast (Yewdell *et al.*, 2011), the lumenal domain of Lem2 has not been functionally studied before. Furthermore, the lumenal domains of many INM proteins tend to be ignored as their primary function are in the nucleoplasm. However, it is possible that the NE lumen forms an important site for the interaction of many INM proteins.

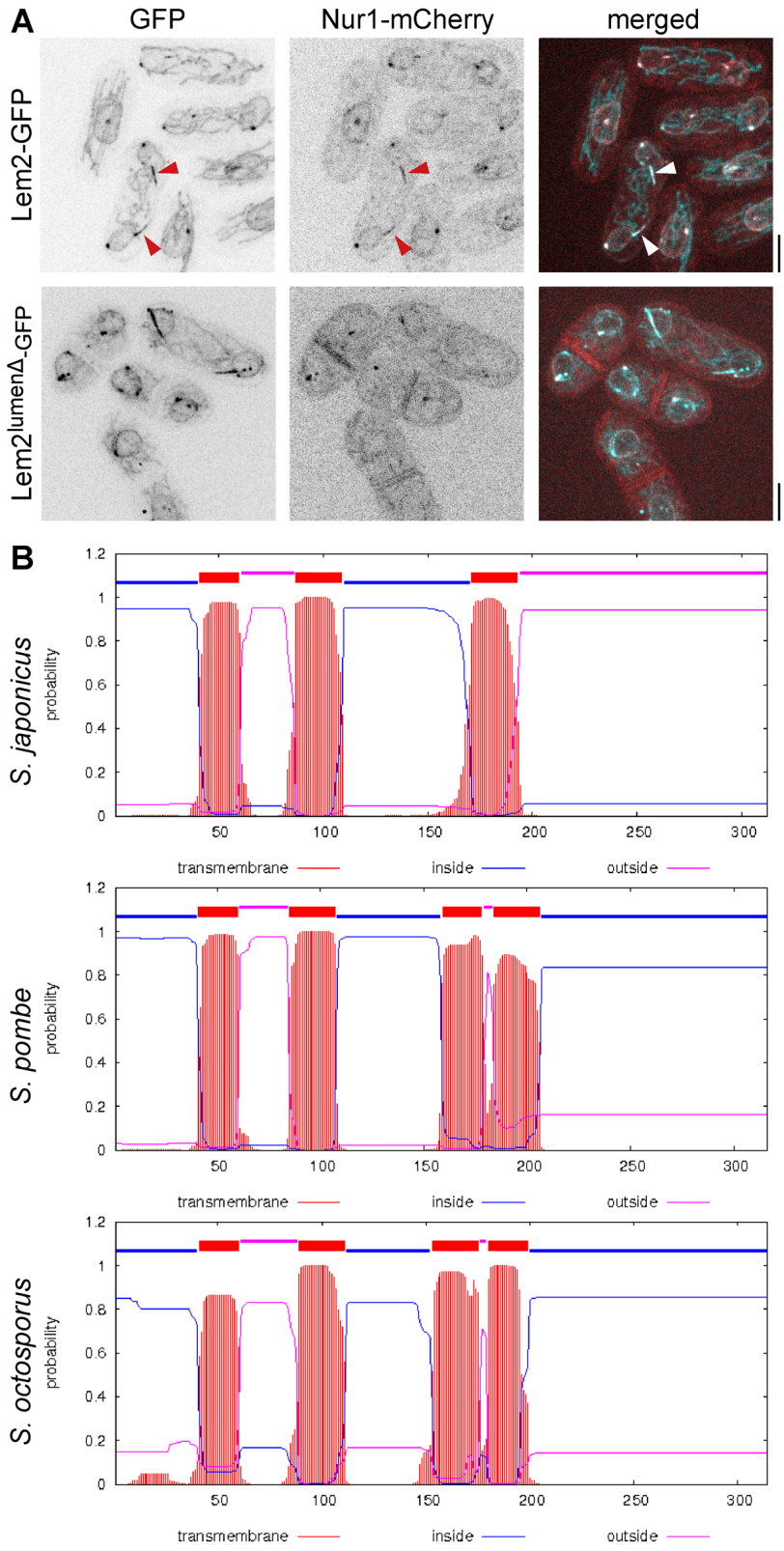

Figure 5-5. Lem2 and Nur1 interact through their lumenal domains.

A) Cells co-expressing Lem2-GFP and Nur1-mCherry for the indicated genotypes. Arrows indicate their enrichment at the tail structures. WT images are the same as presented in Fig. 3-1C. **B)**

Transmembrane helix prediction for fission yeast Nur1 orthologues analysis using the TMHMM online prediction tool.

5.6 Lem2 nuclear envelope clusters exclude nuclear pore complexes

In budding yeast NPCs become clustered in a small fraction of cells (~10%) of ESCRT-III/Vps4 mutants and *heh1Δ* or *heh2Δ* mutants (Webster *et al.*, 2014). The budding yeast Cmp7 orthologue Chm7 can form clusters on the NE which correspond to these NPC clusters (Webster *et al.*, 2016). These NPC clusters were termed "SINCs" and are thought to be storage domains of misassembled NPCs (Webster *et al.*, 2014). We therefore asked if the Lem2-ESCRT-III/Vps4 clusters that we observed correlate to such structures as well. We analysed two of the NPC components which are enriched in SINCs, Nup184 and Nup85 (*S. cerevisiae* Nup188 and Nup85) and found that they were excluded from Lem2 clusters in *vps4Δ* cells (Fig. 5-6). Of note, we have never seen any clustering of NPCs in exponentially growing cells either in the WT or in ESCRT-III/Vps4 mutants (not shown). This correlates to the exclusion of Lem2 from the nuclear poles which are enriched for NPCS and the other fission yeast LEM-domain protein Man1 during anaphase (Fig. 3-2). Thus, we conclude that Lem2 clusters exclude NPCs and that generally Lem2 and NPCs appear to exclude each other, occupying different domains on the NE.

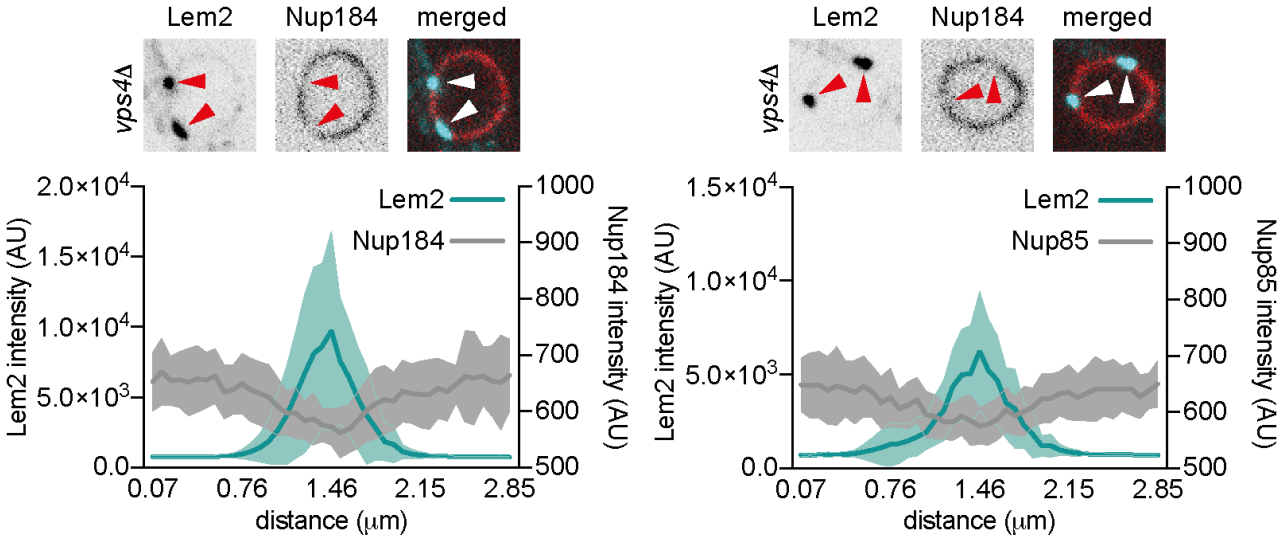

Figure 5-6. Lem2 clusters exclude NPCs.

Shown are single confocal slices of representative nuclei of cells expressing either Nup184-mCherry or Nup85-mCherry with Lem2-GFP in the *vps4Δ* genetic background. Arrows point to the Lem2

cluster that corresponds to a dip in NPC signal. Shown is the quantification of the Lem2 signal and NPC signal centred on Lem2 clusters (N=20).

5.7 Conclusions

In this chapter we have defined a mechanism by which ESCRT-III/Vps4 interacts with Lem2-Nur1. We have shown using an *in vitro* system, that ESCRT-III assemblies can form on Lem2. The AAA-ATPase Vps4 can disassemble these complexes by specifically disassembling the interaction between Lem2 and Cmp7. A $Vps4^{EQ}$ mutant that lacks ATPase activity could not dissolve this interaction and instead bound stably to the entire complex. We have shown that this mechanism is also in place in living cells. In the absence of Vps4, Lem2-Nur1 forms large clusters on the NE together with Cmp7, suggesting that the interaction between Lem2 and Cmp7 is also not disassembled in cells. In cells lacking single ESCRT-III components Lem2 also forms NE clusters. This is likely due to the inability to recruit Vps4 to these clusters, showing again that Vps4 is main force that disassembles Lem2-ESCRT-III complexes also in life cells. We have furthermore shown that Vps4 can also explore the NE in WT cells, this function likely prevents the formation of Lem2-ESCRT-III clusters. The Lem2-Nur1 complex interacts with Cmp7 through the C-terminal domain of Lem2 and the ESCRT-III like C-terminal domain of Cmp7. Next, Cmp7, together with Vps32 can recruit Vps4. Lem2 and Nur1 interact through their lumenal domains. Our data is not clear on what happens to the interaction between Lem2 and Nur1 during the process of Lem2-ESCRT-III remodelling by Vps4. Interestingly, it has been noted that the highly conserved MSC domain of human MAN1 bears structural similarity to the winged helix domain of ESCRT-II subunit Vps25 (Caputo *et al.*, 2006). Thus, it might be hypothesised that Lem2 might serve the same function as Vps25 (Teis *et al.*, 2010) in activating ESCRT-III subunits to undergo a conformational switch into the active form and assemble on Lem2.

Chapter 6 – ESCRT-III/Vps4 control heterochromatin-nuclear envelope attachments through Lem2-Nur1

6.1 Lem2-Nur1 nuclear envelope clusters correspond to heterochromatin domains

We wondered if the Lem2-Nur1-ESCRT-III nuclear envelope clusters corresponded to any specific domains on the NE. Since the Lem2-Nur1 complex is involved in heterochromatin maintenance and its tethering to the NE (Gonzalez *et al*., 2012; Banday *et al.*, 2016; Barrales *et al.*, 2016; Tange *et al.*, 2016), we analysed if the Nur1-Lem2 clusters in ESCRT-III-deficient cells co-localised with heterochromatin. As described before, in fission yeast, all heterochromatin including sub-telomeric and peri-centromeric sequences are localised to the nuclear periphery during interphase (Allshire and Ekwall, 2015) and are marked by the heterochromatin protein 1 (HP1) orthologue Swi6 (Chen *et al.*, 2008). At the NE centromeres are clustered together at the SPB and telomeres form several clusters on opposite parts of the NE. We found that in interphase most Lem2-GFP clusters were adjacent to heterochromatic domains at the INM marked by Swi6-mCherry in all ESCRT-III/Vps4 mutants (Fig. 6-1A). This suggests that Lem2-Nur1 clusters are preferentially formed on heterochromatin. In *cmp7Δ* and *vps24Δ* mutants clusters disappeared during mitosis (Fig. 5-2). Interestingly, we found that in *vps32Δ* and *vps4Δ* mutants Lem2-GFP clusters persisted and remained adjacent to Swi6 throughout mitosis (Fig. 6-1A). This observation will be explored in more detail later in this chapter. The severe association of Lem2 with heterochromatin in *vps4Δ* mutant cells was prevented in the absence of Nur1 (Fig. 6-1B). This indicated that either Nur1 linked Lem2 to heterochromatin or Lem2 requires Nur1 to be stabilised onto heterochromatin, similar to the requirement of Nur1 for Lem2 stabilisation on the tail (Fig. 3-1E).

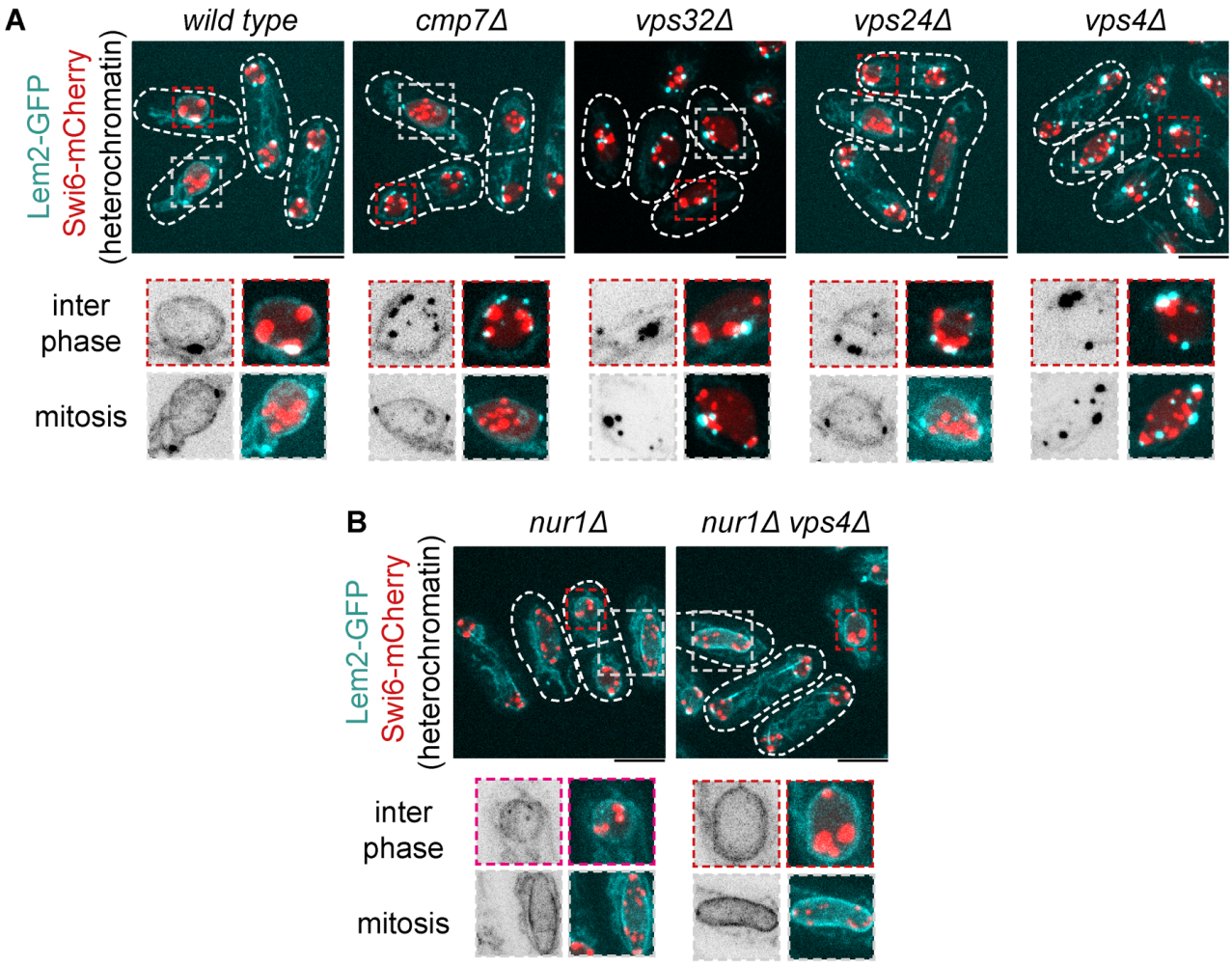

Figure 6.1. Lem2 nuclear envelope clusters correspond to heterochromatic domains.

A) Maximum projections of spinning disk confocal Z-stacks of cells of the indicated genotypes co-expressing Lem2-GFP and Swi6-mCherry (top). Interphase and mitotic nuclei are highlighted in magnified images (bottom). **B)** Same as in A) but for mutants deficient for Nur1.

6.2 Increased affinity of Lem2 for heterochromatin in the absence of Vps4

We next asked if the clustering of Lem2 adjacent to heterochromatin was due to an increased affinity of Lem2 for heterochromatin in the absence of ESCRT-III/Vps4 function. We performed chromatin-immunoprecipitation (ChIP) on Lem2-GFP followed by qPCR. We tested a WT strain, the *vps4Δ* mutant where we predict stronger affinity of Lem2 for heterochromatin, the *nur1Δ* mutant and the *vps4Δ nur1Δ* double mutant where we predict that the affinity of Lem2 is abrogated. In *S. pombe*, Lem2 binds to the central domain of the centromere (Banday *et al.*, 2016; Barrales *et al.*, 2016). This domain is where the kinetochore is assembled on CENP-A nucleosomes and does not

contain heterochromatin. The central core domain is surrounded by heterochromatic peri-centromeric DNA repeats (Allshire and Ekwall, 2015). However, *S. pombe* Lem2 was not enriched at this surrounding heterochromatin (Barrales *et al*., 2016). This same report did not find Lem2 to be enriched at sub-telomeric heterochromatin. However, using ChIP-seq another report found that *S. pombe* Lem2 was binding to only small domains of the sub-telomeric heterochromatin (Banday *et al*., 2016). This suggests that either the affinity of Lem2 for heterochromatin is not very high, or interaction is very transient.

The centromere of *S. japonicus* is markedly different from the other fission yeasts. Its sequence was not fully assembled due to the fact that it consists of retrotransposons, which have almost all been eliminated from the other fission yeasts (Rhind *et al.*, 2011). It has been suggested that the entire centromere of *S. japonicus* consists of retrotransposons covered by heterochromatin, with CENP-A assembling on particular types of retrotransposons (Tong *et al.*, 2019). Because of the unassembled centromere sequence of *S. japonicus* we could not design qPCR primers for the "central" centromere domain. We therefore tested binding of Lem2 over a region of 90kb on the left side of the centromere of chromosome 1 and over 50kb on the right side (Fig. 6-2A). We also probed for Lem2 binding in the subtelomeric region up to 65kb from the end of chromosome 1 (Fig. 6-2A).

We first tested if we could detect heterochromatin surrounding the centromere and in the subtelomeric region by doing ChIP-qPCR against H3K9 di-methylation, the main heterochromatic histone mark of the related *S. pombe* (H3K9me2; Allshire and Ekwall, 2015). Consistent with the fact that Swi6 can be found up to 50kb away from the chromosome end (Kanoh *et al.*, 2005), we found H3K9me2 over the entire tested subtelomere range, with varying levels (Fig. 6-2B). We also detected H3K9me2 surrounding the chromosome 1 centromere, with the amount of H3K9me2 tailing off further away on both sides. On the right chromosome arm the distance of heterochromatin coverage correlated more closely to that of *S. pombe* (Fig. 6-2B), where H3K9me2 spreads ~15kb away from the central centromere domain (Barrales *et al*., 2016). We did find significant H3K9me2 enrichment up to 75kb away from the centromere on the left chromosome arm, covering the region containing a large amount

of tRNA genes (Fig. 6-2B). Notably, we did not detect heterochromatin on the gene encoding actin, which is found in a gene-dense region of chromosome 2 (Fig. 6-2B).

We next investigated whether we could detect Lem2-GFP on these heterochromatic regions. Fig. 6-2C shows the Lem2-GFP ChIP results of the individual qPCR primer sets. In order to infer information about the overall effect of the genotype on Lem2-heterochromatin interaction, we combined the Lem2-GFP ChIP results of each genomic locus with high levels of heterochromatin as defined by higher than median H3K9me2 levels (Fig. 6-2E) and did the same for the peri-centromeric and subtelomeric regions (Fig. 6-3F, G). Firstly, in WT cells we only saw a very mild enrichment of Lem2 as compared to an untagged strain overall (Fig. 6-2C, D), stratifying for centromeres and telomeres we found that Lem2 in the WT was only mildly enriched on the peri-centromere (Fig. 6-3E, F, G). Importantly, in the absence of Vps4 we saw a dramatic increase in the association of Lem2 over all heterochromatic regions (Fig. 6-2C, E, F, G). This enrichment in the *vps4Δ* mutant linearly correlated to the presence of H3K9me2 (Fig. 6-2G), this highly suggests that Lem2 is indeed bound to heterochromatin in this mutant. Lem2 enrichment in the *vps4Δ* background decreased further away from the centromere and was present throughout the sub-telomeric region (Fig. 6-2C). This enrichment was rescued by the additional deletion of *nur1*, which reduced Lem2 association with both peri-centromeric and subtelomeric heterochromatin back to WT levels (Fig. 6-3C, E, F, G).

In conclusion, in the absence of Vps4 function the affinity of Lem2 for heterochromatin is drastically increased. This correlates to the enrichment of Lem2 onto heterochromatin as observed by microscopy (Fig. 6-2). Further corresponding to our microscopic observations, the strong Lem2-heterochromatin interaction is prevented in the *vps4Δ nur1Δ* mutant.

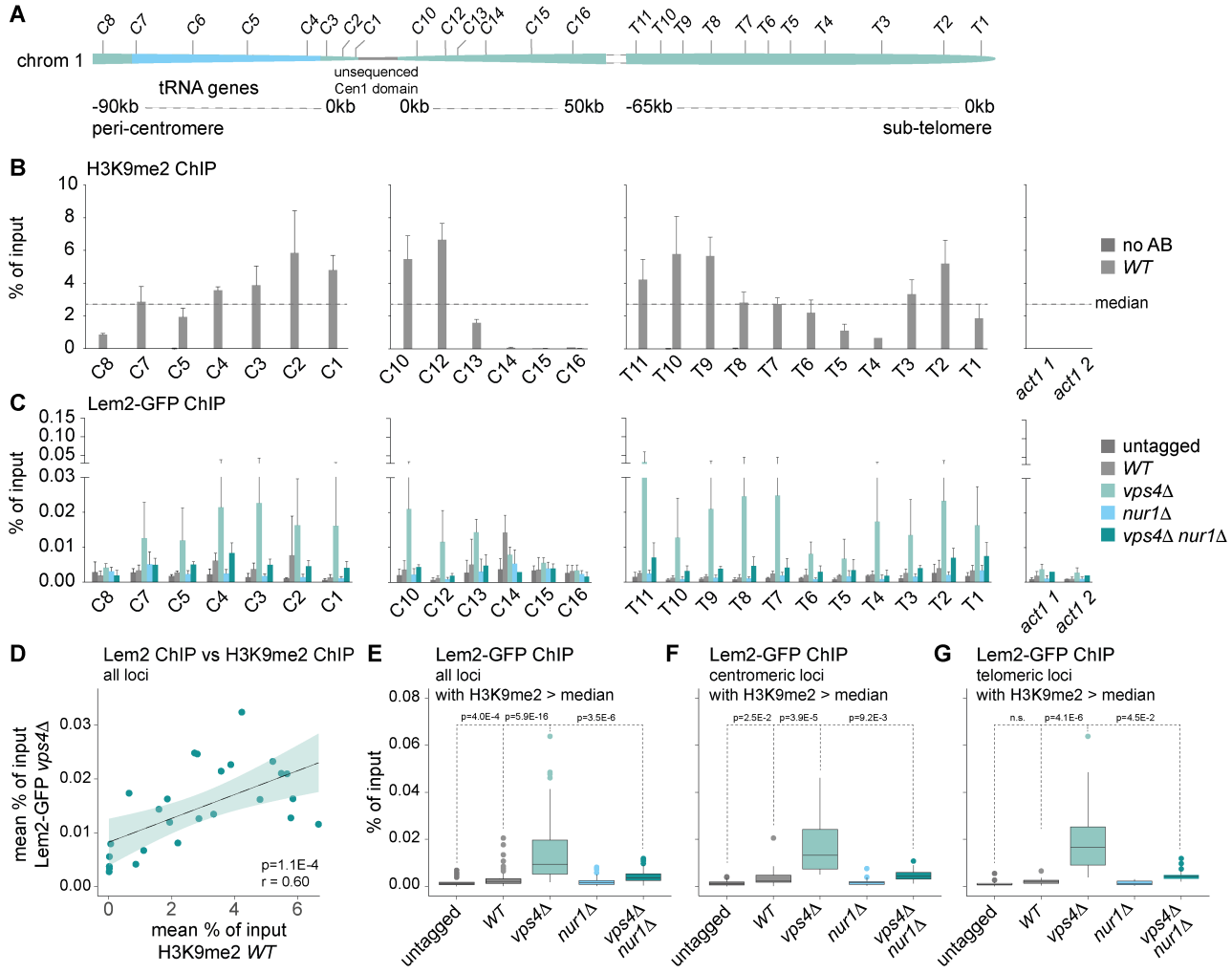

Figure 6-2. Increased affinity of Lem2 for heterochromatin in the absence of Vps4.

A) Scheme depicting the peri-centromeric and sub-telomeric regions of chromosome 1 of *S. japonicus* (not to scale). The locations of the qPCR primer sets are indicated to scale. **B)** ChIP-qPCR of H3K9me2 in WT cells (N=3). **C)** ChIP-qPCR of Lem2-GFP in strains of indicated genotypes (N=3) of the same genomic loci as in (B). **D)** Correlation plot of mean Lem2-GFP ChIP signal vs the mean H3K9me2 ChIP signal for each of the genomic loci. Dotted line corresponds to the linear trendline, shaded area corresponds to the 95% confidence interval. Pearson correlation coefficient: r = 0.60 and p = 1.1E-4. **E)** Pooled Lem2-GFP ChIP data of each of the genomic loci with higher than median H3K9me2 levels (See B). Kruskal-Wallis test, followed by Dunn post-hoc test Benjamini-Hochberg false discovery rate correction **F,G)** Same as in (E) but for the peri-centromeric and subtelomeric regions respectively.

6.3 Vps4 maintains levels of H3K9me2 at peri-centromeric and subtelomeric heterochromatin

We next wondered if the levels of H3K9me2 were affected by the higher affinity of Lem2 for heterochromatin in the *vps4Δ* mutant. We performed H3K9me2 ChIP-qPCR in the same set of mutants. Interestingly, despite the fact that much more chromatin was associated with Lem2 in the *vps4Δ* mutant (Fig. 6-2), we found significantly lower levels of H3K9me2 in this mutant (Fig. 6-3A, B). When looking specifically at the genomic loci with high heterochromatin levels we found a mild rescue of this loss in the *vps4Δ nur1Δ* double mutant (Fig. 6-3B). However, when looking at either the centromeric and subtelomeric regions alone we could not detect a rescue of this phenotype by the additional deletion of *nur1* (Fig. 6-3C, D). Thus, we conclude that in the absence of Vps4 function the heterochromatic state of peri-centromeric and subtelomeric regions is affected. We suggest that further investigation is needed to identify whether the loss of the H3K9me2 mark in the *vps4Δ* mutant is NE-chromatin tethering depended or independent.

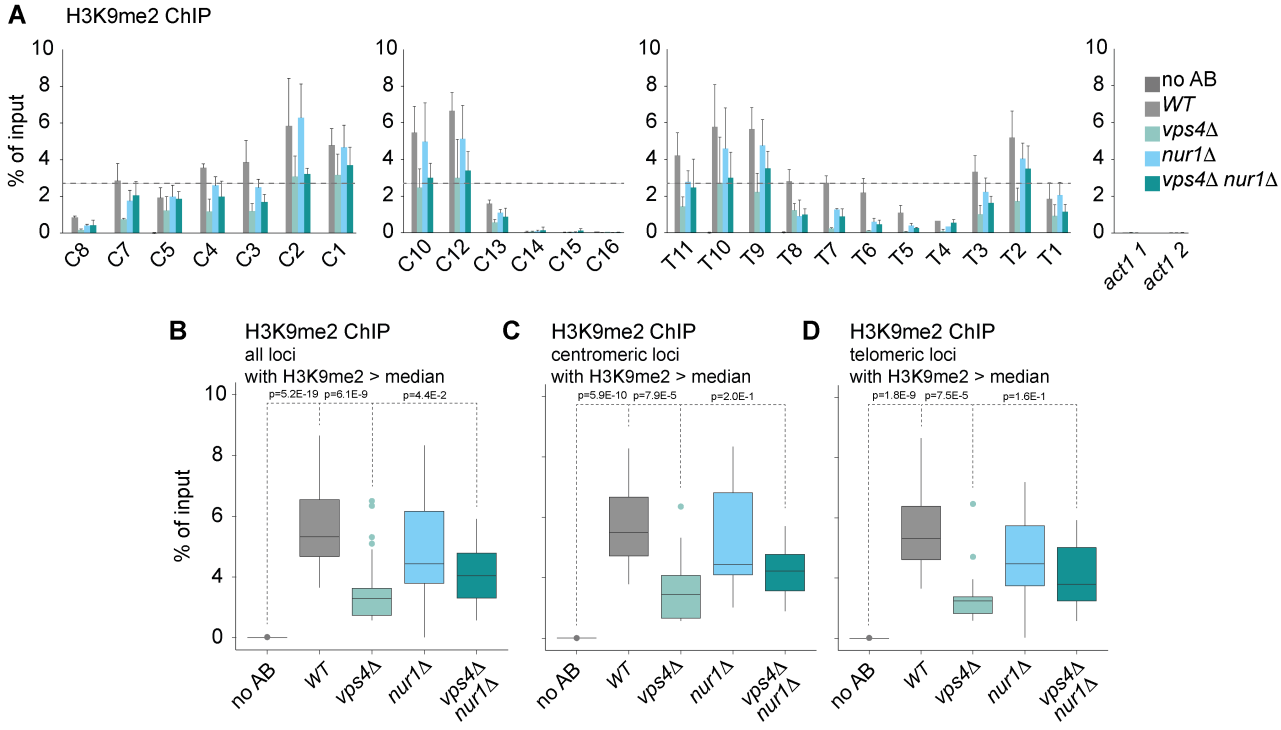

Figure 6-3. Vps4 maintains levels of H3K9me2 at peri-centromeric and subtelomeric heterochromatin.

A) ChIP-qPCR of H3K9me2 in strains of indicated genotypes on the same genomic loci as in Fig. 6-2 (N=3). **B)** Pooled H3K9me2 ChIP data of each of the genomic loci with higher than median H3K9me2

levels (See A and Fig. 6-3). Kruskal-Wallis test, followed by Dunn post-hoc test Benjamini-Hochberg false discovery rate correction **C, D)** Same as in (B) but for the peri-centromeric and subtelomeric regions respectively.

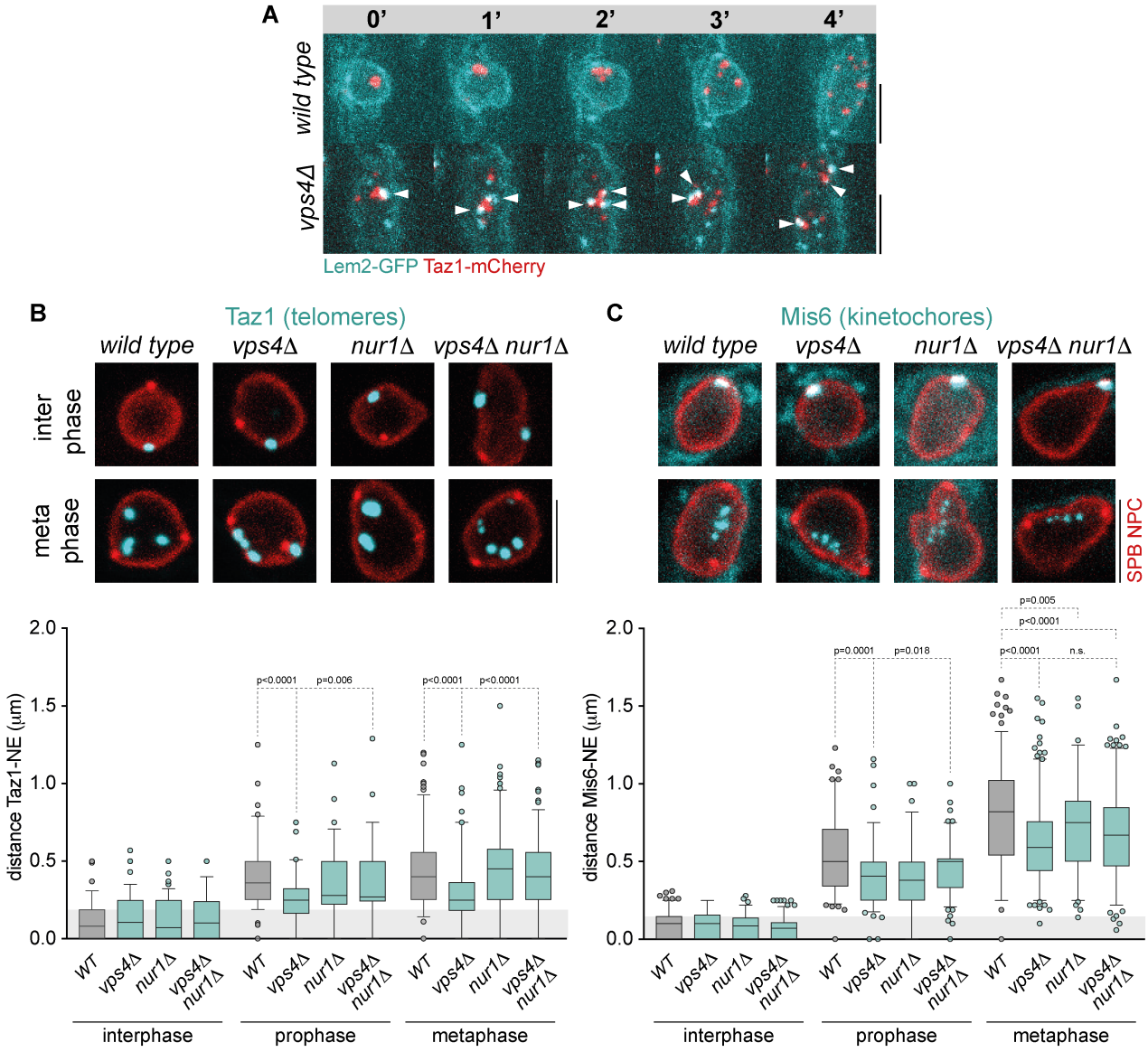

Figure 6-4. Persistent association of chromatin with the nuclear envelope throughout mitosis.

A) Time-lapse maximum projection sequences of WT and *vps4Δ* cells expressing Lem2-GFP and Taz1-mCherry, focusing on mitotic nuclei. Arrows indicate the fate of a single Lem2-associated telomere cluster that splits and the separated telomeres that stay associated with Lem2 throughout mitosis. **B)** Z-projections of the middle confocal slices of nuclei of WT and *vps4Δ* cells expressing Taz1-GFP Nup189-mCherry Pcp1-mCherry. Box-plots of the quantification of Taz1-NE distance at indicated stages of the cell cycle are presented. Quantification of Taz1-NE distance is described in Materials

and Methods. Shown in gray is the lower three quartiles of the WT interphase data. Kruskal-Wallis test Dunn's test for multiple comparisons, multiplicity-adjusted p-values are presented. **C)** Same set-up as in (B) but for Mis6-NE distance.

6.4 Persistent association of chromatin with the nuclear envelope throughout mitosis

S. japonicus, like other eukaryotes, releases chromosomes from the INM as it enters mitosis (Hediger *et al.*, 2002; Güttinger *et al*., 2009; Ebrahimi and Cooper, 2012; Fujita *et al.*, 2012; Kanoh, 2013; Yam *et al*., 2013). The observation that Lem2 clusters stay adjacent to heterochromatin during mitosis in *vps32Δ* and *vps4Δ* mutants, combined with the stronger affinity of Lem2 for heterochromatin in the absence of Vps4, suggested that chromatin-NE interactions are maintained throughout mitosis in these mutants. We investigated the fate of persistent Lem2 clusters in mitotic *vps4Δ* cells by performing time-lapse imaging of Lem2-GFP together with a telomere marker Taz1-mCherry. In WT cells, the NE-bound telomere clusters dispersed during early mitosis (Fig. 6-4A) and moved away from the NE, indicating that chromosome arms were released (Fujita *et al.*, 2012; Yam *et al*., 2013). However, in *vps4Δ* cells Taz1 remained associated with Lem2 clusters throughout mitosis, which co-segregated together with telomeres (Fig. 6-4A).

To fully test if chromosomes are not released during mitosis we measured the distance between the two main heterochromatic domains that are tethered by Lem2, centromeres and kinetochores, to the NE throughout interphase and mitosis. Indeed, as mitosis progressed most telomeres did not appear to move away from the NE in mitotic *vps4Δ* cells as compared to the WT (Fig. 6-4B). When breaking the interaction between Lem2 and chromosomes by additionally deleting *nur1*, telomeres were still associated with the NE in interphase, but would no longer stay attached during mitosis (Fig. 6-4B). Kinetochores of *vps4Δ* cells labelled by Mis6-GFP were still able to fully detach from the NE, however they did show decreased movement away from the NE (Fig. 6-4C). A slight decrease in kinetochore-NE distance was also observed in *nur1Δ* cells.

In conclusion, we show chromosome-NE attachments persist throughout mitosis in the absence of Vps4 function. Based on the persistent Lem2 clusters of both *vps32Δ* and *vps4Δ* mutants this data suggests that also in *vps32Δ* cells these attachments

persist. We hypothesise that centromeres can still be released from the NE due to the fact they are associated with SPB, rather than the NE.

6.5 ESCRT-III/Vps4 regulated chromosome-NE association is conserved between fission yeasts

We asked if the ESCRT-III/Vps4 mutant associated persistent tethering was a feature unique to *S. japonicus*, which performs a semi-open mitosis, or if it was also conserved to *S. pombe*, which performs a completely closed mitosis and therefore segregates its chromosomes within an intact nuclear membrane. Indeed, it has been shown that *S. pombe* also releases its chromosomes from the NE during mitosis (Fujita *et al.*, 2012). We first determined that in *S. pombe* Lem2-GFP has a similar localisation pattern to *S. japonicus*, with the exception that in *S. pombe* Lem2 is not enriched at the SPB during mitosis (Fig. 6-5). Although this feature has not been mentioned before in literature, this phenotype could already be observed in imaging data of an earlier report (Hiraoka *et al.*, 2011). Notably, Lem2 is also enriched at the tail structure (Fig. 6-5). Interestingly, when we deleted *vps4*, we observed the same Lem2 clustering phenotype as in *S. japonicus*, with Lem2 clusters persisting throughout mitosis. (Fig. 6-5). This suggests that also in *S. pombe* chromosome-NE attachments are maintained throughout the cell-cycle in the absence of Vps4 function. Additionally, due to the similar localisation of Lem2 it also suggests that Lem2 might perform a function in maintaining nuclear compartmentalisation during mitotic exit in *S. pombe*.

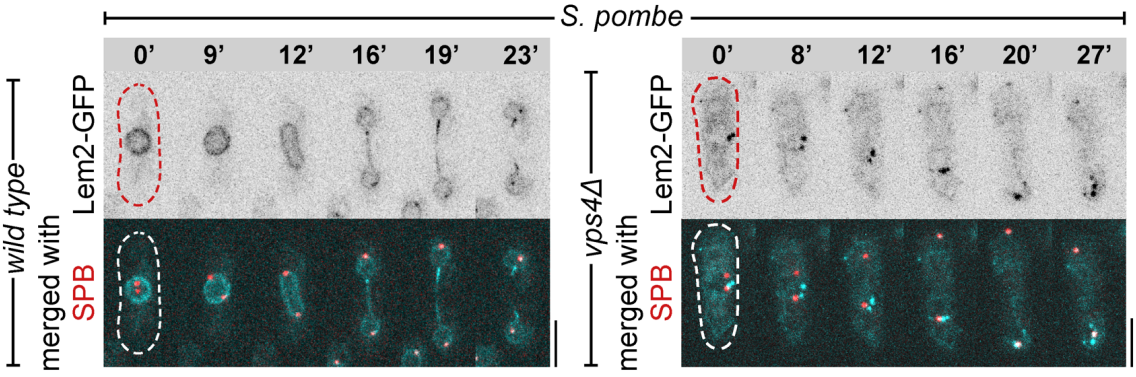

Figure 6-5. Localisation of Lem2 in *S. pombe*.

Maximum projections of Z-stacks of a time-lapse sequence of *S. pombe* cells expressing Lem2-GFP and Pcp1-mCherry (n≥7 cells for both genotypes).

6.6 Abnormal mitotic progression in the absence of Vps4

We asked if the persistent chromosome-NE attachments during mitosis deregulated mitotic progression in *vps4Δ* cells in *S. japonicus*. In the WT, the spindle assembly checkpoint (SAC) protein Mad2-GFP (Musacchio, 2015) typically remained on kinetochores for 5-10 minutes (Fig. 6-6). However, in *vps4Δ* cells, whereas the mean duration of Mad2 on kinetochores was not affected, we observed an abnormally broad distribution of the duration of SAC activation (Fligner-Killeen test for homogeneity of variances p = 0.001). Whereas some cells were delayed at the metaphase to anaphase transition, others had a marked decrease in the duration of Mad2 kinetochore recruitment (Fig. 6-6). This suggested that the persistent chromosome-NE attachments do not necessarily delay mitotic progression. However, it suggests that there is rather a deregulation of mitotic progression.

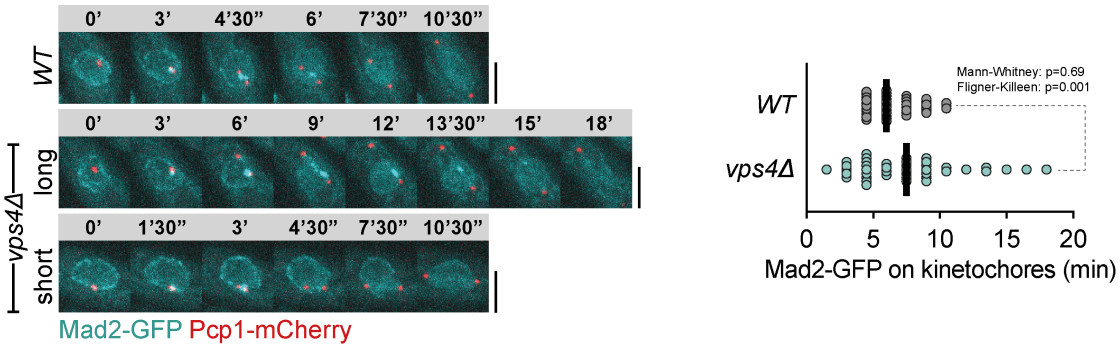

Figure 6-6. Deregulation of the SAC in the absence of Vps4.

Time-lapse maximum projection images of representative cells of indicated genotypes expressing Mad2-GFP and Pcp1-mCherry. Presented is the quantification of the duration of Mad2-GFP presence at kinetochores in WT (n=40 cells) and *vps4Δ* (n=41 cells. Mann-Whitney U test p = 0.69, Fligner-Killeen test for homogeneity of variances p = 0.001.

6.7 Persistent chromosome-nuclear envelope attachments induce severe growth defects

We hypothesised that the persistent chromosome-NE association of *vps32Δ* and *vps4Δ* are deleterious to the cell. We used a colony forming unit (CFU) assay to systematically quantify ESCRT-III/Vps4-associated growth defects. In this assay we plated cells from exponentially growing cultures in equal densities on rich media agar plates and counted

the number of colonies that appeared as a measure for viability and the quantified the size of these colonies as a measure for growth. We observed mild growth defects in ESCRT-III mutants that did not have persistent chromosome-NE associations, that is *cmp7Δ* and *vps24Δ*, and also in the *nur1Δ* mutant (Fig. 6-7A, B). However, we observed profound defects in colony growth in both the *vps32Δ* and *vps4Δ* mutants (Fig. 6-7A, B). We were able to partially rescue the growth defect of both mutants by the additional deletion of *nur1*, although not fully in the case of *vps32Δ*. This suggested that these growth defects were at least partially associated with persistent chromatin-NE associations. We also observed a significant decrease in the viability of both *vps32Δ* and *vps4Δ* mutants (Fig. 6-7B). However, we were not able to rescue this defect with the *nur1Δ* deletion (Fig. 6-7B).

In conclusion, we found severe growth defects associated with only in the ESCRT-III/Vps4 mutants that have persistent chromosome-NE associations and we were able to rescue this defect by breaking these chromosome attachments using the *nur1* deletion. This was despite the fact that the nucleocytoplasmic compartmentalisation phenotype of these mutants could not be rescued by the additional deletion of *nur1* (Fig. 3-4D). This is consistent with data from *S. pombe*, where the deletion of *vps4* is also associated with severe growth defects, as was measured by growth curve analysis of yeast cultures (Gu *et al*., 2017). We hypothesize that in both organisms this is due to the persistent chromosome-NE attachments observed in this mutant and are not likely to be due the delayed establishment of compartmentalisation.

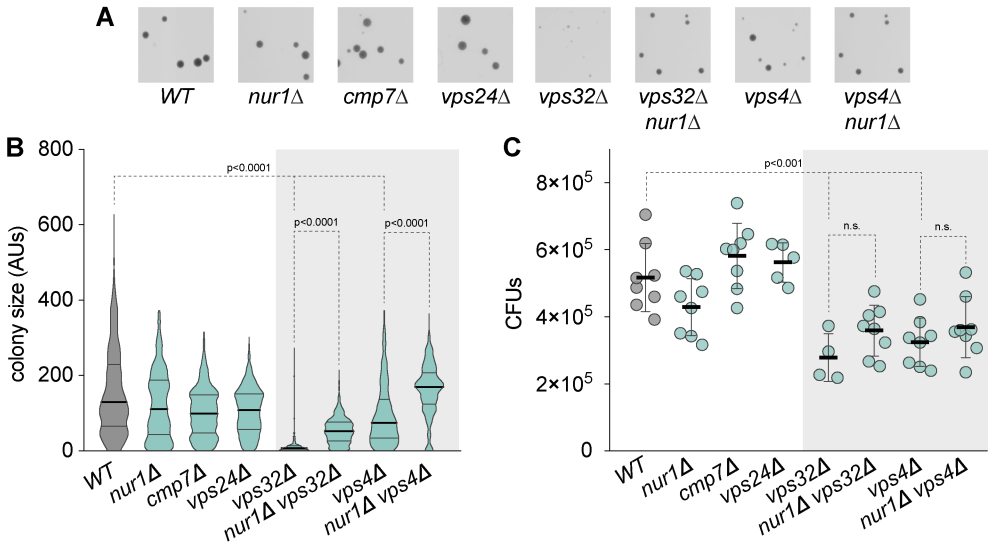

Figure 6-7. Quantification of growth defects associated with ESCRT-III/Vps4 mutants.

A) Representative images of colonies of each mutant of the CFU assay. **B)** Quantification of colony size of the CFU assay. Presented is the pooled data of 3 technical replicates of 3 biological experiments. Kruskal-Wallis test and Dunn's test for multiple comparisons, multiplicity-adjusted p-values are presented. **B)** Quantification of CFU assays for cells of indicated genotypes. One-way ANOVA, Tukey's multiple comparisons test.

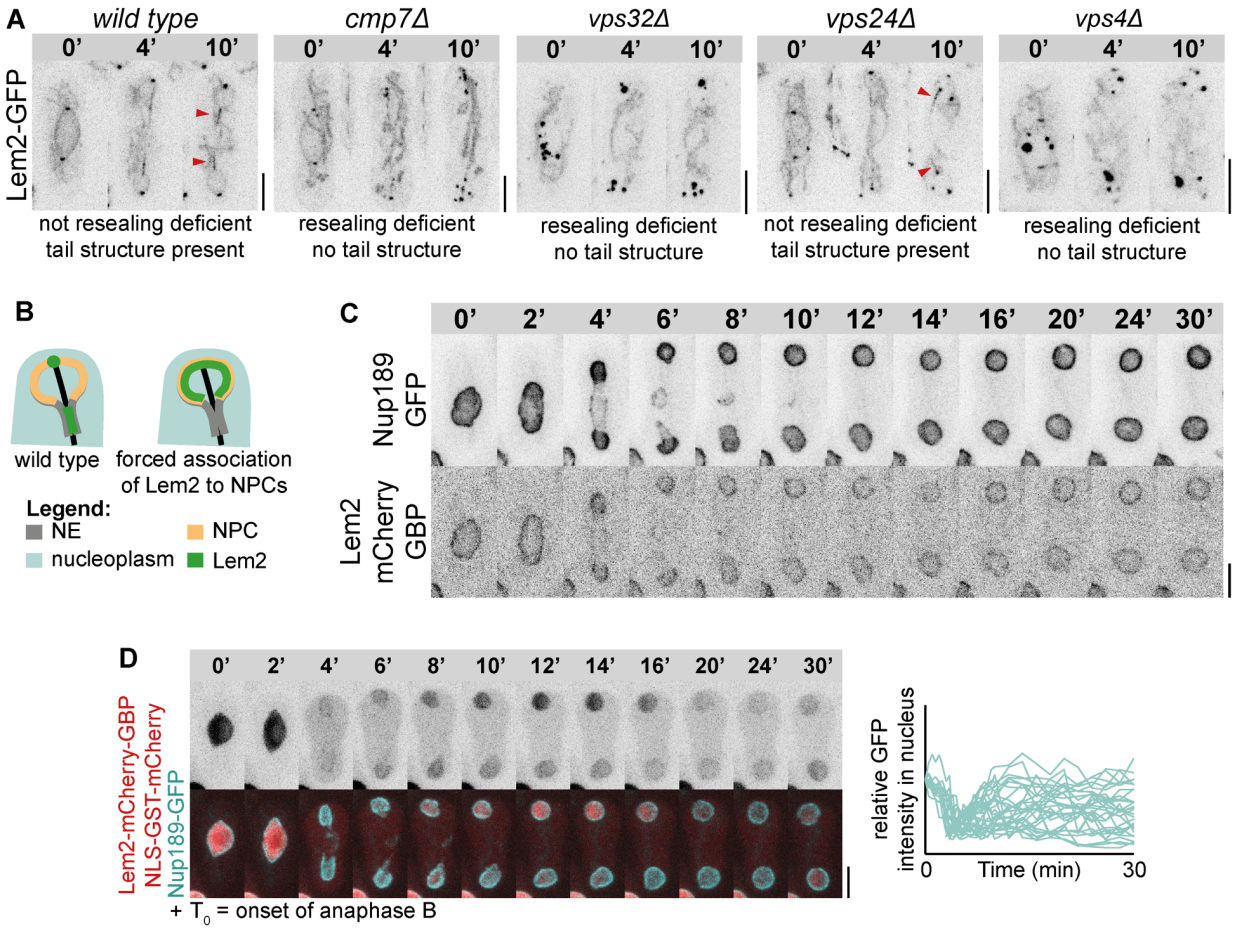

Figure 6-8. A functional ESCRT-III/Vps4 system is required for Lem2 to redistribute to the tail during mitotic exit.

A) Time-lapse images of maximum projections of confocal Z-stacks of cells of indicated genotypes expressing Lem2-GFP starting from prior to NE breakdown. Arrows indicate the presence of Lem2 on tail structures in the WT and *vps24Δ* mutant. **B)** Scheme of the synthetic tethering strategy of Lem2-mCherry-GBP to Nup189-GFP. **C)** Time-lapse sequence of a cell expressing Lem2-mCherry-GBP and Nup189-GFP showing that Lem2 is stably associating with NPCs throughout the cell-cycle. **D)** Shown is a representative cell from the synthetic tethering experiment expressing additionally Nhp6-mCherry as a nucleoplasmic marker. Presented is the quantification of relative mCherry intensity in the nuclei of 15 cells (30 nuclei), analysed as in Fig. 1.

6.8 A functional ESCRT-III/Vps4 system is required for Lem2 to redistribute to the tail during mitotic exit

Based on our data that Lem2 stays permanently locked on heterochromatin in *vps32Δ* and *vps4Δ* mutants, we asked what happens to the tail localisation of Lem2 during mitotic exit in these mutants. Indeed, in the mutants that were deficient in nuclear re-compartmentalisation, *cmp7Δ*, *vps32Δ, vps4Δ* and also *nur1Δ*, Lem2 failed to enrich on tail structures (Fig. 6-8A for ESCRT-III/Vps4 mutants and Fig. 3-1E for *nur1Δ*). In the *vps24Δ* mutant that was not defective in this process, Lem2 was still present at the 'tails' (Fig. 6-8A). We hypothesized that the function of ESCRT-III/Vps4 in releasing Lem2 from heterochromatin was required for Lem2 to enrich at the 'tails'. To formally test this hypothesis, we tagged Lem2 with GFP-binding-protein (GBP) and expressed it together with the NPC component Nup189-GFP (Fig. 6-8B). Because NPCs are excluded from the tail (Yam *et al*., 2013), this permanent association between Lem2 and NPCs forced Lem2 away from the tail, instead localising around the NE together with NPCs (Fig. 6-8C). When we analysed the establishment of compartmentalisation in this strain we observed marked deficiency in re-establishing nucleocytoplasmic compartmentalisation during mitotic exit (Fig. 6-8D), reminiscent of Lem2-Nur1 mutants (Fig. 3-3) and ESCRT-III/Vps4 mutants (Fig. 3-4).

Thus, under conditions where ESCRT-III and Vps4 were fully functional and Lem2 was present, but was sequestered away from the regions where the spindle intersects with the NE, *S. japonicus* cells are not able compartmentalise the nucleus during mitotic exit. We conclude that Lem2-Nur1 must be first released by the ESCRT-III/Vps4 machinery from heterochromatin during interphase to be able to enrich at the NE sealing sites in order to re-establish nucleocytoplasmic compartmentalisation.

6.9 Conclusions

In this chapter we have shown that chromosome-NE attachments persist throughout mitosis in the absence of Vps4 function. Our data suggests that this is due to a higher affinity of the INM protein Lem2 for heterochromatin in the absence of Vps4. Lem2 is known to tether chromatin during interphase, therefore this likely represents an extreme state of tethering which carries over into mitosis and is not affected by normal

mitotic regulation. These persistent tethering results in a deregulated mitotic progression and severe growth defects. All of these phenotypes can be rescued by the deletion of *nur1*, which abrogates the interaction between Lem2 and heterochromatin. Interestingly, in the absence of Vps4 function, not only are chromosomes strongly associated with Lem2, but vice versa Lem2 is also strongly associated with chromosomes. This results in Lem2 being sequestered away from the tail structure during mitotic exit. Thus, we suggest that one of the main reasons that ESCRT-III/Vps4 are defective in the establishment of nuclear compartmentalisation during mitotic exit is not because they are defective in membrane resealing, but because Lem2 is kept away from the tail structure.

Chapter 7 – Discussion

7.1 Conclusions

In this thesis, we set out to elucidate the mechanism by which Lem2 establishes nucleocytoplasmic compartmentalisation during mitotic exit and address the question if there could be the role for the ESCRT-III/Vps4 machinery in this process. We established that in *S. japonicus* Lem2 works together in a complex with Nur1 both for its interphase and mitotic exit functions. Based on deletion mutants we found that Lem2-Nur1 works together with a non-canonical ESCRT-III/Vps4 complex to establish nucleocytoplasmic compartmentalisation during mitotic exit. Of note, this data combined with localisation data of ESCRT-III/Vps4 suggested that ESCRT-III/Vps4 does not "reseal" the NE, as it is hypothesised to do in human cells (Olmos *et al.*, 2015; Vietri *et al.*, 2015). Rather it aids in the stabilisation of the 'tail' structure to establish and maintain compartmentalisation before spindle breakdown. We next showed that both *in vitro* and *in vivo* ESCRT-III can form a stable complex with the C-terminal MSC domain of Lem2 and that the AAA-ATPase Vps4 can subsequently disassemble this complex (Fig. 7-1). When Vps4 activity is lacking, these stable complexes persist on Lem2, and at the same time, Lem2-Nur1 forms big clusters on heterochromatin. We have shown using ChIP that the fraction of heterochromatin bound to Lem2 is indeed much increased in

this case. Thus, we hypothesise that when Vps4 remodels the interaction between Lem2 and ESCRT-III, at the same time it also releases the interaction of Lem2 with

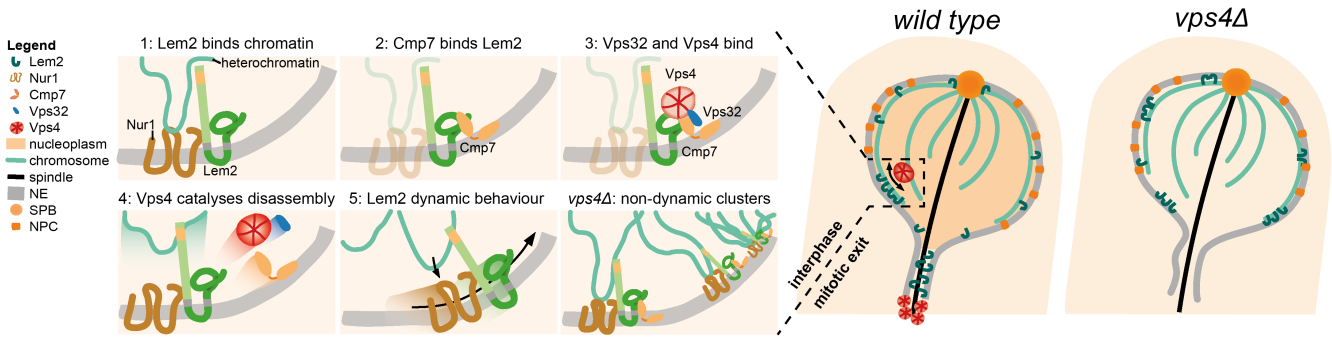

Figure 7-1. Schematic summary of the main findings of thesis.

A cartoon explaining our model for ESCRT-III/Vps4 function in interphase chromatin tethering to the NE and the resulting NE sealing phenotypes during mitosis. 1: Lem2 binds heterochromatin, for which Nur1 is required. 2: Cmp7 recognises the heterochromatin bound state of Lem2-Nur1. 3: Cmp7 then recruits Vps32 and the AAA-ATPase Vps4. 4: Vps4 now catalyses the disassembly of the Lem2-Cmp7 interaction. 5: This results in Lem2-Nur1 complex releasing heterochromatin and being free to move around the NE and re-engage heterochromatin in cycles of binding and unbinding. In the absence of Vps4 function the interaction between Lem2 and Cmp7 persists, resulting in the stable association of Lem2-Nur1 with Cmp7 and heterochromatin. During mitotic exit, such a stable engagement prevents Lem2 from enriching at the 'tail', which we hypothesise results in a destabilised interfase between membrane and the spindle and a delay in re-establishing the nucleocytoplasmic compartmentalisation.

heterochromatin (Fig. 7-1). We hypothesise that Cmp7 can somehow recognise the heterochromatin-bound state of Lem2-Nur1, which induces ESCRT-III to assemble. One pertinent side effect of the fact that Lem2-heterochromatin association is not broken down is that Lem2 fails to enrich at the tail during mitotic exit. This appears to be the case only in the mutants with very strong Lem2-heterochromatin interaction: *vps32Δ* and *vps4Δ.* By synthetically forcing Lem2 away from the tail we have shown that the absence of Lem2 from the tail is likely to be the main contributing cause to the fact that these ESCRT-III/Vps4 mutants are defective in the establishment of nucleocytoplasmic compartmentalisation.

We found that the persistent association of chromosomes with the NE leads to severe growth defects and a deregulated mitosis. The artificial tethering of histones to

ER membranes in cultured human cells leads to chromatin bridges and failure in chromosome segregation and chromatin organisation (Champion *et al.*, 2018). Even tethering a single chromosomal locus on a single chromosome leads to either delayed segregation or often complete mis-segregation of chromosomes in budding yeast (Chen, 2019). We did not observe actual chromosome mis-segregation occurring in *vps4Δ* mutants. However, it should be noted that many cells in these cultures appear very sick and these often did not appear to undergo mitosis. Considering the rate with which *vps4Δ* mutants pick up suppressor mutations in *S. pombe* (Gu *et al*., 2017), it might be possible that cells undergoing mitosis in our system might have developed mutations to alleviate this phenotype. One instance where chromosome mis-segregation events can be easily monitored is during meiosis, as all the chromosome segregation products are visible within one ascus. Indeed, *vps4Δ* was identified in a screen for sporulation and meiotic chromosome segregation defects as having many meiotic chromosome mis-segregation events (Blyth *et al.*, 2018).

7.2 Lem2-Nur1 and ESCRT-III/Vps4 seal the nuclear membrane around the mitotic spindle during mitotic exit

Our data suggests that it is important to make a distinction between “resealing” of the nuclear membrane and “sealing” of the NE. Whereas the first is a membrane remodelling event that leads to an intact membrane, the latter is a situation in which protein factors can stabilise membranes and effectively “seal” the hole without fusing the membrane. This is the case in *S. japonicus*, where the tail structure is able to create a barrier between the nucleoplasm and the cytoplasm for around 20-25 min, while the spindle is still spanning the two daughter nuclei. Similar mechanisms of membrane “sealing” can likely be found in different cellular contexts. The nucleus of *S. pombe*, which performs a closed mitosis, likely forms a similar membrane “seal”. At the same stage during mitotic exit in *S. pombe*, the nuclear membrane connecting the daughter nuclei is also tightly associated with the mitotic spindle and also forms a diffusion barrier between the two daughter nuclei (Lucena *et al*., 2015). In fact, even the spindle midzone area, between the two daughter nuclei forms a distinct zone delimited by diffusion barriers (Lucena *et al.*, 2015). These are likely established at the tail site. The same is true for budding yeast, where a diffusion barrier exists between the two daughter nuclei

(Boettcher *et al.*, 2012). A similar structure might establish nuclear compartmentalisation in human cells where spindle microtubules are also piercing through the nuclear membrane during telophase (von Appen *et al*., 2019 preprint).

What could ESCRT-III/Vps4 be doing at the tail if not resealing the NE? The dynamic localisation of ESCRT-III/Vps4 at this single defined site is markedly different from the described dynamics of the ESCRT-III/Vps4 complex at endosomes or HIV budding sites (Adell *et al.*, 2017; Jouvenet *et al.*, 2011; Johnson *et al*., 2018) and therefore does not correspond with the idea of ESCRT-III/Vps4 performing a membrane remodelling event. Most ESCRT-III/Vps4 complexes mediating membrane budding events at endosomes last no longer than 50 seconds. Roughly 80% of all ESCRT-III/Vps4 assemblies last no longer than 10 seconds. For most of these assemblies, the analysed ESCRT-III subunits Snf7 and Vps24 assembled in a coordinated manner. This was also coordinated with the appearance of at least two Vps4 hexamers (Adell *et al*., 2017). ESCRT-III/Vps4 is much more dynamic than early ESCRT complexes, which slowly increase in size until the rapid coordinated assembly of ESCRT-III/Vps4 (Wenzel *et al.*, 2018). This coordinated manner of assembly is different from the sequential assembly that has been hypothesised before (Teis *et al*., 2008). Potentially, many short filaments form here rather than a single long filament, which has consistently been the main model for ESCRT-III function (Schöneberg *et al.*, 2016; Adell *et al.*, 2017). All these events also end abruptly, with all of the proteins disappearing in one go. A similar kinetics is observed during the budding of HIV particles. First, there is a slow increase in the amount of the viral protein GAG, followed by rapid recruitment of ESCRT-III/Vps4 and abrupt disassembly of the entire complex (Jouvenet *et al.*, 2011; Johnson *et al*., 2018).

For budding into endosomes, each individual resolved ESCRT-III/Vps4 event results in a single membrane remodelling event producing a single intraluminal vesicle (Adell *et al.*, 2017; Wenzel *et al.*, 2018). At the tail in *S. japonicus*, it is unlikely that the appearance and disappearance of ESCRT-III/Vps4 throughout its existence represents a single event, as the tail is not resolved until the breakdown of the spindle, which happens in an ESCRT-III independent way. We know based on our *in vitro* data that Vps4 can specifically disassemble the interaction between Lem2 and Cmp7 and we hypothesised that this also affects the affinity for Lem2-Nur1 to heterochromatin. Lem2 has an affinity for microtubules of the spindle (von Appen *et al*., 2019 preprint). We

hypothesise that, just as ESCRT-III/Vps4 can remodel the interaction or affinity for Lem2-Nur1 and heterochromatin, ESCRT-III/Vps4 can also remodel the interaction between Lem2-Nur1 and microtubules. This is then part of a two-step model, in which during interphase ESCRT-III/Vps4 needs to release Lem2-Nur1 from chromatin to allow it to enrich at the tails. Here, Lem2-Nur1 can then again be regulated by ESCRT-III/Vps4 to help stabilise this structure.

To fully test this hypothesis, we would need to design a situation where we could separate these two functions. Ideally, a Lem2 mutant which does not interact with chromatin, but can still engage with microtubules and the ESCRT-III/Vps4 machinery would solve this question. However, our data suggests that Lem2 needs Nur1, with which it interacts through its lumenal domain (Fig.5-5) to both interact with chromatin and to stably associate with the tail (Fig. 6-1, 6-2; Fig. 3-2C). Lem2 mutants lacking the C-terminal MSC domain also likely fail to interact with ESCRT-III and are also not enriched at the tail (Fig. 5-4). This makes it difficult to genetically unravel the two spatially and temporally segregated functions of Lem2-Nur1 regulation by ESCRT-III/Vps4.

7.3 A novel mechanism regulating chromatin-NE attachments mediated by ESCRT-III/Vps4

In this work we have uncovered a mechanism by which ESCRT-III/Vps4 regulates the interaction between the INM complex Lem2-Nur1. By conditionally inactivating Vps4 we have shown that Lem2 becomes gradually locked onto heterochromatin (Fig. 5-2). We suggest that ESCRT-III/Vps4 continuously monitors and remodels chromatin-NE attachments during interphase (Fig. 7-1). To our knowledge this is the first description of a mechanism that can regulate the tethering state of chromatin during a single interphase. Most descriptions of chromatin-NE tethering have been on large scale chromosome movements, for example during differentiation. Mostly there has been a focus on “steady states” of chromatin distribution in the nucleus, for example before differentiation or after differentiation (Peric-Hupkes *et al.*, 2010; Robson *et al.*, 2017). This might be partly because it would be technically challenging to monitor the tethering state of genomic loci in live cells. Methods such as DamID have successfully defined NE associated chromatin domains that can be observed to move away after contact with the NE (Kind *et al.*, 2013). With this method it was observed that there is a local region

near the NE to which LADs are constrained, and where they potentially can have intermittent contact with the NE (Kind *et al*., 2013). Yet, it was not defined how these intermittent contacts could be mediated or regulated.

Another angle of looking at chromatin-NE attachments could be by looking at the INM proteins mediating this tethering. A screen of several INM proteins using FRAP identified a wide range of different mobilities and different mobile fractions for these proteins (Zuleger *et al.*, 2011). The low mobile fraction of some of these proteins is likely due to specific interactions with other proteins or with chromatin at the INM. Thus, the respective mobility versus immobility of INM proteins could potentially be used to assess the tethering state of chromatin to INM proteins. The turnover rate of INM proteins is a combination of both lateral movement within the nucleus, but also for a large part due to new proteins imported from the ER (Zuleger *et al*., 2011). Interestingly, when ATP was depleted the mobility of only some INM proteins, Emerin and SUN2, was drastically decreased both in the ER and at the INM, indicating that the lower mobility was not due to deficient ER to nuclear translocation (Zuleger *et al.*, 2011). Rather it suggests an ATP dependent step of remodelling interactions with binding partners both in the ER and the INM. In light of our data, it might be interesting to speculate if the action of ATPases such as Vps4 might responsible for this. In WT *S. pombe* cells, Lem2 has a high mobility around the NE and also experiences a certain turnover rate at the SPB. The protein Bqt4 is required to maintain Lem2's presence at the NE, whereas the protein Csi1 stabilises it at the SPB (Ebrahimi *et al.*, 2018; Hirano *et al.*, 2018). In a *bqt4Δ csi1Δ* double mutant, the turnover rate of Lem2 at the SPB is drastically increased (Ebrahimi *et al.*, 2018), suggesting that indeed the dynamicity of Lem2 on the NE or SPB is a reflection of its interaction with other proteins and potentially also chromatin. We speculate that in ESCRT-III/Vps4 mutants Lem2 indeed becomes immobilised on heterochromatin, which could be tested by FRAP or photo-activation experiments.

Another way in which large scale chromatin-NE tethering is regulated is during the beginning of mitosis, when all chromosomes are released from the NE. Here, phosphorylation events are known to play an important role. In S. *pombe*, the release of telomeres from the NE is regulated through phosphorylation of Rap1 by the CDK Cdc2 (Fujita *et al*., 2012; Hu *et al.*, 2018). In *C. elegans* and human cells the association of BAF with both chromatin and the NE through LEM-domain proteins is regulated by both

phosphorylation and dephosphorylation events by VRK-1 kinase and PP2A respectively (Gorjánácz *et al.*, 2007; Asencio *et al.*, 2012). The lack of VRK-1 kinase in worms lead to the persistent association of chromatin to LEM-2 and Emerin and thus to the NE during mitosis. This leads to gross NE morphology defects during NE reformation and interphase (Gorjánácz *et al*., 2007). Many other INM proteins such as Lamins are also known to become phosphorylated at the onset of NE breakdown (Güttinger *et al*., 2009).

How could ESCRT-III/Vps4 perform its regulation of Lem2 chromatin tethering? We can envision two possible mechanisms: The first mechanism is that Cmp7 and Vps32 directly interact with Lem2 in its heterochromatin-bound state, which then recruits Vps4 to remodel this interaction. Thus, in this model polymerisation of any ESCRT-III components would not necessarily have to occur and after binding Vps4 could induce a conformational change in either Cmp7, Vps32 or Lem2 which would release the complex and also release Lem2-Nur1 from heterochromatin. This latter would in line with the function of some other AAA-ATPases. For example, the ATPase TRIP13 induces an activating conformational change in the SAC protein MAD2 by inserting and pulling through only a small peptide stretch through its centrail pore, which unwinds a stabilising α-helix (Alfieri *et al*., 2018). Based on *in vitro* data that Vps4 can translocate and unfold entire ESCRT-III subunits through its central pore in an ATPase dependent manner it would be likely that the remodelling function of Vps4 is performed on either Cmp7 or Vps32 (Yang *et al.*, 2015; Monroe *et al.*, 2017; Su *et al.*, 2017). In the second model ESCRT-III forms filaments on the INM that could entrap Lem2 and potentially chromatin. These filaments would necessarily consist of Cmp7 and not of Vps32, the latter being considered to be the main filament component on endosomal ESCRT assemblies (Babst *et al.*, 2002; Teis *et al*., 2008), because in the complete absence of Vps32 Lem2 is still severely trapped on heterochromatin (Fig. 6-1). Genetic data in budding yeast suggests that the LEM-domain Heh1 could “activate” Chm7 to form assemblies on the INM (Thaller *et al.*, 2019). Furthermore, *in vitro* data of human ESCRT proteins suggests that the C-terminus of LEM2 can induce the formation of CHMP7 filaments (von Appen *et al.*, 2019, *preprint*). In the absence of Vps4 these hypothetical filaments could not be disassembled, resulting in Lem2 being trapped in these filaments. At the current time, we are not able to differentiate between these two models.

One question that arises from both models is what Lem2-ESCRT-III clusters look like at a molecular level? And what is the reason that they are refractive to mitotic regulation? One hypothesis is that mitotic regulation cannot access chromatin. We hypothesise that the persistent and strong tethering of chromatin might exert a pushing force on the NE that causes it to deform, leading to some chromatin domains becoming locked away in membrane pouches, inaccessible to mitotic regulation. Using correlative light-electron microscopy (CLEM) techniques, several different types of NE deformation associated with ESCRT-III disfunction have already been described. These include INM derived cisternae intruding into the nucleoplasm, NE evaginations into the cytoplasm and also NE ruptures observed when expressing an "active" form of Chm7 in budding yeast (Thaller *et al.*, 2019). Others have observed complicated networks of membrane associated with the NE and also have observed LEM2 clusters that are associated with sheets of membrane parallel to the INM that can be shaped into large membrane networks (Vietri *et al*., 2019 *preprint*). Another possibility is that persistent chromatin-NE attachments lead to chromatin, potentially from different chromosomes, becoming entangled at the NE. Over time such entangled chromatin could become a physical obstruction for soluble factors mediating chromatin release. Proof of some form of entangled chromatin in ESCRT-III mutants can be found in human cultured cells, where topoisomerase IIB is localised to CHMP7 foci at the NE, suggestive of torsional stress (Vietri *et al*., 2019 *preprint*). Indeed, it has been suggested that in budding yeast, chromosome-NE attachments might prevent the removal of torsional stress (Titos *et al*., 2014). It can be envisioned that in cells with deregulated ESCRT-III, persistent chromatin-NE attachments can lead to both membrane deformations and chromosome torsional stress by the drawing in of both chromatin and nuclear membrane. We have attempted to answer the question of Lem2-ESCRT-III structure using CLEM. Preliminary data suggests that cells expressing the $Vps4^{EQ}$ exhibit large NE deformations and bulges. However, work is still ongoing to confirm this.

What could be the function of dynamic regulation of chromatin-NE attachments? We hypothesise that dynamic tethering might play a role in chromatin-related processes that occur at the NE or alternatively that it might be important for the maintenance of chromatin structure. One dynamic process occurring at the NE is the replication of late-replicating DNA regions (Ogawa *et al.*, 2018). The Lem2 interacting

protein Bqt4 is involved in tethering replicating telomeres to the NE during S-phase (Ebrahimi *et al*., 2018; Ogawa *et al*., 2018). Suggesting a possible role in this, *lem2Δ*, *nur1Δ* and the ESCRT-III mutants *vps24Δ* and *did4Δ* were identified as being sensitive to hydroxyurea in *S. pombe* screens (Deshpande *et al.*, 2009; Han *et al.*, 2010; Hayles *et al.*, 2013). Hydroxyurea prevents DNA replication by limiting dNTP pools (Chabes *et al.*, 2003; Koç *et al.*, 2004). Normally, cells can block cell-cycle progression during S-phase when they fail to properly replicate their genomes. However, mutants deficient in this block do not arrest the cell-cycle in S-phase and instead can enter mitosis with under-replicated DNA and fail to properly segregate their genomes, resulting in lack of growth in the presence of hydroxyurea (Enoch *et al*., 1992). Additionally, *lem2Δ* mutants were also sensitive to the DNA damage inducing drug methyl-methane-sulfonate (Zhurinsky *et al.*, 2019). Hydroxyurea induces replication stress, which WT cells can survive by inducing a cell cycle checkpoint that prevents cells from going through mitosis without replicated chromosomes or a checkpoint that arrests the cell cycle in response to DNA damage during S-phase (Enoch *et al*., 1992; Al-Khodairy *et al.*, 1994). Mutants that are defective in this checkpoint attempt mitosis, eventually fail and try to divide the cell without segregated chromosomes, resulting in a "cut" phenotype where the septum cuts the undivided nucleus in two. Notably, mutants of *lem2* have been observed to exhibit a cut phenotype (Hayles *et al.*, 2013; Xu, 2015). Indeed, in *S. pombe* Lem2 helps facilitate Rad3 mediated checkpoint signalling in response to hydroxyurea (Xu, 2015).

Secondly, we showed that *vps4Δ* mutants have much lower H3K9me2 levels in both the peri-centromeric and subtelomeric regions (Fig. 6-3), although our data is not definitive on whether this is dependent on tethering or not. Considering that Lem2 interacts with different heterochromatin maintenance factors (Barrales *et al*., 2016), we suggest that the transient organisation of chromatin at the NE might bring chromatin into contact with its regulators. It should be noted that if the lower H3K9me2 levels associated with *vps4Δ* could be rescued by the *nur1* deletion, another hypothesis for the lower H3K9me2 levels could be a similar one to why chromatin is not released from the NE during mitosis. If in ESCRT-III mutants chromatin becomes inaccessible for mitotic regulation because it becomes locked away in NE "pouches", for the same reason heterochromatin maintenance factors might also not gain access to it. However, our data suggests that it might not be rescued, which would point to a tethering-

independent function of Vps4 in maintaining H3K9me2 levels on heterochromatin. In the next section we will discuss a potential role for ESCRT-III/Vps4 mediated NE-chromatin tethering in NE maintenance in human cells.

7.4 A potential model for the role of ESCRT-III/Vps4 in NE maintenance and resealing based on regulating chromatin-NE tethering

Since the discovery of a role for ESCRT-III/Vps4 in NE reformation during telophase several years ago (Olmos *et al.*, 2015; Vietri *et al.*, 2015), the canonical model has been that ESCRT-III/Vps4 is actively remodelling the membrane during this process. This is not a surprise, considering the established role for this machinery in membrane remodelling in various cellular contexts and a host of *in vitro* data of ESCRT-III subunits deforming membranes. However, several works have indicated that ESCRT-III/Vps4 might at least be partially dispensable for this process in cultured human cells. Combined with our work suggesting that this machinery regulates chromatin-NE tethering, some of the conclusions regarding ESCRT-III/Vps4 function at the NE might have to be re-examined.

A recent paper supporting this, identified that BAF, the protein that links chromatin to LEM-domain proteins in metazoa, plays a vital role in NE repair (Halfmann *et al.*, 2019). Upon NE rupture induced by either mechanical compression, laser or constrained migration, cytosolic BAF is recruited to the rupture site. Here it binds to the exposed DNA, BAF then recruits the LEM-domain proteins LEM2, MAN1, Emerin and Lap2α to the rupture site. Next, CHMP7 is recruited to the rupture site, its recruitment depending on both BAF and LEM2. The depletion of BAF prevented the recruitment of membrane to the rupture site (Halfmann *et al*., 2019). Thus, BAF recruits INM proteins to the rupture site, which bring membrane with them, meaning that membrane recruitment fully depended on NE-chromatin associations. It was not investigated whether CHMP7 was also required for this membrane recruitment. This lack of membrane recruitment in BAF knockdown cells correlated to a failure of reinstating nucleocytoplasmic compartmentalisation after NE rupture, either laser-induced or induced by constrained migration. Most nucleoplasmic protein was re-localised to the nucleus around 15 min after rupture, but cells lacking BAF did not appear to be able to repair the nucleus, even after a period of two hours. Interestingly, upon knockdown of either LEM2 or CHMP7, cells had no problem with repairing the nucleus. Only

knockdown of several LEM-domain proteins together could mimic the BAF associated inability to repair the NE (Halfmann *et al.*, 2019).

This data suggests that the main factor contributing to the repair of NE ruptures is the recruitment of membrane to the site of rupture that is brought there by INM proteins. Indeed, CHMP7 was completely dispensable for at least the repair of laser-induced NE rupture (Halfmann *et al*., 2019). In another cell culture system, knockdown of CHMP4B also did not result in a delay of NE repair after spontaneous rupture (Robijns *et al.*, 2016). Furthermore, even though there is an enrichment of both LEM-2 and VPS-32 at the site where membranes of the reforming NE interact with microtubules in *C. elegans* oocytes after the second meiotic division, knockdown of LEM-2 or deletion of *CHMP-7* did not result in delayed compartmentalisation (Penfield *et al.*, 2019; *preprint*). Defects in compartmentalisation were only observed in mutants affecting CNEP1 (*S. j.* and *S. c.*: Nem1), a phosphatase which regulates the protein Lipin and thus directs the flow of phosphatidic acid to either membrane phospholipids or storage lipids (Santos-Rosa *et al.*, 2005; Han *et al*., 2006; Kim *et al.*, 2007). Deletion of *cnep1* resulted in excessive ER membrane production and infiltration of the nuclear interior by ER membranes during reformation of the oocyte derived pronucleus after the second meiotic division (Penfield *et al*., 2019; *preprint*). However, these nuclei also eventually established compartmentalisation. However, some form of unstable membrane integrity was maintained, as oocyte derived pronuclei exhibited premature loss of compartmentalisation in the first mitotic division. This phenotype was acerbated by additional depletion of either LEM-2 or CHMP-7 and could be fully rescued by the additional depletion of CDGS-1, which prevents the formation of excessive membrane sheets (Penfield *et al*., 2019; *preprint*). This was interpreted as CNEP-1 and LEM-2/CHMP-7 playing redundant roles in establishing compartmentalisation. However, this data does suggest that even in the absence of ESCRT-III and even LEM2 in this case, *C. elegans* oocyte nuclei were able to maintain nuclear integrity. Another report on *C. elegans* oocytes showed that LEM-2 and VPS-32 are recruited to NE ruptures in Lamin-deficient mutants (Penfield *et al.*, 2018). However, it was not tested whether lack of these proteins also resulted in deficient nuclear repair. Other reports on migration induced NE rupture showed that indeed ESCRT-III is recruited to NE blebs and protrusions (Denais *et al.*, 2016; Raab *et al.*, 2016) and reinstating nucleocytoplasmic

compartmentalisation is delayed upon knockdown of ESCRT-III components. However, despite a severe delay, most nuclei were eventually able to reseal (Denais *et al.*, 2016; Raab *et al.*, 2016). This is similar to post-mitotic NE resealing in human cells, which after knockdown of ESCRT-III subunits are still able to fully reinstate nuclear compartmentalisation despite a delay in this process (Olmos *et al.*, 2015; Vietri *et al.*, 2015; Olmos *et al*., 2016). Indeed, the idea that ESCRT-III/Vps4 is actively "resealing" the membrane appears to be mostly based on its enrichment at resealing sites, despite a lot of evidence suggesting that compartmentalisation can be establishment in the absence of these proteins. Due to the fact that many events occur at this time during the resealing process and that it has not been completely possible to untangle these events, the data is not completely clear about which stage of this process ESCRT-III/Vps4 could potentially execute. These events include membrane spreading, regulation of chromatin-NE interactions, clearing of microtubules, rebuilding the nuclear lamina and finally membrane fusion.

What then does ESCRT-III/Vps4 do at the NE if not resealing the membrane? One mechanism that has been suggested is that the reinstatement of nucleocytoplasmic compartmentalisation after NE rupture might be performed by proteins forming a diffusion barrier for nucleoplasmic and cytoplasmic components at the rupture site, rather than an actual resealing of the membrane (King and Lusk, 2019). Support for this hypothesis is found by the fact that LEM2 and CHMP7 can co-polymerise around microtubules perforating the reforming NE, which has been suggested to form a molecular glue or seal that helps establish compartmentalisation in the presence of spindle microtubules (von Appen *et al.*, 2019 *preprint*), similar to the way that Lem2 appears to stabilise the nuclear membrane around the spindle at the tail structure in *S. japonicus*. Additionally, i*n vitro* data suggests that CHMP2B can act as a diffusion barrier on reconstituted membranes preventing diffusion of both lipid membrane components and trans-membrane proteins (De Franceschi *et al.*, 2019). Here, again, another mechanism would be responsible for the actual fusing of the membrane, be it other factors or spontaneous fusion induced by the pulling together of membrane by chromatin.

Other potential mechanisms could be hypothesised based on the ability of ESCRT-III/Vps4 to regulate chromatin-INM interactions. For example, INM LEM-domain

proteins might distribute membrane over the rupture site through their dual association with both chromatin and membrane. This spreading might be guided by ESCRT-III/Vps4 in a Brownian-ratchet like mechanism, similar to the spreading of ER membrane over chromatin during telophase (Anderson and Hetzer, 2007; Anderson *et al.*, 2009). Alternatively, ESCRT-III/Vps4 might stabilise the interaction between chromatin and membrane at the rupture site by prolonging the interaction between LEM-domain proteins and chromatin. Such a mechanism is supported by our data. Subsequently, other factors that could fuse the membrane could come in. However, at this moment no fusogenic factors are known that could perform this function at the NE, apart from ESCRT-III. Therefore, we suggest another hypothesis where the stable association between chromatin and membrane could provide the force necessary for the fusing of the membrane by first bringing the membrane in proximity and then forcing the fusion of the opposing membranes. This hypothesis would have to be tested by more careful analysis of the molecular events that occur during NE resealing. Related to this, the tethering of chromatin to the NE could be used as a way to locally and rapidly stabilise the membrane in response to mechanical forces.

It might therefore be important to differentiate between NE repair in the presence and absence of spindle microtubules. That is, NE resealing during mitotic exit is likely vitally different than the repair of interphase ruptures. In the first instance, a temporary nucleocytoplasmic barrier, depending on Lem2 and Cmp7, might be established around microtubules. Due to the formation of such a structure being restricted to telophase this barrier formation might be cell-cycle regulated. It is potentially highly conserved as well. Similar structures of spindle microtubules piercing the nuclear membrane during mitotic exit can be found in budding yeast, fission yeasts and human cells. Indeed, the enrichment of Lem2 to this structure is critical to establishment of compartmentalisation in the presence of spindle in *S. japonicus* (Fig. 6-8) and in human cultured cells (von Appen *et al*., 2019 preprint). As mentioned before, the fact that Lem2 behaves in exactly the same manner during the closed mitosis of *S. pombe* is highly suggestive of it performing the same function here. Also in budding yeast mitosis, during the formation of the dumbbell stage the two daughter nuclei, although still connected by membrane and the mitotic spindle, are compartmentalised by a diffusion barrier formed by the geometry of membrane tightly wrapping around

the spindle (Boettcher *et al.*, 2012). In this case, Lem2 still depends on its chromatin-binding ability to be recruited to the NE. In the second instance resealing of interphase NE ruptures more likely to be explained by the chromatin-tethering ability of Lem2 and other INM proteins, which might be regulated by ESCRT-III/Vps4.

Would this model of ESCRT-III/Vps4 mediated chromatin-NE attachments explain some of the phenotypes that are associated with ESCRT-III dysfunction at the NE? De-regulated ESCRT-III results in the accumulation of DNA damage at the nuclear periphery enriched for CHMP7 and CHMP4 (Vietri *et al.*, 2019 *preprint*; Willan *et al.*, 2019). Deregulated ESCRT-III associated DNA damage might be induced by Topoisomerase IIB, which is attempting to relieve stress on the chromosome by inducing DNA breaks (Vietri *et al*., 2019 *preprint*). It was suggested that in micronuclei ESCRT-III enrichment might induce DNA damage (Willan *et al*., 2019). Knockdown of CHMP7, but not of VPS4 was able to partially rescue the accumulation of DNA damage in micronuclei. Our model supports this, as the accumulation of ESCRT-III at micronuclei might be indicative of strong chromatin-NE tethers that might deform both the membrane and the chromatin. In agreement with their data, knockdown of VPS4 would lock ESCRT-III on the micronuclear envelope and lock chromatin onto it as well. Our model would predict that knockdown of CHMP7 would prevent the formation of such aberrant ESCRT-III complexes, and this was indeed observed (Willan *et al*., 2019). Interestingly, in micronuclei both CHMP7 and CHMP4 could be observed to penetrate deep into the chromatin core of micronuclei by STED microscopy, not just associating with the periphery like in the main nucleus. This might be linked to the invasion of ER membrane into these micronuclei (Willan *et al*., 2019).

7.5 Potential other chromatin related functions of ESCRT-III

Is the function of ESCRT-III/Vps4 limited to chromatin-NE attachments, or is it also involved in other chromatin-related functions, as some of our data suggests (Fig. 6-3)? Only one ESCRT-III subunit has so far been described to potentially play such a role. The human ESCRT-III subunit CHMP1A was identified to function both in the MVB pathway and in the nucleus (Howard *et al.*, 2001; Stauffer *et al.*, 2001). Overexpressed CHMP1 was found to create structures in the nucleus containing condensed chromatin, which CHMP1 surrounded like a shell. This CHMP1 shell colocalised with locally altered

chromatin enriched for acetylated and phosphorylated H3 (H3K9/14Ac and H3-S10P). The inside of these structures was enriched for the Polycomb protein BMI1, broadly involved in gene silencing. Overexpression of CHMP1 in *Xenopus* embryos resulted in increased silencing of the developmental genes *En-2* and *Rx2A*. Additionally, CHMP1 overexpressed cells were blocked in S-phase (Stauffer *et al.*, 2001). CHMP1A has also been observed to localise as nuclear puncta, apart from endosomal localisation, in mouse primary cultures of cerebellar granule cells (Mochida *et al*., 2012). In the brain, CHMP1A is required for the recruitment of Polycomb protein BMI1 to specific chromosomal loci, although it was not shown whether this depended on the nuclear function of CHMP1A (Mochida *et al*., 2012). Loss of function mutants of CHMP1A occurring in patients with pontocerebellar hypoplasia resulted in loss of silencing of a negative regulator of stem cell proliferation, INK4, leading to a massive decrease in cerebral cortical size in humans, mice and zebrafish (Mochida *et al.*, 2012). Lastly, overexpressed CHMP1A in a human pancreatic cancer cell line localised exclusively to the nucleus, where it was able to activate the DNA DSB-break repair ATM kinase, resulting in growth defects (Manohar *et al.*, 2011).

A potential problem of two of these studies (Stauffer *et al.*, 2001; Manohar *et al.*, 2011) is that they are based on high levels of CHMP1A overexpression. Overexpression of CHMP1A appears to drive it exclusively into the nucleus, whereas endogenous CHMP1A is found in both the cytoplasm and the nucleus (Howard *et al.*, 2001; Mochida *et al.*, 2012). ESCRT-III subunits usually only function in the context of larger ESCRT-III complexes, however, no other ESCRT-III subunits were analysed in these studies, making it unclear whether these chromatin functions are CHMP1A specific. It is also not clear whether the phenotypes observed upon CHMP1A overexpression are due to a potential nuclear function or due to a propensity of overexpressed ESCRT-III subunits to form oligomeric aggregates. Overexpression of a single ESCRT-III subunit CHMP2B or CHMP4A/B in cells can form tubular aggregates which can deform the plasma-membrane (Hanson *et al.*, 2008; Bodon *et al.*, 2011). These tubules are outside of the context of normal ESCRT-III stoichiometry and their ability to form filaments is potentially due the high abundance of unregulated ESCRT-III subunits, similar to what is often observed *in vitro* (Lata *et al.*, 2008; McCullough *et al.*, 2015). Thus, it is possible that the overexpressed CHMP1A, which is driven into the nucleus, might distort

chromatin by formation of polymers or aggregates. It would be useful to study the nuclear function of CHMP1A at endogenous levels and combine this with a thorough analysis of the other ESCRT-III subunits and VPS4. Certainly, the nuclear speckle-like localisation of endogenous CHMP1A is indicative of a function there (Mochida *et al*., 2012). It should be noted that its nuclear localisation was not observed in some common cell types such as 3T3 and HEK 239T cells (Mochida *et al*., 2012) and therefore a potential nuclear function of CHMP1A or other ESCRT-III subunits might not have been noticed before and might be restricted to specific cell-types.

7.6 The ubiquitous functions of the ESCRT-III/Vps4 machinery

As described in section 1-7 of the introduction, the ESCRT-III/Vps4 machinery is involved in diverse functions in the cell (Fig. 7-6). These include the formation of intralumenal vesicles during MVB formation (Katzmann *et al*., 2001; Babst *et al.*, 2002; Babst *et al.*, 2002), the last step of cytokinesis where the midbody is pinched off after furrow ingression (Carlton and Martin-Serrano, 2007; Morita *et al.*, 2007), the control of the abscission checkpoint (Carlton *et al.*, 2012), viral budding from the plasma membrane (Garrus *et al.*, 2001; Martin-Serrano *et al*., 2001; Demirov *et al.*, 2002), plasma membrane and endosomal membrane repair (Jimenez *et al.*, 2014; Radulovic *et al.*, 2018; Skowyra *et al.*, 2018), the budding of small signalling vesicles from the plasma membrane into the exterior (Matusek *et al.*, 2014), the formation of peroxisomes from the ER (Mast *et al.*, 2018), neuron pruning (Loncle *et al.*, 2015), microautophagy of the ER (Schäfer *et al.*, 2019) and autophagosome closure (Zhen *et al.*, 2019; Zhou *et al.*, 2019). Several nuclear functions have been ascribed to this machinery as well (Fig. 7-6): The resealing of the NE during telophase (Olmos *et al*., 2015; Vietri *et al*., 2015), NPC assembly quality control in budding yeast (Webster *et al*., 2014), the maintenance of nuclear morphology in *S. pombe* (Gu *et al*., 2017) and the budding of viral particles from the nucleus through the nuclear membranes (Arii *et al.*, 2018).

Based on the model presented in this thesis an additional function can be added to this list: The regulation of heterochromatin-NE tethering by regulating the interaction of the Lem2-Nur1 complex with heterochromatin. How does this model fit in with the other cellular functions of ESCRT-III/Vps4? We present a model were, despite occurring on a membrane, the main function of ESCRT-III/Vps4 is to act on membrane proteins,

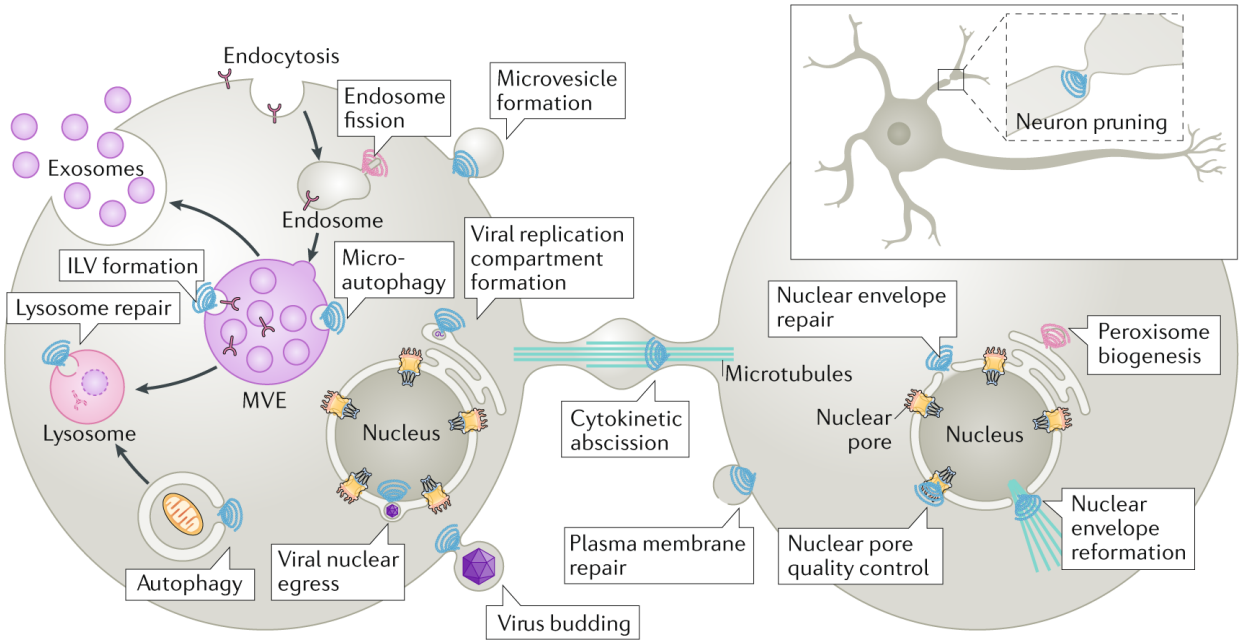

Figure 7-6. The ubiquitous functions of the ESCRT-III/Vps4 machinery.

Schematic overview of the different functions of ESCRT-III/Vps4. ESCRT-III is represented by as blue spiral

Figure taken from Vietri et al. (2019)

with the AAA-ATPase Vps4 not remodelling membranes, but the interaction between membrane proteins and heterochromatin. The apparent difference is that in its other functions it is thought that the role of ESCRT-III is to execute some form of membrane remodelling and scission. However, when looking further into the context in which ESCRT-III/Vps4 functions and the proteins that it interacts with to perform these functions, it might become clear that the way this machinery functions in these contexts is not very different from the model presented here.

Firstly, assembly of ESCRT-III/Vps4 is tightly regulated in relation to its substrates. This is not always obvious from reviewing the isolated function of this machinery based on *in vitro* studies. These often present very specific circumstances that do not directly relate to *in vivo* function. In *in vitro* studies where ESCRT-III is studied in the context of membrane remodelling very high concentrations of ESCRT-III/Vps4 subunits are often added to membranes (Lata *et al.*, 2008; Chiaruttini *et al.*, 2015). However, in living cells the amount of ESCRT-III/Vps4 subunits that function in remodelling events is likely much lower. By lattice light-sheet microscopy of the formation of ESCRT-III/Vps4 complexes on endosomes during MVB formation in budding yeast it was found that on average only 75-200 molecules of Snf7/Vps32 assembled

during the lifespan of the complex (Adell *et al.*, 2017). Furthermore, this recruitment first requires the slower build-up of early ESCRT complexes before the more abrupt assembly of ESCRT-III (Wenzel *et al.*, 2018). *In vitro* studies also often lack endogenous ESCRT-III/Vps4 substrates. Indeed, ESCRT-III/Vps4 appears to only function on specific substrates such as ubiquitinated cargo during MVB formation, which then recruits ESCRT-I (Katzmann *et al*., 2001). During HIV-1 budding the viral GAG protein interacts with ESCRT-I protein Tsg101, eventually recruiting ESCRT-III and Vps4 (Garrus *et al.*, 2001; Martin-Serrano *et al*., 2001). Furthermore, this machinery is recruited to the cytokinetic midbody by the spindle component Cep55 (Carlton and Martin-Serrano, 2007). Thus, ESCRT does not function without cargo and might in fact function in cargo crowding (Adell *et al*., 2017; Wenzel *et al*., 2018). In conclusion, the formation of ESCRT-III/Vps4 complexes appears to be tightly controlled in time and in size and also depends on substrates and early recruiters. In the model presented here, Lem2 is the substrate that, similarly to other ESCRT functions, can circumvent early ESCRTs by directly interacting with Cmp7.

Lastly, another important part of Vps4 function is the fact that it does not remodel membranes themselves, rather it remodels ESCRT-III subunits. This is also observed *in vitro* where Vps4 is required for the turnover of ESCRT-III subunits within spiral polymers and for spiral growth (Mierzwa *et al.*, 2017). Although the molecular mechanism is not yet known, it is likely the changes in ESCRT-III subunits or changes in the actual assemblies that mediate membrane remodelling. This also fits with our model, were a likely mechanism for the function of Vps4 in disassembling the interaction between Lem2 and Cmp7 is by acting directly on the ESCRT-III subunit Cmp7.

Thus, when viewing ESCRT-III as a machinery that acts on specific cargo's or substrates such as ubiquitinated proteins, viral proteins or INM proteins and Vps4 as an enzyme that acts to induce some change in ESCRT-III subunits it can be seen how, by changing the adaptor for the different substrates this machinery can be repurposed to perform different functions throughout the cell. However, one aspect that is not addressed in this thesis is the consequences for the nuclear membrane when Vps4 is absent. Considering the membrane-remodelling functions of ESCRT-III/Vps4 it should be investigated if NE deformations indeed follow lack of ESCRT-III/Vps4 function and if these are directly caused by the deregulation of heterochromatin-NE tethering.

Furthermore, it should be assessed if the function of ESCRT-III/Vps4 at Lem2-Nur1 is completely separate from membrane remodelling. Also, our data does not indicate whether any form of ESCRT-III polymerisation is important for it to remodel heterochromatin-Lem2 interactions. More insight into the molecular mode of action of ESCRT-III/Vps4 at the NE might also shed light on its interaction with its substrates in the different cellular processes in which its functions.

7.7 Outlook

The data presented in this thesis lays the groundwork for a new line of investigation regarding the ESCRT-III/Vps4 machinery, a complex that is canonically known as a membrane remodelling machine, and its novel role in the regulation of INM proteins. Several interesting questions arise from this. For example: How exactly does ESCRT-III/Vps4 affect the interaction between Lem2 and chromatin? How does the ATPase activity of Vps4 affect the disassembly of the Lem2-Cmp7 interaction? Some of these questions might be complemented by *in vitro* systems, such as the membrane-free system we used here (Fig. 5-1). An on-bead binding assay was already used with GST-Lem2 fragments to identify that the HEH-domain of *S. pombe* Lem2 directly binds DNA (Hirano *et al.*, 2018). An adaptation of this system to use chromatin instead of naked DNA and the addition of ESCRT-III/Vps4 components which we have already been able to purify and use in functional assays might be a start to elucidate the molecular mechanisms of Lem2 ESCRT-III/Vps4 interactions. Importantly, what is the cellular function of this mechanism and what are the functional consequences of abnormal chromatin-NE tethering? Further studies into, for example, DNA replication, DNA-damage and chromosome segregation will provide insight into this. Using *S. japonicus* or also *S. pombe* would be good way to elucidate a function for this mechanism in nuclear organisation, which could be expanded by looking into mammalian cell systems, where dynamic chromatin organisation occurs during for example differentiation. In addition, the fission yeast *S. japonicus* lends itself to being an excellent model for the study of the establishment of nucleocytoplasmic compartmentalisation, owing to simple architecture and use of conserved proteins. Further investigation into the currently known players could for example elucidate how the switch of Lem2 affinity from the tail to chromatin mediated during mitotic exit? How is the membrane actually resealed after

the breakdown of the spindle? Currently we cannot exclude or prove that ESCRT-III/Vps4 is performing a membrane resealing step in addition to its role in tail maintenance.

One particularly important aspect to follow up on is the mitotic consequences for the persistent heterochromatin-NE attachments that we have observed in the absence of either Vps32 or Vps4. Based on studies in other model systems (Champion *et al.*, 2018; Chen, 2019), it can be predicted that this might induce chromosome segregation errors. There are several ways that this could be tested. Bye staining cells for DNA and analysing the DNA content of single cells using flow-cytometry the extend of aneuploidy in the population of all the different ESCRT-III mutants can be assessed. We have shown that the growth defect that is associated with *vps32* and *vps4* deletion can be rescued with the additional deletion of *nur1* (Fig. 6-7). Therefore, we predict that particularly these first two mutants will exhibit aneuploidy, which might be rescued in the double deletion mutant. Similarly, the rate of aneuploidy could be assessed by performing a time-course of the acute inactivation of Vps4 using the temperature sensitive mutant used in Fig. 5-2. The acute inactivation of Vps4 could also be supplemented by live-imaging of chromosome segregation assess whether over time chromosome segregation errors increase.

Several lines of evidence suggest that the system presented here might be fully or partially conserved in higher eukaryotes including humans. In the first report describing LEM2 in human cells it was observed that overexpression of LEM2 resulted in its clustering at the NE. These clusters contained other NE proteins such as BAF and other LEM-domain proteins Emerin and MAN1 (Brachner *et al.*, 2005). In cultured human cancer cells, the knockdown of CHMP2A resulted in NE foci of CHMP7, CHMP4B and LEMD2, but excluded Lamin B1 (Vietri *et al.*, 2019 *preprint*). In another cell culture system similar results were obtained, the knockdown of VPS4 also resulted in NE foci containing CHMP7, CHMP4, LEM-domain protein LAP2 and Lamin A/C, but were excluded from Lamin B (Willan *et al.*, 2019). VPS4 knockdown increased the fraction of stable CHMP7-CHMP4 foci (Willan *et al*., 2019), similar to the deletion of *vps4* in *S. japonicus* (Fig. 5-4), suggesting that in the WT situation ESCRT-III/VPS4 transiently interacts with chromatin (Willan *et al*., 2019). These interactions are lost in the absence of VPS4, which provides the dynamicity of this process likely through its ATPase activity.

Thus, it might be that the persistent association of ESCRT-III with chromatin is the cause of the observed DNA damage.

Recently, two patients with an unknown genetic disorder were predicted to have some form of progeria using artificial intelligence, which is normally associated with mutations in the *LMNA* gene encoding for Lamin A. Upon genetic analysis of their genomes these two patients were found to share a point mutation in the MSC domain of LEM2 (Marbach *et al.*, 2019). Slightly overexpressing LEM2 already results in its accumulation in NE clusters (Brachner *et al*., 2005). However, this report noted that transfection of cells with lower amounts of plasmid resulted in no LEM2 clustering. When they transfected cells with the LEM2 mutant, they found that it still accumulated in clusters on the NE, sometimes in very large patches decorating the NE. These clusters and patches also contained BAF and Emerin. Nuclei of fibroblasts derived from these patients exhibited very deformed nuclei (Marbach *et al*., 2019). It would be very interesting to further elucidate if these clusters indeed also contain ESCRT-III and if the cellular phenotypes and also the disease phenotypes could be due to the aberrant regulation of chromatin-NE tethering.

Acknowledgements

I would like to thank Snezhka Oliferenko for giving me the opportunity to do my PhD in her lab, it was a great experience. I would further like to thank Snezhka for advice, mentorship and scientific insights. Next I would like to acknowledge our collaborators David Teis and Simon Sprenger, without whom this work would not have been possible. Particularly Simon for all his help with establishing the tagged ESCRT-III/Vps4 strains and the work on the *in vitro* binding assay. But also for the fun times and many coffees and beers. I would like to acknowledge Sigurd Braun, Eugene Makeyev and Jessica Greenwood for all kinds of technical help and advice with setting up and analysing the ChIP experiments. I want the thank the members of my thesis committee Frank Uhlmann, Jeremy Carlton, Dylan Owen and Baljinder Mankoo for all the advice and criticism during all my thesis committee meetings. I want to thank especially the members of the Oliferenko lab Masha Makarova, Risa Mori, Gu Ying, Sherman Foo, Sara Alam and Polina Reichert for the great lab atmosphere and for immediately welcoming

me into their midst when I arrived in London. This support that this small group has for each other is quite unique and all the fun times that we had made my experience in London really great. Lastly I would like to thank Magda Gabrysiak for all the love and support, always being there, listening to presentations and everything else.

References

Abranches, R., Beven, A. F., Aragón-Alcaide, L. and Shaw, P. J. (1998) 'Transcription sites are not correlated with chromosome territories in wheat nuclei', *Journal of Cell Biology*, 143(1), pp. 5–12. doi: 10.1083/jcb.143.1.5.

Adell, M. A. Y., Migliano, S. M. and Teis, D. (2016) 'ESCRT-III and Vps4: a dynamic multipurpose tool for membrane budding and scission', *FEBS Journal*, 283, pp. 3288–3302. doi: 10.1111/febs.13688.

Adell, M. A. Y., Migliano, S. M., Upadhyayula, S., Bykov, Y. S., Sprenger, S., Pakdel, M., Vogel, G. F., Jih, G., Skillern, W., Behrouzi, R., Babst, M., Schmidt, O., Hess, M. W., Briggs, J. A., Kirchhausen, T. and Teis, D. (2017) 'Recruitment dynamics of ESCRT-III and Vps4 to endosomes and implications for reverse membrane budding', *eLife*, 6, p. e31652. doi: 10.7554/eLife.31652.

Adell, M. A. Y. and Teis, D. (2011) 'Assembly and disassembly of the ESCRT-III membrane scission complex', *FEBS Letters*. Federation of European Biochemical Societies, 585(20), pp. 3191–3196. doi: 10.1016/j.febslet.2011.09.001.

Adell, M. A. Y., Vogel, G. F., Pakdel, M., Müller, M., Lindner, H., Hess, M. W. and Teis, D. (2014) 'Coordinated binding of Vps4 to ESCRT-III drives membrane neck constriction during MVB vesicle formation', *Journal of Cell Biology*, 205(1), pp. 33–49. doi: 10.1083/jcb.201310114.

Al-Khodairy, F., Fotou, E., Sheldrick, K. S., Griffiths, D. J. F., Lehmann, A. R. and Carr, A. M. (1994) 'Identification and characterization of new elements involved in checkpoint and feedback controls in fission yeast', *Molecular Biology of the Cell*, 5(2), pp. 147–160. doi: 10.1091/mbc.5.2.147.

Alfieri, C., Chang, L. and Barford, D. (2018) 'Mechanism for remodelling of the cell cycle checkpoint protein MAD2 by the ATPase TRIP13', *Nature*. Springer US, 559, pp. 274–278. doi: 10.1038/s41586-018-0281-1.

Allshire, R. C. and Ekwall, K. (2015) 'Epigenetics regulation of chromatin states in Schizosaccharomyces pombe', *Cold Spring Harbor Perspectives in Biology*, 7, pp. 1–25. doi: 10.1101/cshperspect.a018770.

Anderson, D. J. and Hetzer, M. W. (2007) 'Nuclear envelope formation by chromatin-mediated reorganization of the endoplasmic reticulum.', *Nature Cell Biology*, 9(10), pp. 1160–1166. doi: 10.1038/ncb1636.

Anderson, D. J., Vargas, J. D., Hsiao, J. P. and Hetzer, M. W. (2009) 'Recruitment of functionally distinct membrane proteins to chromatin mediates nuclear envelope formation in vivo.', *The Journal of Cell Biology*, 186(2), pp. 183–91. doi: 10.1083/jcb.200901106.

Aoki, K., Hayashi, H., Furuya, K., Sato, M., Takagi, T., Osumi, M., Kimura, A. and Niki, H. (2011) 'Breakage of the nuclear envelope by an extending mitotic nucleus occurs during anaphase in Schizosaccharomyces japonicus', *Genes to Cells*, 16(9), pp. 911–926. doi: 10.1111/j.1365-2443.2011.01540.x.

Aoki, K., Nakajima, R., Furuya, K. and Niki, H. (2010) 'Novel episomal vectors and a highly efficient transformation procedure for the fission yeast Schizosaccharomyces japonicus', *Yeast*, 27, pp. 1049–1060. doi: 10.1002/yea.

von Appen, A., Lajoie, D., Johnson, I. E., Trnka, M., Pick, S. M., Burlingame, A. L., Ullman, K. S. and Frost, A. (2019) 'A role for liquid-liquid phase separation in ESCRT-mediated nuclear envelope reformation.', *bioRxiv*, p. https://doi.org/10.1101/577460. doi: 10.1101/577460.

Arib, G. and Akhtar, A. (2011) 'Multiple facets of nuclear periphery in gene expression control', *Current Opinion in Cell Biology*, 23(3), pp. 346–353. doi: 10.1016/j.ceb.2010.12.005.

Arii, J., Watanabe, M., Maeda, F., Tokai-Nishizumi, N., Chihara, T., Miura, M., Maruzuru, Y., Koyanagi, N., Kato, A. and Kawaguchi, Y. (2018) 'ESCRT-III mediates budding across the inner nuclear membrane and regulates its integrity', *Nature Communications*. Springer US, 9(1). doi: 10.1038/s41467-018-05889-9.

Asencio, C., Davidson, I. F., Santarella-Mellwig, R., Ly-Hartig, T. B. N., Mall, M., Wallenfang, M. R., Mattaj, I. W. and Gorjánácz, M. (2012) 'Coordination of kinase and phosphatase activities by Lem4 enables nuclear envelope reassembly during mitosis.', *Cell*, 150(1), pp. 122–35. doi: 10.1016/j.cell.2012.04.043.

Babst, M., Katzmann, D. J., Estepa-Sabal, E. J., Meerloo, T. and Emr, S. D. (2002) 'ESCRT-III: An Endosome-Associated Heterooligomeric Protein Complex Required for MVB Sorting', *Developmental Cell*, 3(2), pp. 271–282. doi: 10.1016/S1534-5807(02)00220-4.

Babst, M., Katzmann, D. J., Snyder, W. B., Wendland, B. and Emr, S. D. (2002) 'Endosome-associated complex, ESCRT-II, recruits transport machinery for protein sorting at the multivesicular body', *Developmental Cell*, 3(2), pp. 283–289. doi: 10.1016/S1534-5807(02)00219-8.

Babst, M., Sato, T. K., Banta, L. M. and Emr, S. D. (1997) 'Endosomal transport function in yeast requires a novel AAA-type ATPase, Vps4p', *EMBO Journal*, 16(8), pp. 1820–1831. doi: 10.1093/emboj/16.8.1820.

Babst, M., Wendland, B., Estepa, E. J. and Emr, S. D. (1998) 'The Vps4p AAA ATPase regulates membrane association of a Vps protein complex required for normal endosome function', *EMBO Journal*, 17(11), pp. 2982–2993. doi: 10.1093/emboj/17.11.2982.

Banday, S., Farooq, Z., Rashid, R., Abdullah, E. and Altaf, M. (2016) 'Role of inner nuclear membrane protein complex Lem2-Nur1 in heterochromatic gene silencing in S. pombe', *Journal of Biological Chemistry*, 291(38), pp. 20021–20029. doi: 10.1074/jbc.M116.743211.

Barrales, R. R., Forn, M., Georgescu, P. R., Sarkadi, Z. and Braun, S. (2016) 'Control of heterochromatin localization and silencing by the nuclear membrane protein Lem2', *Genes & Development*, 30, pp. 1–16. doi: 10.1101/gad.271288.115.3.

Bauer, I., Brune, T., Preiss, R. and Kölling, R. (2015) 'Evidence for a non-endosomal function of the Saccharomyces cerevisiae ESCRT-III like protein Chm7', *Genetics*, 201, pp. 1439–1452.

Bleck, M., Itano, M. S., Johnson, D. S., Thomas, V. K., North, A. J., Bieniasz, P. D. and Simon, S. M. (2014) 'Temporal and spatial organization of ESCRT protein recruitment during HIV-1 budding', *Proceedings of the National Academy of Sciences*, 111(33), pp. 12211–12216. doi: 10.1073/pnas.1321655111.

Blyth, J., Makrantoni, V., Barton, R. E., Spanos, C., Rappsilber, J. and Marston, A. L. (2018) 'Genes important for schizosaccharomyces pombe meiosis identified through a functional genomics screen', *Genetics*, 208(2), pp. 589–603. doi: 10.1534/genetics.117.300527.

Bodon, G., Chassefeyre, R., Pernet-Gallay, K., Martinelli, N., Effantin, G., Hulsik, D. L., Belly, A., Goldberg, Y., Chatellard-Causse, C., Blot, B., Schoehn, G., Weissenhorn, W. and Sadoul, R. (2011) 'Charged Multivesicular Body Protein 2B (CHMP2B) of the Endosomal Sorting Complex Required for Transport-III (ESCRT-III) polymerizes into helical structures deforming the plasma membrane', *Journal of Biological Chemistry*, 286(46), pp. 40276–40286. doi: 10.1074/jbc.M111.283671.

Boettcher, B., Marquez-Lago, T. T., Bayer, M., Weiss, E. L. and Barral, Y. (2012) 'Nuclear envelope morphology constrains diffusion and promotes asymmetric protein segregation in closed mitosis', *The Journal of Cell Biology*, 197(7), pp. 921–937. doi: 10.1083/jcb.201112117.

Brachner, A. and Foisner, R. (2011) 'Evolvement of LEM proteins as chromatin tethers at the nuclear periphery', *Biochemical Society Transactions*, 39(6), pp. 1735–1741. doi: 10.1042/BST20110724.

Brachner, A., Reipert, S., Foisner, R. and Gotzmann, J. (2005) 'LEM2 is a novel MAN1-related inner nuclear membrane protein associated with A-type lamins.', *Journal of Cell Science*, 118, pp. 5797–5810. doi: 10.1242/jcs.02701.

Bustin, M. and Misteli, T. (2016) 'Nongenetic functions of the genome', *Science*, 352(6286). doi: 10.1126/science.aad6933.

Capitanchik, C., Dixon, C. R., Swanson, S. K., Florens, L., Kerr, A. R. W. and Schirmer, E. C. (2018) 'Analysis of rna-seq datasets reveals enrichment of tissue-specific splice variants for nuclear envelope proteins', *Nucleus*. Taylor & Francis, 9(1), pp. 410–430. doi: 10.1080/19491034.2018.1469351.

Caputo, S., Couprie, J., Duband-Goulet, I., Kondé, E., Lin, F., Braud, S., Gondry, M., Gilquin, B., Worman, H. J. and Zinn-Justin, S. (2006) 'The carboxyl-terminal nucleoplasmic region of MAN1 exhibits a DNA binding winged helix domain', *Journal of Biological Chemistry*, 281(26), pp. 18208–18215. doi: 10.1074/jbc.M601980200.

Carlton, J. G., Caballe, A., Agromayor, M., Kloc, M. and Martin-Serrano, J. (2012) 'ESCRT-III governs the Aurora B-mediated abscission checkpoint through CHMP4C', *Science*, pp. 220–225. doi: 10.1126/science.1217180.

Carlton, J. G. and Martin-Serrano, J. (2007) 'Parallels between cytokinesis and retroviral budding: a role for the ESCRT machinery.', *Science*, 316(5833), pp. 1908–1912. doi: 10.1126/science.1143422.

Cashikar, A. G., Shim, S., Roth, R., Maldazys, M. R., Heuser, J. E. and Hanson, P. I. (2014) 'Structure of cellular

ESCRT-III spirals and their relationship to HIV budding', *eLife*, 3, pp. 1–17. doi: 10.7554/eLife.02184.

Chabes, A., Georgieva, B., Domkin, V., Zhao, X., Rothstein, R. and Thelander, L. (2003) 'Survival of DNA damage in yeast directly depends on increased dNTP levels allowed by relaxed feedback inhibition of ribonucleotide reductase', *Cell*, 112(3), pp. 391–401. doi: 10.1016/S0092-8674(03)00075-8.

Champion, L., Pawar, S., Luithle, N., Ungricht, R. and Kutay, U. (2018) 'Dissociation of membrane–chromatin contacts is required for proper chromosome segregation in mitosis', *Molecular Biology of the Cell*, 30(4), pp. 427–440. doi: 10.1091/mbc.e18-10-0609.

Chan, J. N. Y., Poon, B. P. K., Salvi, J., Olsen, J. B., Emili, A. and Mekhail, K. (2011) 'Perinuclear cohibin complexes maintain replicative life span via roles at distinct silent chromatin domains', *Developmental Cell*. Elsevier Inc., 20(6), pp. 867–879. doi: 10.1016/j.devcel.2011.05.014.

Chen, E. S., Zhang, K., Nicolas, E., Cam, H. P., Zofall, M. and Grewal, S. I. (2008) 'Cell cycle control of centromeric repeat transcription and heterochromatin assembly', *Nature*, 451(7179), pp. 734–737. doi: 10.1038/nature06561.

Chen, R.-H. (2019) 'Chromosome detachment from the nuclear envelope is required for genome stability in closed mitosis', *Molecular Biology of the Cell*, 30, pp. 1578–1586.

Chiaruttini, N., Redondo-Morata, L., Colom, A., Humbert, F., Lenz, M., Scheuring, S. and Roux, A. (2015) 'Relaxation of loaded ESCRT-III spiral springs drives membrane deformation', *Cell*, 163, pp. 1–14. doi: 10.1016/j.cell.2015.10.017.

Chikashige, Y., Yamane, M., Okamasa, K., Tsutsumi, C., Kojidani, T., Sato, M., Haraguchi, T. and Hiraoka, Y. (2009) 'Membrane proteins Bqt3 and -4 anchor telomeres to the nuclear envelope to ensure chromosomal bouquet formation', *Journal of Cell Biology*, 187(3), pp. 413–427. doi: 10.1083/jcb.200902122.

Cremer, T., Cremer, C., Baumann, H., Luedtke, E.-K., Sperling, K., Teuber, V. and Zorn, C. (1982) 'Rabl's model of the interphase chromosome arrangement tested in Chinese hamster cells by premature chromosome condensation and laser UV-microbeam experiments', *Human Genetics*, 60, pp. 46–56.

Cremer, T., Lichter, P., Borden, J., Ward, D. and Manuelidis, L. (1988) 'Detection of chromosome aberrations in metaphase and interphase tumor cells by in situ hybridization using chromosome-specific library probes', *Human Genetics*, 80(3), pp. 235–246. doi: 10.1007/BF01790091.

Czapiewski, R., Robson, M. I. and Schirmer, E. C. (2016) 'Anchoring a Leviathan: How the nuclear membrane tethers the genome', *Frontiers in Genetics*, 7(MAY), pp. 1–13. doi: 10.3389/fgene.2016.00082.

Dahl, K. N., Ribeiro, A. J. S. and Lammerding, J. (2008) 'Nuclear shape, mechanics, and mechanotransduction', *Circulation Research*, 102(11), pp. 1307–1318. doi: 10.1161/CIRCRESAHA.108.173989.

Demirov, D. G., Ono, A., Orenstein, J. M. and Freed, E. O. (2002) 'Overexpression of the N-terminal domain of TSG101 inhibits HIV-1 budding by blocking late domain function', *Proceedings of the National Academy of Sciences*, 99(2), pp. 955–960. doi: 10.1073/pnas.032511899.

Denais, C. M., Gilbert, R. M., Isermann, P., McGregor, A. L., Lindert, M. te, Weigelin, B., Davidson, P., Friedl, P., Wolf, K. and Lammerding, J. (2016) 'Nuclear envelope rupture and repair during cancer cell migration', *Science*, 352, pp. 353–358. doi: 10.1126/science.aad7297.

Deshpande, G. P., Hayles, J., Hoe, K. L., Kim, D. U., Park, H. O. and Hartsuiker, E. (2009) 'Screening a genome-wide S. pombe deletion library identifies novel genes and pathways involved in genome stability maintenance', *DNA Repair*, 8(5), pp. 672–679. doi: 10.1016/j.dnarep.2009.01.016.

Ding, R., West, R. R., Morphew, D. M., Oakley, B. R. and McIntosh, J. R. (1997) 'The spindle pole body of Schizosaccharomyces pombe enters and leaves the nuclear envelope as the cell cycle proceeds.', *Molecular Biology of the Cell*, 8(8), pp. 1461–1479. doi: 10.1091/mbc.8.8.1461.

Dixon, J. R., Gorkin, D. U. and Ren, B. (2016) 'Chromatin Domains: The Unit of Chromosome Organization', *Molecular Cell*. Elsevier Inc., 62(5), pp. 668–680. doi: 10.1016/j.molcel.2016.05.018.

Dixon, J. R., Selvaraj, S., Yue, F., Kim, A., Li, Y., Shen, Y., Hu, M., Liu, J. S. and Ren, B. (2012) 'Topological domains in mammalian genomes identified by analysis of chromatin interactions', *Nature*. Nature Publishing Group, 485(7398), pp. 376–380. doi: 10.1038/nature11082.

Dundr, M. and Misteli, T. (2010) 'Biogenesis of nuclear bodies.', *Cold Spring Harbor perspectives in biology*, 2(12). doi: 10.1101/cshperspect.a000711.

Ebrahimi, H. and Cooper, J. P. (2012) 'Closed Mitosis : A Timely Move before Separation', *Current Biology*. Elsevier Ltd, 22(20), pp. R880–R882. doi: 10.1016/j.cub.2012.08.034.

Ebrahimi, H., Masuda, H., Jain, D. and Cooper, J. P. (2018) 'Distinct " safe zones " at the nuclear envelope ensure robust replication of heterochromatic chromosome regions', *eLife*, 7, p. e32911. doi: 10.7554/eLife.32911.

Enoch, T., Carr, A. M. and Nurse, P. (1992) 'Fission yeast genes involved in coupling mitosis to completion of DNA replication', *Genes and Development*, 6(11), pp. 2035–2046. doi: 10.1101/gad.6.11.2035.

Fernández-Álvarez, A., Bez, C., O'Toole, E. T., Morphew, M. and Cooper, J. P. (2016) 'Mitotic Nuclear Envelope Breakdown and Spindle Nucleation Are Controlled by Interphase Contacts between Centromeres and the Nuclear Envelope', *Developmental Cell*, pp. 1–16. doi: 10.1016/j.devcel.2016.10.021.

Finlan, L. E., Sproul, D., Thomson, I., Boyle, S., Kerr, E., Perry, P., Ylstra, B., Chubb, J. R. and Bickmore, W. A. (2008) 'Recruitment to the nuclear periphery can alter expression of genes in human cells', *PLoS Genetics*, 4(3), p. e1000039. doi: 10.1371/journal.pgen.1000039.

De Franceschi, N., Alqabandi, M., Miguet, N., Caillat, C., Mangenot, S., Weissenhorn, W. and Bassereau, P. (2019) 'The ESCRT protein CHMP2B acts as a diffusion barrier on reconstituted membrane necks', *Journal of Cell Science*, 132(4), p. jcs217968. doi: 10.1242/jcs.217968.

Fujita, I., Nishihara, Y., Tanaka, M., Tsujii, H., Chikashige, Y., Watanabe, Y., Saito, M., Ishikawa, F., Hiraoka, Y. and Kanoh, J. (2012) 'Telomere-nuclear envelope dissociation promoted by Rap1 phosphorylation ensures faithful chromosome segregation', *Current Biology*. Elsevier Ltd, 22(20), pp. 1932–1937. doi: 10.1016/j.cub.2012.08.019.

Furusawa, T., Rochman, M., Taher, L., Dimitriadis, E. K., Nagashima, K., Anderson, S. and Bustin, M. (2015) 'Chromatin decompaction by the nucleosomal binding protein HMGN5 impairs nuclear sturdiness', *Nature Communications*. Nature Publishing Group, 6, pp. 1–10. doi: 10.1038/ncomms7138.

Furuya, K. and Niki, H. (2009) 'Isolation of heterothallic haploid and auxotrophic mutants of Schizosaccharomyces japonicus', *Yeast*, 26(4), pp. 221–233. doi: 10.1002/yea.1662.

Garrus, J. E., Von Schwedler, U. K., Pornillos, O. W., Morham, S. G., Zavitz, K. H., Wang, H. E., Wettstein, D. A., Stray, K. M., Côté, M., Rich, R. L., Myszka, D. G. and Sundquist, W. I. (2001) 'Tsg101 and the vacuolar protein sorting pathway are essential for HIV-1 budding', *Cell*, 107(1), pp. 55–65. doi: 10.1016/S0092-8674(01)00506-2.

Gerlitz, G., Reiner, O. and Bustin, M. (2013) 'Microtubule dynamics alter the interphase nucleus', *Cellular and Molecular Life Sciences*, 70(7), pp. 1255–1268. doi: 10.1007/s00018-012-1200-5.

Godfrey, M., Kuilman, T. and Uhlmann, F. (2015) 'Nur1 Dephosphorylation Confers Positive Feedback to Mitotic Exit Phosphatase Activation in Budding Yeast', *PLoS Genetics*, 11(1). doi: 10.1371/journal.pgen.1004907.

Goliand, I., Adar-Levor, S., Segal, I., Nachmias, D., Dadosh, T., Kozlov, M. M. and Elia, N. (2018) 'Resolving ESCRT-III Spirals at the Intercellular Bridge of Dividing Cells Using 3D STORM', *Cell Reports*. ElsevierCompany., 24(7), pp. 1756–1764. doi: 10.1016/j.celrep.2018.07.051.

Gonzalez-Sandoval, A., Towbin, B. D., Kalck, V., Cabianca, D. S., Gaidatzis, D., Hauer, M. H., Geng, L., Wang, L., Yang, T., Wang, X., Zhao, K. and Gasser, S. M. (2015) 'Perinuclear Anchoring of H3K9-Methylated Chromatin Stabilizes Induced Cell Fate in C. elegans Embryos', *Cell*. Elsevier Inc., 163(6), pp. 1333–1347. doi: 10.1016/j.cell.2015.10.066.

Gonzalez, Y., Saito, A. and Sazer, S. (2012) 'Fission yeast Lem2 and Man1 perform fundamental functions of the animal cell nuclear lamina', *Nucleus*, 3(1), pp. 60–76. doi: 10.4161/nucl.18824.

Gorjánácz, M., Klerkx, E. P. F., Galy, V., Santarella, R., López-Iglesias, C., Askjaer, P. and Mattaj, I. W. (2007) 'Caenorhabditis elegans BAF-1 and its kinase VRK-1 participate directly in post-mitotic nuclear envelope assembly.', *The EMBO Journal*, 26(1), pp. 132–143. doi: 10.1038/sj.emboj.7601470.

Gu, M., LaJoie, D., Chen, O. S., von Appen, A., Ladinsky, M. S., Redd, M. J., Nikolova, L., Bjorkman, P. J., Sundquist, W. I., Ullman, K. S. and Frost, A. (2017) 'LEM2 recruits CHMP7 for ESCRT-mediated nuclear envelope closure in fission yeast and human cells', *Proceedings of the National Academy of Sciences*, 114(11), pp. E2166–E2175. doi: 10.1073/pnas.1613916114.

Gu, Y. and Oliferenko, S. (2015) 'Comparative biology of cell division in the fission yeast clade', *Current Opinion in Microbiology*. Elsevier Ltd, 28, pp. 18–25. doi: 10.1016/j.mib.2015.07.011.

Gu, Y., Yam, C. and Oliferenko, S. (2012) 'Divergence of mitotic strategies in fission yeasts', *Nucleus*, 3(3), pp. 220–225. doi: 10.4161/nucl.19514.

Guelen, L., Pagie, L., Brasset, E., Meuleman, W., Faza, M. B., Talhout, W., Eussen, B. H., De Klein, A., Wessels, L., De Laat, W. and Van Steensel, B. (2008) 'Domain organization of human chromosomes revealed by mapping of nuclear lamina interactions', *Nature*, 453(7197), pp. 948–951. doi: 10.1038/nature06947.

Güttinger, S., Laurell, E. and Kutay, U. (2009) 'Orchestrating nuclear envelope disassembly and reassembly during mitosis.', *Nature Reviews. Molecular Cell Biology*, 10(3), pp. 178–191. doi: 10.1038/nrm2641.

Halfmann, C. T., Sears, R. M., Katiyar, A., Busselman, B. W., Aman, L. K., Zhang, Q., O'Bryan, C. S., Angelini, T. E., Lele, T. P. and Roux, K. J. (2019) 'Repair of nuclear ruptures requires barrier-to-autointegration factor', *The Journal of Cell Biology*, 28, pp. 2136–2149. doi: 10.1083/jcb.201901116.

Han, G. S., Wu, W. I. and Carman, G. M. (2006) 'The Saccharomyces cerevisiae lipin homolog is a Mg2+-dependent phosphatidate phosphatase enzyme', *Journal of Biological Chemistry*, 281(14), pp. 9210–9218. doi: 10.1074/jbc.M600425200.

Han, T. X., Xu, X. Y., Zhang, M. J., Peng, X. and Du, L. L. (2010) 'Global fitness profiling of fission yeast deletion strains by barcode sequencing', *Genome Biology*, 11(6). doi: 10.1186/gb-2010-11-6-r60.

Hanson, P. I., Roth, R., Lin, Y. and Heuser, J. E. (2008) 'Plasma membrane deformation by circular arrays of ESCRT-III protein filaments', *The Journal of Cell Biology*, 180(2), pp. 389–402. doi: 10.1083/jcb.200707031.

Harada, T., Swift, J., Irianto, J., Shin, J. W., Spinler, K. R., Athirasala, A., Diegmiller, R., Dingal, P. C. D. P., Ivanovska, I. L. and Discher, D. E. (2014) 'Nuclear lamin stiffness is a barrier to 3D migration, but softness can limit survival', *Journal of Cell Biology*, 204(5), pp. 669–682. doi: 10.1083/jcb.201308029.

Hayles, J., Wood, V., Jeffery, L., Hoe, K.-L., Kim, D.-U., Park, H.-O., Salas-Pino, S., Heichinger, C. and Nurse, P. (2013) 'A genome-wide resource of cell cycle and cell shape genes of fission yeast.', *Open biology*, 3(5), p. 130053. doi: 10.1098/rsob.130053.

Hediger, F., Neumann, F. R., Van Houwe, G., Dubrana, K. and Gasser, S. M. (2002) 'Live imaging of telomeres: yKu and Sir proteins define redundant telomere-anchoring pathways in yeast', *Current Biology*, 12(02), pp. 2076–2089. doi: 10.1016/S0960-9822(02)01338-6.

Henne, W. M., Buchkovich, N. J. and Emr, S. D. (2011) 'The ESCRT Pathway', *Developmental Cell*. Elsevier Inc., 21(1), pp. 77–91. doi: 10.1016/j.devcel.2011.05.015.

Herrada, I., Samson, C., Velours, C., Renault, L., Östlund, C., Chervy, P., Puchkov, D., Worman, H. J., Buendia, B. and Zinn-Justin, S. (2015) 'Muscular dystrophy mutations impair the nuclear envelope emerin self-assembly properties', *ACS Chemical Biology*, 10, pp. 2733–2742. doi: 10.1021/acschembio.5b00648.

Hetzer, M. W. (2010) 'The nuclear envelope', *Cold Spring Harbor Perspectives in Biology*, 2, p. a000539.

Hirano, Y., Kinugasa, Y., Asakawa, H., Chikashige, Y., Obuse, C., Haraguchi, T. and Hiraoka, Y. (2018) 'Lem2 is retained at the nuclear envelope through its interaction with Bqt4 in fission yeast', *Genes to Cells*, (December 2017), pp. 1–14. doi: 10.1111/gtc.12557.

Hiraoka, Y., Maekawa, H., Asakawa, H., Chikashige, Y., Kojidani, T., Osakada, H., Matsuda, A. and Haraguchi, T. (2011) 'Inner nuclear membrane protein Ima1 is dispensable for intranuclear positioning of centromeres.', *Genes to Cells*, 16(10), pp. 1000–11. doi: 10.1111/j.1365-2443.2011.01544.x.

Hochstrasser, M., Mathog, D., Gruenbaum, Y., Saumweber, H. and Sedat, J. W. (1986) 'Spatial organization of chromosomes in the salivary gland nuclei of Drosophila melanogaster', *Journal of Cell Biology*, 102(1), pp. 112–123. doi: 10.1083/jcb.102.1.112.

Hoffmann, K., Sperling, K., Olins, A. L. and Olins, D. E. (2007) 'The granulocyte nucleus and lamin B receptor: Avoiding the ovoid', *Chromosoma*, 116(3), pp. 227–235. doi: 10.1007/s00412-007-0094-8.

Horio, T., Kimura, N., Basaki, A., Tanaka, Y., Noguchi, T., Akashi, T. and Tanaka, K. (2002) 'Molecular and structural characterization of the spindle pole bodies in the fission yeast Schizosaccharomyces japonicus var. japonicus', *Yeast*, 19(15), pp. 1335–1350. doi: 10.1002/yea.921.

Howard, T., Stauffer, D., Degnin, C. and Hollenberg, S. (2001) 'CHMP1 functions as a member of a newly defined family of vesicle trafficking proteins', *Journal of Cell Science*, 114(13), pp. 2395–2404.

Hu, C., Inoue, H., Sun, W., Takeshita, Y., Huang, Y., Xu, Y., Kanoh, J. and Chen, Y. (2018) 'Structural insights into chromosome attachment to the nuclear envelope by an inner nuclear membrane protein Bqt4 in fission yeast', *Nucleic Acids Research*. Oxford University Press, pp. 1–12. doi: 10.1093/nar/gky1186.

Hu, C., Inoue, H., Sun, W., Takeshita, Y., Huang, Y., Xu, Y., Kanoh, J. and Chen, Y. (2019) 'The Inner Nuclear Membrane Protein Bqt4 in Fission Yeast Contains a DNA-Binding Domain Essential for Telomere Association with the Nuclear Envelope', *Structure*. Elsevier Ltd., 27(2), p. 335–343.e3. doi: 10.1016/j.str.2018.10.010.

Ikegami, K., Egelhofer, T. a, Strome, S. and Lieb, J. D. (2010) 'Caenorhabditis elegans chromosome arms are anchored to the nuclear membrane via discontinuous association with LEM-2.', *Genome Biology*. BioMed Central Ltd, 11(12), p. R120. doi: 10.1186/gb-2010-11-12-r120.

Jimenez, A. J., Maiuri, P., Lafaurie-Janvore, J., Divoux, S., Piel, M. and Perez, F. (2014) 'ESCRT machinery is required for plasma membrane repair', *Science*, 343(6174), pp. 1247136–1247136. doi: 10.1126/science.1247136.

Jin, Q. W., Fuchs, J. and Loidl, J. (2000) 'Centromere clustering is a major determinant of yeast interphase nuclear organization', *Journal of Cell Science*, 113(11), pp. 1903–1912.

Job, G., Brugger, C., Xu, T., Lowe, B. R., Pfister, Y., Qu, C., Shanker, S., Baños Sanz, J. I., Partridge, J. F. and Schalch, T. (2016) 'SHREC Silences Heterochromatin via Distinct Remodeling and Deacetylation Modules', *Molecular Cell*, 62(2), pp. 207–221. doi: 10.1016/j.molcel.2016.03.016.

Johnson, D. S., Bleck, M. and Simon, S. M. (2018) 'Timing of ESCRT-III protein recruitment and membrane scission during HIV-1 assembly.', *eLife*, 7, pp. 1–20. doi: 10.7554/eLife.36221.

Jouvenet, N., Zhadina, M., Bieniasz, P. D. and Simon, S. M. (2011) 'Dynamics of ESCRT protein recruitment during retroviral assembly', *Nature Cell Biology*. Nature Publishing Group, 13(4), pp. 394–402. doi: 10.1038/ncb2207.

Kanoh, J. (2013) 'Release of chromosomes from the nuclear envelope: A universal mechanism for eukaryotic mitosis?', *Nucleus*, 4(2), pp. 100–104. doi: 10.4161/nucl.23984.

Kanoh, J., Sadaie, M., Urano, T. and Ishikawa, F. (2005) 'Telomere binding protein Taz1 establishes Swi6 heterochromatin independently of RNAi at telomeres', *Current Biology*, 15(20), pp. 1808–1819. doi: 10.1016/j.cub.2005.09.041.

Katzmann, D. J., Babst, M. and Emr, S. D. (2001) 'Ubiquitin-dependent sorting into the multivesicular body pathway requires the function of a conserved endosomal protein sorting complex, ESCRT-I', *Cell*, 106(2), pp. 145–155. doi: 10.1016/S0092-8674(01)00434-2.

Kim, Y., Gentry, M. S., Harris, T. E., Wiley, S. E., Lawrence, J. C. and Dixon, J. E. (2007) 'A conserved phosphatase cascade that regulates nuclear membrane biogenesis', *Proceedings of the National Academy of Sciences of the United States of America*, 104(16), pp. 6596–6601. doi: 10.1073/pnas.0702099104.

Kind, J., Pagie, L., Ortabozkoyun, H., Boyle, S., De Vries, S. S., Janssen, H., Amendola, M., Nolen, L. D., Bickmore, W. A. and Van Steensel, B. (2013) 'Single-cell dynamics of genome-nuclear lamina interactions', *Cell*. Elsevier Inc., 153(1), pp. 178–192. doi: 10.1016/j.cell.2013.02.028.

Kind, J., Pagie, L., De Vries, S. S., Nahidiazar, L., Dey, S. S., Bienko, M., Zhan, Y., Lajoie, B., De Graaf, C. A., Amendola, M., Fudenberg, G., Imakaev, M., Mirny, L. A., Jalink, K., Dekker, J., Van Oudenaarden, A. and Van Steensel, B. (2015) 'Genome-wide Maps of Nuclear Lamina Interactions in Single Human Cells', *Cell*. Elsevier Inc., 163(1), pp. 134–147. doi: 10.1016/j.cell.2015.08.040.

King, M. C. and Lusk, C. P. (2019) 'Loss of nuclear envelope integrity? No probLEM—BAF has it covered', *The Journal of Cell Biology*, 218(7), p. jcb.201905155. doi: 10.1083/jcb.201905155.

Koç, A., Wheeler, L. J., Mathews, C. K. and Merrill, G. F. (2004) 'Hydroxyurea Arrests DNA Replication by a Mechanism that Preserves Basal dNTP Pools', *Journal of Biological Chemistry*, 279(1), pp. 223–230. doi: 10.1074/jbc.M303952200.

Korfali, N., Wilkie, G. S., Swanson, S. K., Srsen, V., de las Heras, J., Batrakou, D. G., Malik, P., Zuleger, N., Kerr, A. R. W., Florens, L. and Schirmer, E. C. (2012) 'The nuclear envelope proteome differs notably between tissues',

Nucleus, 3(6). doi: 10.4161/nucl.22257.

Kubai, D. F. and Ris, H. (1969) 'Division in the dinoflagellate Gyrodinium cohnii (Schiller). A new type of nuclear reproduction.', *The Journal of cell biology*, 40(2), pp. 508–528. doi: 10.1083/jcb.40.2.508.

Kumaran, R. I. and Spector, D. L. (2008) 'A genetic locus targeted to the nuclear periphery in living cells maintains its transcriptional competence', *The Journal of Cell Biology*, 180(1), pp. 51–65. doi: 10.1083/jcb.200706060.

Lata, S., Schoehn, G., Jain, A., Pires, R., Piehler, J., Gottlinger, H. G. and Weissenhorn, W. (2008) 'Helical structures of ESCRT-III are disassembled by VPS4.', *Science*, 321(5894), pp. 1354–7. doi: 10.1126/science.1161070.

Lieberman-aiden, E., Berkum, N. L. Van, Williams, L., Imakaev, M., Ragoczy, T., Telling, A., Amit, I., Lajoie, B. R., Sabo, P. J., Dorschner, M. O., Sandstrom, R., Bernstein, B., Bender, M. A., Groudine, M., Gnirke, A., Stamatoyannopoulos, J., Mirny, L. A., Lander, E. S. and Dekker, J. (2009) 'Comprehensive Mapping of Long-Range Interactions Reveals Folding Principles of the Human Genome', *Science*, 33292(October), pp. 289–294.

Lim, G. H. W., Huber, G., Torii, Y., Hirata, A., Miller, J. and Sazer, S. (2007) 'Vesicle-like biomechanics governs important aspects of nuclear geometry in fission yeast.', *PloS one*, 2(9), p. e948. doi: 10.1371/journal.pone.0000948.

Lin, C. H., MacGurn, J. A., Chu, T., Stefan, C. J. and Emr, S. D. (2008) 'Arrestin-related ubiquitin-ligase adaptors regulate endocytosis and protein turnover at the cell surface', *Cell*, 135(4), pp. 714–725. doi: 10.1016/j.cell.2008.09.025.

Loncle, N., Agromayor, M., Martin-Serrano, J. and Williams, D. W. (2015) 'An ESCRT module is required for neuron pruning', *Scientific Reports*, 5, p. 8461. doi: 10.1038/srep08461.

Lu, L., Ladinsky, M. S. and Kirchhausen, T. (2011) 'Formation of the postmitotic nuclear envelope from extended ER cisternae precedes nuclear pore assembly', *Journal of Cell Biology*, 194(3), pp. 425–440. doi: 10.1083/jcb.201012063.

Lucena, R., Dephoure, N., Gygi, S. P., Kellogg, D. R., Tallada, V. A., Daga, R. R. and Jimenez, J. (2015) 'Nucleocytoplasmic transport in the midzone membrane domain controls yeast mitotic spindle disassembly', *The Journal of Cell Biology*, 209(3), pp. 387–402. doi: 10.1083/jcb.201412144.

Makarova, M., Gu, Y., Chen, J.-S., Beckley, J. R., Gould, K. L. and Oliferenko, S. (2016) 'Temporal regulation of lipin activity diverged to account for differences in mitotic programs', *Current Biology*, 26, pp. 1–7. doi: 10.1016/j.cub.2015.11.061.

Makarova, M. and Oliferenko, S. (2016) 'Mixing and matching nuclear envelope remodeling and spindle assembly strategies in the evolution of mitosis', *Current Opinion in Cell Biology*. Elsevier Ltd, 41, pp. 43–50. doi: 10.1016/j.ceb.2016.03.016.

Manohar, S., Harlow, M., Nguyen, H., Li, J., Hankins, G. R. and Park, M. (2011) 'Chromatin modifying protein 1A (Chmp1A) of the endosomal sorting complex required for transport (ESCRT)-III family activates ataxia telangiectasia mutated (ATM) for PanC-1 cell growth inhibition', *Cell Cycle*, 10(15), pp. 2529–2539. doi: 10.4161/cc.10.15.15926.

Mans, B. J., Anantharaman, V., Aravind, L. and Koonin, E. V. (2004) 'Comparative genomics, evolution and origins of the nuclear envelope and nuclear pore complex', *Cell Cycle*, 3(12), pp. 1612–1637. doi: 10.4161/cc.3.12.1316.

Marbach, F., Rustad, C. F., Riess, A., Đukić, D., Hsieh, T. C., Jobani, I., Prescott, T., Bevot, A., Erger, F., Houge, G., Redfors, M., Altmueller, J., Stokowy, T., Gilissen, C., Kubisch, C., Scarano, E., Mazzanti, L., Fiskerstrand, T., Krawitz, P. M., Lessel, D. and Netzer, C. (2019) 'The Discovery of a LEMD2-Associated Nuclear Envelopathy with Early Progeroid Appearance Suggests Advanced Applications for AI-Driven Facial Phenotyping', *American Journal of Human Genetics*, 104(4), pp. 749–757. doi: 10.1016/j.ajhg.2019.02.021.

Martin-Serrano, J., Zang, T. and Bieniasz, P. D. (2001) 'HIV-1 and Ebola virus encode small peptide motifs that recruit Tsg101 to sites of particle assembly to facilitate egress', *Nature Medicine*, 7(12), pp. 1313–1319. doi: 10.1038/nm1201-1313.

Mast, F. D., Herricks, T., Strehler, K. M., Miller, L. R., Saleem, R. A., Rachubinski, R. A. and Aitchison, J. D. (2018) 'ESCRT-III is required for scissioning new peroxisomes from the endoplasmic reticulum.', *Journal of Cell Biology*, pp. 1–24. doi: 10.1083/jcb.201706044.

Masuda, K., Xu, Z. J., Takahashi, S., Ito, A., Ono, M., Nomura, K. and Inoue, M. (1997) 'Peripheral framework of carrot cell nucleus contains a novel protein predicted to exhibit a long α-helical domain', *Experimental Cell Research*, 232(1), pp. 173–181. doi: 10.1006/excr.1997.3531.

Matusek, T., Wendler, F., Polès, S., Pizette, S., D'Angelo, G., Fürthauer, M. and Therond, P. P. (2014) 'The ESCRT machinery regulates the secretion and long-range activity of Hedgehog', *Nature*, 516(729), pp. 99–103. doi: 10.1038/nature13847.

McCullough, J., Clippinger, A. K., Talledge, N., Skowyra, M. L., Saunders, M. G., Naismith, T. V., Colf, L. A., Afonine, P., Arthur, C., Sundquist, W. I., Hanson, P. I. and Frost, A. (2015) 'Structure and membrane remodeling activity of ESCRT-III helical polymers', *Science*, 350(6267), pp. 1548–1551. doi: 10.1126/science.aad8305.

Meier, I., Phelan, T., Gruissem, W., Spiker, S. and Schneider, D. (1996) 'MFP1, a novel plant filament-like protein with affinity for matrix attachment region DNA', *Plant Cell*, 8(11), pp. 2105–2115. doi: 10.1105/tpc.8.11.2105.

Meister, P., Towbin, B. D., Pike, B. L., Ponti, A. and Gasser, S. M. (2010) 'The spatial dynamics of tissue-specific promoters during C. elegans development', *Genes and Development*, 24(8), pp. 766–782. doi: 10.1101/gad.559610.

Mekhail, K. and Moazed, D. (2010) 'The nuclear envelope in genome organization, expression and stability.', *Nature reviews. Molecular cell biology*. Nature Publishing Group, 11(5), pp. 317–28. doi: 10.1038/nrm2894.

Mekhail, K., Seebacher, J., Gygi, S. P. and Moazed, D. (2008) 'Role for perinuclear chromosome tethering in maintenance of genome stability', *Nature*, 456(7222), pp. 667–670. doi: 10.1038/nature07460.

Meuleman, W., Peric-Hupkes, D., Kind, J., Beaudry, J. B., Pagie, L., Kellis, M., Reinders, M., Wessels, L. and Van Steensel, B. (2013) 'Constitutive nuclear lamina-genome interactions are highly conserved and associated with A/T-rich sequence', *Genome Research*, 23(2), pp. 270–280. doi: 10.1101/gr.141028.112.

Mierzwa, B. E., Chiaruttini, N., Redondo-morata, L., Filseck, J. M. Von, König, J., Larios, J., Poser, I., Müller-reichert, T., Scheuring, S., Roux, A. and Gerlich, D. W. (2017) 'Dynamic subunit turnover in ESCRT-III assemblies is regulated by Vps4 to mediate membrane remodelling during cytokinesis', *Nature Cell Biology*, 19(7), pp. 787–798. doi: 10.1038/ncb3559.

Mochida, G. H., Ganesh, V. S., De Michelena, M. I., Dias, H., Atabay, K. D., Kathrein, K. L., Huang, H. T., Sean Hill, R., Felie, J. M., Rakiec, D., Gleason, D., Hill, A. D., Malik, A. N., Barry, B. J., Partlow, J. N., Tan, W. H., Glader, L. J., James Barkovich, A., Dobyns, W. B., Zon, L. I. and Walsh, C. A. (2012) 'CHMP1A encodes an essential regulator of BMI1-INK4A in cerebellar development', *Nature Genetics*. Nature Publishing Group, 44(11), pp. 1260–1264. doi: 10.1038/ng.2425.

Monroe, N., Han, H., Shen, P. S., Sundquist, W. I. and Hill, C. P. (2017) 'Structural basis of protein translocation by the Vps4-Vta1 AAA ATPase', *eLife*, 6, pp. 1–22. doi: 10.7554/eLife.24487.001.

Moreno, S., Klar, A. and Nurse, P. (1991) 'Molecular Genetic Analysis of Fission Yeast Schizosaccharomyces pombe', *Methods in Enzymology*, 194, pp. 795–823. doi: 10.1038/289119a0.

Morita, E., Sandrin, V., Chung, H.-Y., Morham, S. G., Gygi, S. P., Rodesch, C. K. and Sundquist, W. I. (2007) 'Human ESCRT and ALIX proteins interact with proteins of the midbody and function in cytokinesis.', *The EMBO Journal*, 26(19), pp. 4215–27. doi: 10.1038/sj.emboj.7601850.

Musacchio, A. (2015) 'The Molecular Biology of Spindle Assembly Checkpoint Signaling Dynamics', *Current Biology*. Elsevier Ltd, 25(20), pp. R1002–R1018. doi: 10.1016/j.cub.2015.08.051.

Obita, T., Saksena, S., Ghazi-Tabatabai, S., Gill, D., Perisic, O., Emr, S. and Williams, R. (2007) 'Structural basis for selective recognition of ESCRT-III by the AAA ATPase Vps4', *Nature*, 449(7163), pp. 735–739. doi: 10.1038/nature06171.

Ogawa, S., Kido, S., Handa, T., Ogawa, H., Asakawa, H., Takahashi, T. S., Nakagawa, T., Hiraoka, Y. and Masukata, H. (2018) 'Shelterin promotes tethering of late replication origins to telomeres for replication-timing control', *The EMBO Journal*, 37, p. e98997. doi: 10.15252/embj.201898997.

Olmos, Y., Hodgson, L., Mantell, J., Verkade, P. and Carlton, J. G. (2015) 'ESCRT-III controls nuclear envelope reformation', *Nature*, 522, pp. 236–239. doi: 10.1038/nature14503.

Olmos, Y., Perdrix-rosell, A. and Carlton, J. G. (2016) 'Membrane binding by CHMP7 coordinates ESCRT- III-

dependent nuclear envelope reformation', *Current Biology*. Elsevier Ltd., 26, pp. 1–7. doi: 10.1016/j.cub.2016.07.039.

Otsuka, S., Bui, K. H., Schorb, M., Hossain, M. J., Politi, A. Z., Koch, B., Eltsov, M., Beck, M. and Ellenberg, J. (2016) 'Nuclear pore assembly proceeds by an inside-out extrusion of the nuclear envelope', *eLife*, 5, pp. 1–23. doi: 10.7554/eLife.19071.

Otsuka, S., Steyer, A. M., Schorb, M., Hériché, J. K., Hossain, M. J., Sethi, S., Kueblbeck, M., Schwab, Y., Beck, M. and Ellenberg, J. (2018) 'Postmitotic nuclear pore assembly proceeds by radial dilation of small membrane openings', *Nature Structural and Molecular Biology*. Springer US, 25(1), pp. 21–28. doi: 10.1038/s41594-017-0001-9.

Parada, L. and Misteli, T. (2002) 'Chromosome positioning in the interphase nucleus.', *Trends in cell biology*, 12(9), pp. 425–32. Available at: http://www.ncbi.nlm.nih.gov/pubmed/12220863.

Paulin, J. J. and Brooks, A. S. (1975) 'Macronuclear differentiation during oral regeneration in Stentor coeruleus', *Journal of Cell Science*, 19(3), pp. 531–541.

Penfield, L., Shankar, R., Szentgyörgyi, E., Laffitte, A., Mauro, M., Audhya, A., Müller-Reichtert, T. and Bahmanyar, S. (2019) 'Local regulation of lipid synthesis controls ER sheet insertion into nuclear envelope holes to complete nuclear closure Lauren', *bioRxiv*, p. doi: http://dx.doi.org/10.1101/757013.

Penfield, L., Wysolmerski, B., Mauro, M., Farhadifar, R., Martinez, M. A., Biggs, R., Wu, H.-Y., Broberg, C., Needleman, D. and Bahmanyar, S. (2018) 'Dynein-pulling forces counteract lamin-mediated nuclear stability during nuclear envelope repair.', *Molecular Biology of the Cell*, 29, pp. 852–868. doi: 10.1091/mbc.E17-06-0374.

Peric-Hupkes, D., Meuleman, W., Pagie, L., Bruggeman, S. W. M., Solovei, I., Brugman, W., Gräf, S., Flicek, P., Kerkhoven, R. M., van Lohuizen, M., Reinders, M., Wessels, L. and van Steensel, B. (2010) 'Molecular Maps of the Reorganization of Genome-Nuclear Lamina Interactions during Differentiation', *Molecular Cell*, 38(4), pp. 603–613. doi: 10.1016/j.molcel.2010.03.016.

Petersen, J. and Russell, P. (2016) 'Growth and the environment of Schizosaccharomyces pombe', *Cold Spring Harbor Protocols*, p. doi:10.1101/pdb.top079764. doi: 10.1101/pdb.top079764.

Pickersgill, H., Kalverda, B., De Wit, E., Talhout, W., Fornerod, M. and Van Steensel, B. (2006) 'Characterization of the Drosophila melanogaster genome at the nuclear lamina', *Nature Genetics*, 38(9), pp. 1005–1014. doi: 10.1038/ng1852.

Poleshko, A., Smith, C. L., Nguyen, S. C., Sivaramakrishnan, P., Wong, K. G., Murray, J. I., Lakadamyali, M., Joyce, E. F., Jain, R. and Epstein, J. A. (2019) 'H3K9me2 orchestrates inheritance of spatial positioning of peripheral heterochromatin through mitosis', *eLife*, 8, pp. 1–24. doi: 10.7554/elife.49278.

R Core Team (2019) 'R: A language and environment for statistical computing. R Foundation for Statistical Computing', p. https://www.R-project.org/.

Raab, M., Gentili, M., Belly, H. De, Thiam, H. R., Vargas, P., Jimenez, A. J., Lautenschlaeger, F., Manel, N. and Piel, M. (2016) 'ESCRT III repairs nuclear envelope ruptures during cell migration to limit DNA damage and cell death', *Science*, 352(6283), pp. 359–362. doi: 10.1126/science.aad7611.

Radulovic, M., Bongiovanni, A., Schink, K. O., Nähse-Kumpf, V., Wenzel, E. M., Lafont, F. and Stenmark, H. (2018) 'ESCRT-mediated lysosome repair precedes lysophagy and promotes cell survival', *EMBO Journal*, 37, p. e99753. doi: 10.1101/313866.

Raikhel, N., Paulin, J. J. and Skarlato, S. O. (1981) 'Mitosis of Micronuclei During Division and Regeneration in the Ciliate Stentor coeruleus', *The Journal of Protozoology*, 28(1), pp. 103–107. doi: 10.1111/j.1550-7408.1981.tb02812.x.

Reddy, K. L., Zullo, J. M., Bertolino, E. and Singh, H. (2008) 'Transcriptional repression mediated by repositioning of genes to the nuclear lamina', *Nature*, 452(7184), pp. 243–247. doi: 10.1038/nature06727.

Rhind, N., Chen, Z., Yassour, M., Thompson, D. A., Haas, B. J., Habib, N., Wapinski, I., Roy, S., Lin, M. F., Heiman, D. I., Young, S. K., Furuya, K., Guo, Y., Pidoux, A., Chen, H. M., Robbertse, B., Goldberg, J. M., Aoki, K., Bayne, E. H., Berlin, A. M., Desjardins, C. A., Dobbs, E., Dukaj, L., Fan, L., FitzGerald, M. G., French, C., Gujja, S., Hansen, K., Keifenheim, D., Levin, J. Z., Mosher, R. A., Müller, C. A., Pfiffner, J., Priest, M., Russ, C., Smialowska, A., Swoboda, P., Sykes, S. M., Vaughn, M., Vengrova, S., Yoder, R., Zeng, Q., Allshire, R., Baulcombe, D., Birren, B. W., Brown,

W., Ekwall, K., Kellis, M., Leatherwood, J., Levin, H., Margalit, H., Martienssen, R., Nieduszynski, C. A., Spatafora, J. W., Friedman, N., Dalgaard, J. Z., Baumann, P., Niki, H., Regev, A. and Nusbaum, C. (2011) 'Comparative functional genomics of the fission yeasts.', *Science*, 332(6032), pp. 930–6. doi: 10.1126/science.1203357.

Robijns, J., Molenberghs, F., Sieprath, T., Corne, T. D. J., Verschuuren, M. and De Vos, W. H. (2016) 'In silico synchronization reveals regulators of nuclear ruptures in lamin A/C deficient model cells', *Scientific Reports*, 6(July), p. 30325. doi: 10.1038/srep30325.

Robson, M. I., de las Heras, J. I., Czapiewski, R., Lê Thành, P., Booth, D. G., Kelly, D. A., Webb, S., Kerr, A. R. W. and Schirmer, E. C. (2016) 'Tissue-Specific Gene Repositioning by Muscle Nuclear Membrane Proteins Enhances Repression of Critical Developmental Genes during Myogenesis', *Molecular Cell*, 62(6), pp. 834–847. doi: 10.1016/j.molcel.2016.04.035.

Robson, M. I., De Las Heras, J. I., Czapiewski, R., Sivakumar, A., Kerr, A. R. W. and Schirmer, E. C. (2017) 'Constrained release of lamina-associated enhancers and genes from the nuclear envelope during T-cell activation facilitates their association in chromosome compartments', *Genome Research*, 27(7), pp. 1126–1138. doi: 10.1101/gr.212308.116.

Russell, J. J., Theriot, J. A., Sood, P., Marshall, W. F., Landweber, L. F., Fritz-Laylin, L., Polka, J. K., Oliferenko, S., Gerbich, T., Gladfelter, A., Umen, J., Bezanilla, M., Lancaster, M. A., He, S., Gibson, M. C., Goldstein, B., Tanaka, E. M., Hu, C.-K. and Brunet, A. (2017) *Non-model model organisms*, *BMC Biology*. BMC Biology. doi: 10.1186/s12915-017-0391-5.

Rüthnick, D. and Schiebel, E. (2018) 'Duplication and Nuclear Envelope Insertion of the Yeast Microtubule Organizing Centre, the Spindle Pole Body', *Cells*, 7(5), p. 42. doi: 10.3390/cells7050042.

Santos-Rosa, H., Leung, J., Grimsey, N., Peak-Chew, S. and Siniossoglou, S. (2005) 'The yeast lipin Smp2 couples phospholipid biosynthesis to nuclear membrane growth', *EMBO Journal*, 24(11), pp. 1931–1941. doi: 10.1038/sj.emboj.7600672.

Schäfer, J. A., Schessner, J. P., Bircham, P. W., Tsuji, T., Funaya, C., Schaeff, K., Ruffini, G., Papagiannidis, D., Knop, M., Fujimoto, T. and Schuck, S. (2019) 'ESCRT machinery mediates selective microautophagy of endoplasmic reticulum', *EMBO Journal*, p. e102586. doi: 10.1101/661306.

Schindelin, J., Arena, E. T., DeZonia, B. E., Hiner, M. C., Eliceiri, K. W., Rueden, C. T. and Walter, A. E. (2017) 'ImageJ2: ImageJ for the next generation of scientific image data', *BMC Bioinformatics*. BMC Bioinformatics, 18(1), pp. 1–26. doi: 10.1186/s12859-017-1934-z.

Schindelin, J., Arganda-Carreras, I., Frise, E., Kaynig, V., Longair, M., Pietzsch, T., Preibisch, S., Rueden, C., Saalfeld, S., Schmid, B., Tinevez, J. Y., White, D. J., Hartenstein, V., Eliceiri, K., Tomancak, P. and Cardona, A. (2012) 'Fiji: An open-source platform for biological-image analysis', *Nature Methods*, 9(7), pp. 676–682. doi: 10.1038/nmeth.2019.

Schirmer, E. C., Florens, L., Guan, T., Yates, J. R. and Gerace, L. (2003) 'Nuclear Membrane Proteins with Potential Disease links Found By Subtractive Proteomics', *Science*, 301(5638), pp. 1380–1382. doi: 10.1126/science.1088176.

Schirmer, E. C. and Gerace, L. (2005) 'The nuclear membrane proteome: extending the envelope', *Trends in Biochemical Sciences*, 30(10), pp. 551–558. doi: 10.1016/j.tibs.2005.08.003.

Schober, H., Ferreira, H., Kalck, V., Gehlen, L. and Gasser, S. (2009) 'Yeast telomerase and the SUN domain protein Mps3 anchor telomeres and repress subtelomeric recombination', *Genes & development*, 23, pp. 928–938. doi: 10.1101/gad.1787509.nuclear.

Schöneberg, J., Lee, I.-H., Iwasa, J. H. and Hurley, J. H. (2016) 'Reverse-topology membrane scission by the ESCRT proteins.', *Nature reviews. Molecular cell biology*. Nature Publishing Group, 18, pp. 5–17. doi: 10.1038/nrm.2016.121.

Schreiner, S. M., Koo, P. K., Zhao, Y., Mochrie, S. G. J. and King, M. C. (2015) 'The tethering of chromatin to the nuclear envelope supports nuclear mechanics', *Nature Communications*, 6, p. DOI: 10.1038/ncomms8159. doi: 10.1038/ncomms8159.

Segura-Totten, M. and Wilson, K. L. (2004) 'BAF: Roles in chromatin, nuclear structure and retrovirus integration', *Trends in Cell Biology*, 14(5), pp. 261–266. doi: 10.1016/j.tcb.2004.03.004.

Shestakova, A., Hanono, A., Drosner, S., Curtiss, M., Davies, B., Katzmann, D. and Babst, M. (2010) 'Assembly of the AAA ATPase Vps4 on ESCRT-III', *Molecular Biology of the Cell*, 21, pp. 1059–1071. doi: 10.1091/mbc.E09.

Sivakumar, A., de las Heras, J. I. and Schirmer, E. C. (2019) 'Spatial genome organization: From development to disease', *Frontiers in Cell and Developmental Biology*, 7(MAR), p. doi: 10.3389/fcell.2019.00018. doi: 10.3389/fcell.2019.00018.

Skowyra, M. L., Schlesinger, P. H., Naismith, T. V. and Hanson, P. I. (2018) 'Triggered recruitment of ESCRT machinery promotes endolysosomal repair', *Science*, 360(6384), p. eaar5078. doi: 10.1126/science.aar5078.

Smoyer, C. J., Katta, S. S., Gardner, J. M., Stoltz, L., McCroskey, S., Bradford, W. D., McClain, M., Smith, S. E., Slaughter, B. D., Unruh, J. R. and Jaspersen, S. L. (2016) 'Analysis of membrane proteins localizing to the inner nuclear envelope in living cells', *The Journal of Cell Biology*, 215(4), pp. 575–590. doi: 10.1083/jcb.201607043.

De Souza, C., Osmani, A., Hashmim, S. and Osmani, S. (2004) 'Partial nuclear pore complex disassembly during closed mitosis in Aspergillus nidulans', *Current Biology*, 23, pp. 1973–1984. doi: 10.1016/j.

Stauffer, D. R., Howard, T. L., Nyun, T. and Hollenberg, S. M. (2001) 'CHMP1 is a novel nuclear matrix protein affecting chromatin structure and cell-cycle progression.', *Journal of Cell Science*, 114, pp. 2383–2393.

Steglich, B., Filion, G., van Steensel, B. and Ekwall, K. (2012) 'The inner nuclear membrane proteins Man1 and Ima1 link to two different types of chromatin at the nuclear periphery in S. pombe', *Nucleus*, 3(1), pp. 77–87. doi: 10.4161/nucl.18825.

Stewart, C. L., Roux, K. J. and Burke, B. (2007) 'Blurring the boundary: the nuclear envelope extends its reach.', *Science*, 318(5855), pp. 1408–1412. doi: 10.1126/science.1142034.

Su, M., Guo, E. Z., Ding, X., Li, Y., Tarrasch, J. T., Brooks, C. L., Xu, Z. and Skiniotis, G. (2017) 'Mechanism of Vps4 hexamer function revealed by cryo-EM', *Science Advances*, 3(4), pp. 1–8. doi: 10.1126/sciadv.1700325.

Sugiyama, T., Cam, H. P., Sugiyama, R., Noma, K. ichi, Zofall, M., Kobayashi, R. and Grewal, S. I. S. (2007) 'SHREC, an Effector Complex for Heterochromatic Transcriptional Silencing', *Cell*, 128(3), pp. 491–504. doi: 10.1016/j.cell.2006.12.035.

Taddei, A., Hediger, F., Neumann, F. R., Bauer, C. and Gasser, S. M. (2004) 'Separation of silencing from perinuclear anchoring functions in yeast Ku80, Sir4 and Esc1 proteins.', *The EMBO journal*, 23(6), pp. 1301–12. doi: 10.1038/sj.emboj.7600144.

Tange, Y., Chikashige, Y., Takahata, S., Kawakami, K., Higashi, M., Mori, C., Kojidani, T., Hirano, Y., Asakawa, H., Murakami, Y., Haraguchi, T. and Hiraoka, Y. (2016) 'Inner nuclear membrane protein Lem2 augments heterochromatin formation in response to nutritional conditions', *Genes to Cells*, pp. 1–21. doi: 10.1111/gtc.12385.

Teis, D., Saksena, S. and Emr, S. D. (2008) 'Ordered Assembly of the ESCRT-III Complex on Endosomes Is Required to Sequester Cargo during MVB Formation', *Developmental Cell*. Elsevier Inc., 15(4), pp. 578–589. doi: 10.1016/j.devcel.2008.08.013.

Teis, D., Saksena, S., Judson, B. L. and Emr, S. D. (2010) 'ESCRT-II coordinates the assembly of ESCRT-III filaments for cargo sorting and multivesicular body vesicle formation.', *EMBO Journal*. Nature Publishing Group, 29(5), pp. 871–83. doi: 10.1038/emboj.2009.408.

Thaller, D., Allegretti, M., Borah, S., Ronchi, P., Beck, M. and Lusk, C. P. (2019) 'An ESCRT-LEM protein surveillance system is poised to directly monitor the nuclear envelope and nuclear transport system', *eLife*, 8, p. e45284. doi: 10.1101/523670.

Titos, I., Ivanova, T. and Mendoza, M. (2014) 'Chromosome length and perinuclear attachment constrain resolution of DNA intertwines', *The Journal of Cell Biology*, 206(6), pp. 719–733. doi: 10.1083/jcb.201404039.

Tong, P., Pidoux, A. L., Toda, N. R., Ard, R., Berger, H., Shukla, M., Torres-Garcia, J., Mueller, C. A., Nieduszynski, C. A. and Allshire, R. C. (2019) 'Inter-species conservation of organisation and function between non-homologous regional centromeres', *Nature Communications*. Springer US, 10(2343), p. https://doi.org/10.1038/s41467-019-09824-4. doi: 10.1101/309815.

Tran, P. T., Marsh, L., Doye, V., Inoué, S. and Chang, F. (2001) 'A mechanism for nuclear positioning in fission yeast based on microtubule pushing', *Journal of Cell Biology*, 153(2), pp. 397–411. doi: 10.1083/jcb.153.2.397.

Vietri, M., Radulovic, M. and Stenmark, H. (2019) 'The many functions of ESCRTs', *Nature Reviews Molecular Cell Biology*. Springer US, 21(January). doi: 10.1038/s41580-019-0177-4.

Vietri, M., Schink, K. O., Campsteijn, C., Wegner, C. S., Schultz, S. W., Christ, L., Thoresen, S. B., Brech, A., Raiborg, C. and Stenmark, H. (2015) 'Spastin and ESCRT-III coordinate mitotic spindle disassembly and nuclear envelope sealing', *Nature*, 522, pp. 231–235. doi: 10.1038/nature14408.

Vietri, M., Schultz, S. W., Bellanger, A., Jones, C. M., Raiborg, C., Skarpen, E., Pedurupillay, C. R. J., Kip, E., Timmer, R., Jain, A., Collas, P., Knorr, R. L., Grellscheid, S. N., Kusumaatmaja, H., Brech, A., Micci, F., Stenmark, H. and Campsteijn, C. (2019) 'Unrestrained ESCRT-III drives chromosome fragmentation and micronuclear catastrophe', *bioRxiv*, p. 517011. doi: 10.1101/517011.

Voeltz, G. K., Rolls, M. M. and Rapoport, T. A. (2002) 'Structural organization of the endoplasmic reticulum', *EMBO Reports*, 3(10), pp. 944–950. doi: 10.1093/embo-reports/kvf202.

Webster, B. M., Colombi, P., Jäger, J. and Lusk, C. P. (2014) 'Surveillance of nuclear pore complex assembly by ESCRT-III/Vps4', *Cell*, 159(2), pp. 388–401. doi: 10.1016/j.cell.2014.09.012.

Webster, B. M., Thaller, D. J., Jäger, J., Ochmann, S. E., Borah, S., Lusk, C. P. and Webster, B. M. (2016) 'Chm7 and Heh1 collaborate to link nuclear pore complex quality control with nuclear envelope sealing', *The EMBO Journal*, p. e201694574.

Wenzel, E. M., Schultz, S. W., Schink, K. O., Pedersen, N. M., Nähse, V., Carlson, A., Brech, A., Stenmark, H. and Raiborg, C. (2018) 'Concerted ESCRT and clathrin recruitment waves define the timing and morphology of intraluminal vesicle formation', *Nature Communications*. Springer US, 9(1), p. 2932. doi: 10.1038/s41467-018-05345-8.

Willan, J., Cleasby, A. J., Flores-Rodriguez, N., Stefani, F., Rinaldo, C., Pisciottani, A., Grant, E., Woodman, P., Bryant, H. E. and Ciani, B. (2019) 'ESCRT-III is necessary for the integrity of the nuclear envelope in micronuclei but is aberrant at ruptured micronuclear envelopes generating damage', *Oncogenesis*. Springer US, 8(5). doi: 10.1038/s41389-019-0136-0.

Wollert, T. and Hurley, J. H. (2010) 'Molecular mechanism of multivesicular body biogenesis by ESCRT complexes.', *Nature*. Nature Publishing Group, 464(7290), pp. 864–869. doi: 10.1038/nature08849.

Wollert, T., Wunder, C., Lippincott-Schwartz, J. and Hurley, J. H. (2009) 'Membrane scission by the ESCRT-III complex', *Nature*. Nature Publishing Group, 458(7235), pp. 172–177. doi: 10.1038/nature07836.

Xu, Y. (2015) 'Inner nuclear membrane protein Lem2 facilitates Rad3-mediated checkpoint signaling under replication stress induced by nucleotide depletion in fission yeast', *Cellular Signalling*. Elsevier B.V., p. doi: 10.1016/j.cellsig.2015.12.009. doi: 10.1016/j.cellsig.2015.12.009.

Yam, C., Gu, Y. and Oliferenko, S. (2013) 'Partitioning and remodeling of the Schizosaccharomyces japonicus mitotic nucleus require chromosome tethers', *Current Biology*. Elsevier Ltd, 23(22), pp. 2303–2310. doi: 10.1016/j.cub.2013.09.057.

Yam, C., He, Y., Zhang, D., Chiam, K. H. and Oliferenko, S. (2011) 'Divergent strategies for controlling the nuclear membrane satisfy geometric constraints during nuclear division', *Current Biology*. Elsevier Ltd, 21(15), pp. 1314–1319. doi: 10.1016/j.cub.2011.06.052.

Yang, B., Stjepanovic, G., Shen, Q., Martin, A. and Hurley, J. H. (2015) 'Vps4 disassembles an ESCRT-III filament by global unfolding and processive translocation', *Nature Structural and Molecular Biology*, 22(6), pp. 492–498. doi: 10.1038/nsmb.3015.

Yewdell, W. T., Colombi, P., Makhnevych, T. and Lusk, C. P. (2011) 'Lumenal interactions in nuclear pore complex assembly and stability.', *Molecular Biology of the Cell*, 22(8), pp. 1375–1388. doi: 10.1091/mbc.E10-06-0554.

Zhang, D. and Oliferenko, S. (2013) 'Remodeling the nuclear membrane during closed mitosis', *Current Opinion in Cell Biology*, 25(1), pp. 1–7. doi: 10.1016/j.ceb.2012.09.001.

Zhang, X., Cook, P. C., Zindy, E., Williams, C. J., Jowitt, T. A., Streuli, C. H., Macdonald, A. S. and Redondo-mu, J. (2015) 'Integrin alpha 4 beta 1 controls G9a activity that regulates epigenetic changes and nuclear properties required for lymphocyte migration', *Nucleic Acids Research*, 44(7), pp. 3031–3044. doi: 10.1093/nar/gkv1348.

Zhen, Y., Spangenberg, H., Munson, M. J., Brech, A., Schink, K. O., Tan, K.-W., Sørensen, V., Wenzel, E. M.,

Radulovic, M., Engedal, N., Simonsen, A., Raiborg, C. and Stenmark, H. (2019) 'ESCRT-mediated phagophore sealing during mitophagy', *Autophagy*. Taylor & Francis, 0(0), pp. 1–16. doi: 10.1080/15548627.2019.1639301.

Zhou, F., Wu, Z., Zhao, M., Murtazina, R., Cai, J., Zhang, A., Li, R., Sun, D., Li, W., Zhao, L., Li, Q., Zhu, J., Cong, X., Zhou, Y., Xie, Z., Gyurkovska, V., Li, L., Huang, X., Xue, Y., Chen, L., Xu, H., Xu, H., Liang, Y. and Segev, N. (2019) 'Rab5-dependent autophagosome closure by ESCRT', *The Journal of Cell Biology*, 218(6), p. jcb.201811173. doi: 10.1083/jcb.201811173.

Zhu, Q., Zheng, F., Liu, A. P., Qian, J., Fu, C. and Lin, Y. (2016) 'Shape Transformation of the Nuclear Envelope during Closed Mitosis', *Biophysical Journal*. Biophysical Society, 111(10), pp. 2309–2316. doi: 10.1016/j.bpj.2016.10.004.

Zhurinsky, J., Salas-Pino, S., Iglesias-Romero, A. B., Torres-Mendez, A., Knapp, B., Flor-Parra, I., Wang, J., Bao, K., Jia, S., Chang, F. and Daga, R. R. (2019) 'Effects of the microtubule nucleator Mto1 on chromosomal movement, DNA repair, and sister chromatid cohesion in fission yeast', *Molecular Biology of the Cell*, 30(21), pp. 2695–2708. doi: 10.1091/mbc.e19-05-0301.

Zuleger, N., Boyle, S., Kelly, D. A., de las Heras, J. I., Lazou, V., Korfali, N., Batrakou, D. G., Randles, K. N., Morris, G. E., Harrison, D. J., Bickmore, W. A. and Schirmer, E. C. (2013) 'Specific nuclear envelope transmembrane proteins can promote the location of chromosomes to and from the nuclear periphery', *Genome Biology*, 14(2). doi: 10.1186/gb-2013-14-2-r14.

Zuleger, N., Kelly, D. A., Richardson, A. C., Kerr, A. R. W., Goldberg, M. W., Goryachev, A. B. and Schirmer, E. C. (2011) 'System analysis shows distinct mechanisms and common principles of nuclear envelope protein dynamics', *Journal of Cell Biology*, 193(1), pp. 109–123. doi: 10.1083/jcb.201009068.